"Design and Synthesis of Novel Associating Polymers"

Thesis submitted to,

University of Pune

For the degree of

Doctor in Philosophy

In

CHEMISTRY

By

NIVIKA RAJENDRA GUPTA

Under the Guidance Of

Dr. Manohar V. Badiger

Polymer Science & Engineering Division

CSIR-National Chemical Laboratory

Pune- 411008

March 2013

राष्ट्रीय रासायनिक प्रयोगशाला
(वैज्ञानिक तथा औद्योगिक अनुसंधान परिषद)
डॉ. होमी भाभा रोड, पुणे - 411 008. भारत
NATIONAL CHEMICAL LABORATORY
(Council of Scientific & Industrial Research)
Dr. Homi Bhabha Road, Pune - 411008. India

Certificate

Certified that the work presented in the thesis entitled **"Design and Synthesis of Novel Associating Polymers"** submitted by **Ms. Nivika Rajendra Gupta** was carried out by the candidate under my Supervision. Material obtained from other sources has been duly acknowledged in the thesis.

Place: Pune

Date: 28/03/2013

Dr. Manohar V. Badiger
(Research Guide)
CSIR-NCL, Pune
March 2013

Communications Channels ☎ +91 20 25902000 +91 20 25893300 +91 20 25893400 Fax +91 20 25902601 (Director) +91 20 25902660 (Admin.) +91 20 25902639 (Business Development) URL : www.ncl-india.org

TABLE OF CONTENTS

Abstract

Design and Synthesis of Novel Associating Polymers

This thesis work reports on the design, synthesis and characterization of new Associating Polymers (APs) and Superabsorbent Polymers (SAPs) based on Polysaccharides namely, Carboxymethyl guar (CMG), Carboxymethyl tamarind (CMT) and Hydroxypropyl guar (HPG).

APs have attracted increasing attention recently because of their unique rheological properties such as, super-viscosifying, shear-thickening/shear-thinning, thermo-associating and strain-hardening etc. Due to these properties, they find a large number of applications in various areas such as thickeners for cosmetic creams, lotions, pharmaceutical formulations, paints, oil-recovery, paper, textile and other industrial products.

APs consists of water-soluble polymer backbone with a small amount (typically < 2-8 mol %) of covalently bound hydrophobe moieties called "stickers" either dispersed along the polymer chains (grafts) or specifically located at the ends of the polymer chains (telechelic). Their thickening ability in aqueous solution arises through reversible intermolecular associations caused by the unfavorable interactions between water molecules and hydrophobic groups/stickers.

More recently, thermo-associating polymers have emerged as promising materials wherein, the reversible associations are prompted w.r.t temperature as a stimuli by the presence of stickers characterized by a Lower Critical Solution Temperature (LCST). They have potential application as injectables in controlled release technology. In this thesis work, thermo-associating graft copolymers of CMG/CMT and semi-telechelic, LCST, amino terminated poly (N-isopropylacrylamide) (PNIPAm)/ poly(ethylene oxide-co-propylene oxide) (PEPO) were synthesized by coupling reaction between them using a coupling agent namely, 1-Ethyl-3-(3-dimethylaminopropyl)carbodiimide hydrochloride (EDC). The incorporation of PNIPAm/PEPO side chains was confirmed by FT-IR and NMR spectroscopy. The graft copolymers, CMG-g-PNIPAm, CMG-g-PEPO and CMT-g-PEPO in aqueous solutions exhibited interesting thermo-associating property which was investigated using rheology and fluorescence spectroscopy. These thermo-associating polymers

with biodegradable nature of CMG and CMT can have potential applications as injectables in controlled release technology.

We also demonstrated the application of these thermo-associating polymers in the preparation of metal nanoparticles as both reducing and stabilizing agents. Conventional reducing agents such as, borohydrides, and phosphines used for the synthesis of nanoparticles have some disadvantages like toxicity and stability of the obtained nanoparticles. Therefore, we have reported here on the synthesis and characterization of silver-nanoparticles (AgNPs) using CMG-g-PEPO as reducing and capping agent. The confirmation of AgNPs was performed by using UV-Vis spectroscopy which gave a surface plasmon resonance in the range of 400-420 nm. The TEM images indicated the size of the obtained nanoparticles in the range of 10-20 nm. We also showed the use of these nanoparticles for controlled release applications, wherein an anticancer drug, Doxorubicin hydrochloride (Dox) was incorporated onto the AgNPs. The incorporation of the drug was confirmed by XPS and Raman Spectroscopy. The release of Dox from the polymer encapped AgNPs could be controlled taking the advantage of thermo-associating behavior of the polymer.

The research work was also focused on development of new SAPs based on polysaccharides namely, CMG and HPG. SAPs are lightly crosslinked hydrophilic polymers that are capable of absorbing large amounts of water and saline solutions in the range of 10-1000 times their own weight. They have been extensively used in various applications such as baby diapers, sanitary napkins, and controlled release systems and as industrial thickeners. Most of the commercially available SAPs are partially crosslinked acrylates and have no biodegradability. Thus, their extensive usage may result in environmental pollution problem. In view of this we have worked on the synthesis and characterization of new SAP based on crosslinked CMG:HPG. The crosslinking was effected using two different crosslinking agents namely, Citric Acid (CA) and Divinyl sulphone (DVS). The characterization of SAPs in terms of swelling capacity and mechanical strength was performed by swelling ratio and Dynamic Mechanical Analysis (DMA). The biodegradability, toxicity and cell viability studies were performed on these SAPs.Finally, an attempt was made to synthesize APs based on Hyaluronic acid (HA) using a ‘Click Chemistry’ approach.

HA was modified with alkyne and azide groups which were connected to HA backbone through hydrolysable carbonate esters or cleavable disulphide groups. These azide and alkyne modified HA were subsequently crosslinked via ‘click’ in the presence of copper catalyst. The APs obtained were characterized in terms of their chemical structure using FT-IR and NMR spectroscopy. It was observed that the azide and alkyne modified HA exhibited highly viscous /gel nature even before the click reaction which could be attributed to the extensive intermolecular interactions by hydrophobic associations. However, this needs to be investigated further in detail.

LIST OF SCHEMES

LIST OF TABLES

LIST OF FIGURES

Literature

Chapter - I

1.1. Introduction

Associating Polymers (APs) or Hydrophobically Modified Polymers (HMPs) are a class of complex and partially ordered systems, which have attracted a great deal of research and commercial interest in the past 2-3 decades [1-3]. These materials are aqueous soluble and contain both water-soluble (hydrophilic) and water insoluble (hydrophobic) components of varying levels of hydrophobicity. Due to this amphiphilic character of the molecules, they act as effective rheological modifiers even at low concentrations. They can therefore, find various applications in which a careful control of the rheology of solution is required, e.g. paints, foods and pharmaceuticals [2, 4-6]. Depending on the location of hydrophobic groups in the macromolecule chain, a large number of molecular architectures have been envisaged in associating polymers (**see figure 1.1**). The hydrophobic groups can either be dispersed along the hydrophilic polymer chains or present as terminal groups (telechelic/hydrophobically end-capped polymers). The driving force for the association process in the aqueous media is the interaction between the hydrophobic segments that arises in order to minimize their exposure to water. The resulting association gives rise to a transient network, which enhances the viscosity of the solution. The network can break and reform continuously due to thermal fluctuations. The hydrophobic associations indeed play an important role in governing co-operative aggregation processes in aqueous environment such as, surfactant self –assembly, protein folding, formation of biological membranes and molecular recognition. The first report on hydrophobically modified polymers was made by Strauss and coworkers in 1951[7], who derivatized poly (4-vinyl pyridine) with a mixture of ethyl and dodecyl groups to form a polyelectrolyte which self-associate in water.

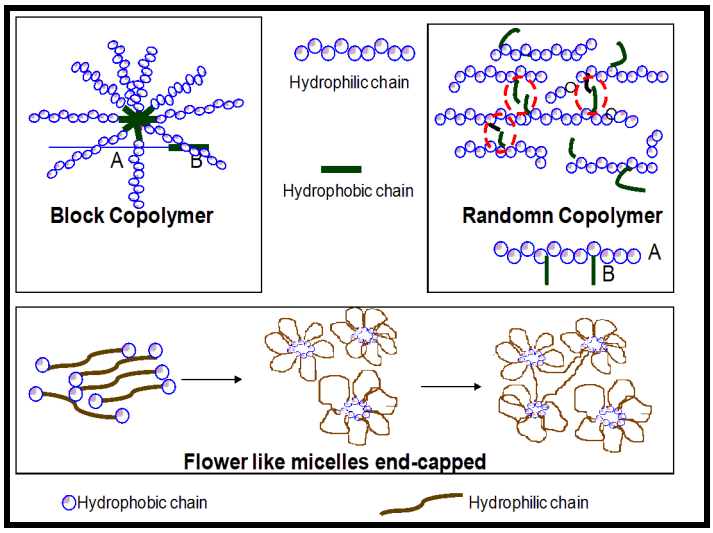

Figure 1.1: *Different molecular architectures in APs*

Subsequently, in 1970 other key contributions were made by Strauss et al. in the area of associating polymers [7, 8]. A few books have been published in the literature [9] which provide an excellent introduction to the field of associating polymers. At the same time, Hester and Squire wrote a review on the influence of associative polymers on the rheology of water-borne coatings [10]. The synthesis of various associating polymer structures is reviewed by Schulz et al. [9] Landoll was amongst the first few ones who developed Cellulose as hydrophobically associating water-soluble polymers [11]. In his work, non-ionic Cellulose ethers such as Hydroxyethyl Cellulose (HEC), hydroxypropyl Cellulose (HPC) and methyl Cellulose (MC) were employed as raw materials for hydrophobization by reactions with long chain n-alkyl epoxides. This new class of polymers exhibited unique rheological properties due to inter-chain association. Following his research, a substantial amount of literature dealing with this class of polymers was developed and reported later [12,13]. However, in almost in all cases, the cellulose derivatives were modified with hydrophobic compounds such as alkyl halides, acid halides, acid anhydrides, isocyanates or epoxides.

1.1.1. Types of APs

APs or HMPs can be classified into different categories namely (i) hydrophobically modified alkali-swellable emulsions (HASE) (ii) hydrophobically modified Cellulose polymers (iii) Telechelic polymers (iv) hydrophobically modified poly(acrylamides) and amphiphilic block copolymers and (v) Thermo-associating Polymers.

Hydrophobically modified alkali-swellable/soluble emulsions (HASE) consists of polyelectrolyte backbone with hydrophobic pendant groups. The polyelectrolyte backbone invariably comprises of carboxylic acid and acrylate ester groups in a proper balance so that the polymer is stable as latex at acid pH, but dissolves and expands at pH above 6.0.

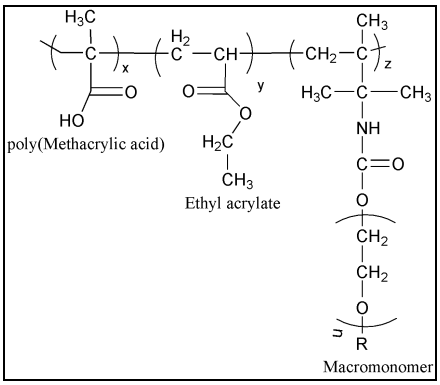

Figure 1.2: *Structure of HASE polymer: EA-50mol%; MA-49.1 mol% & macromonomer with R = $C_{20}H_{41}$ -0.9mol%*

A classic example of HASE polymer is prepared by emulsion polymerization of Methacrylic acid and ethyl acrylate along with a small amount of hydrophobic macro monomer. The chemical structure of this polymer is shown in **figure 1.2**. HASE polymers are extensively used as thickeners in paints, textiles and cosmetics.

One of the first APs synthesized and studied is Hydroxyethyl Cellulose (HEC) containing a small fraction of n-alkyl substituents which is typically of C_{16} hydrocarbon chain. Hydrophobically modified ethyl Hydroxyethyl Cellulose (HM-

EHEC) is prepared by reacting EHEC with hydrophobic compounds such as long chain alkyl halides, alkyl epoxides, alkyl Isocyanates and alkyl anhydrides etc. Extensive studies on rheology and solution behavior of this class of polymers are reported in the literature [14-17].

Telechelic polymers have received considerable attention for the past several years. In general, these are hydrophilic, linear water–soluble polymers, normally based on PEO with hydrophobic end groups. The hydrophobic moieties typically contain 8-18 carbon atoms which are alkyl, perfluoroalkyl or aromatic groups. A representative example of this class of polymers is hydrophobically modified ethoxylated urethanes (HEUR). The first reports on the studies of HEUR polymers appeared in the mid-1980s by Glass and coworkers [18-20]. HEURs have been widely investigated from a fundamental point of view as model associative thickeners. Jenkin's group [21] and Annable et al. [22] examined a series of HEUR polymers prepared by chain extension reaction of an oligomeric PEO with a diisocyanate, followed by end-capping with an aliphatic alcohol. The chemical structure of one of the representative HEUR polymers is shown in **figure 1.3**.

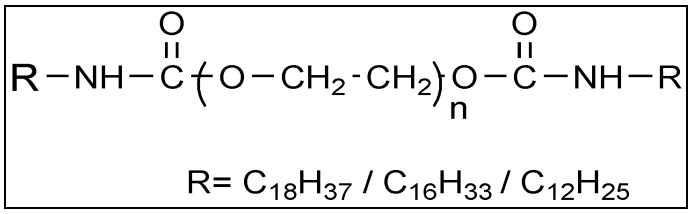

Figure 1.3: *Structure of hydrophobically modified ethoxylated urethanes (HEUR)*

Different molecular architectures such as comb, block and star HEUR polymers have been synthesized and characterized. Such polymers are found to have very effective associating property in urethane paints and coatings [23, 24].

Associating Polymers based on poly(acrylamide) and hydrophobic co-monomers have emerged as promising materials in enhanced oil recovery (EOR), drilling fluids, hydraulic fracture and drag reduction. McCormick and coworkers [5, 25] have made major contribution towards the design and synthesis of APs based upon polysaccharides. Selb etal [26] reported on the rheological properties of a series of acrylic acid-acrylamide copolymers with C_{16} substituents. Hogen–Esch and coworkers [27, 28] have investigated on the series of poly(N,N-dimethylacrylamide) copolymers with fluorocarbon pendant groups. Many aspects of hydrophobically modified poly(acrylamide) including synthesis, rheology and applications have been dealt and reported in the literature [29-35] . The generalized chemical structure of HM-PAM is shown in **figure 1.4**

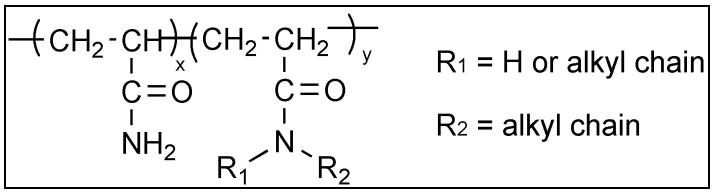

Figure 1.4: *A general chemical structure of HM-PAM*

The most commonly studied hydrophobically modified polyelectrolyte is poly(acrylic acid) [PAA] wherein, PAA was modified with different hydrophobic groups in organic solvent [36, 37].

Amphiphilic polymers, which have received major scientific attention and extensive industrially use are block copolymers of the AB, ABA or BAB type. Amongst the most useful block copolymers are amphiphilic block copolymers of poly(ethylene oxide) - poly(propylene oxide)-poly(ethylene oxide), PEO_y-PPO_x-PEO_y (Poloxamers, ICI or pluronics, BASF). Pluronic block copolymers are known to self-assemble in water into micelles consisting of hydrophobic core of PPO and a corona of the

solvated PEO. The hydrophobic blocks can be poly(propylene oxide), poly(butylene oxide), poly(styrene) or poly(methylmethacrylate) and the hydrophilic blocks can be PEO, PVME, poly (acrylic acid), poly(methylmethacrylic acid), poly(styrene sulfonate) etc. These amphiphilic block copolymers are usually synthesized by living polymerization techniques such as anionic polymerization, cationic polymerization, ATRP etc. Amphiphilic block copolymers form micellar aggregation reversibly due to the hydrophobic associations or electrostatic interactions between the blocks of the copolymers. Depending on the type of the block copolymer, concentration of the block copolymer and temperature of the system, different micelles and phases of self-assemblies can be formed in aqueous media [2,34,38]. Amphiphilic block copolymers find wide range of applications in cosmetics, surfactants and pharmaceutical industries [39].

Associating Polymers exhibiting thermally induced properties in aqueous solutions are termed as thermo-associating Polymers. These polymers show a thermo-thickening behavior i.e. increases in viscosity upon heating which is rather exceptional, as most of the conventional fluids are characterized by a well-known Arrhenius thermo-thinning behavior. In most of the Thermo-associating polymers, polymers with lower critical solution temperature (LCST) are involved. A chapter is dedicated to these polymers in this thesis and hence will be discussed in detail in Chapter - III.

1.1.2. Synthesis of APs

Generally, APs or HMPs are synthesized by two approaches: (i) by direct copolymerization of hydrophilic (water-soluble) monomers with hydrophobic (oil-soluble) monomers by micellar polymerization or (ii) by post functionalisation or chemical modification of water-soluble polymers with hydrophobic groups.

1.1.2.1. Copolymerization

Copolymerization is a widely used industrial process for the synthesis of hydrophobically modified polymers [40-44]. However, direct copolymerization of hydrophilic monomer with hydrophobic monomer has difficulties in identifying a common solvent for both the monomers for the reaction to proceed. Furthermore, a limited solubility of monomers often leads to heterogeneous copolymer composition and low hydrophobic modification [29, 45-47]. In order to overcome these problems, a micellar polymerization/copolymerization technique is routinely used [25, 29, 31-33, 40-45, 48-51]. For example, in the micellar copolymerization of acrylamide, the hydrophobic monomer is solubilized within surfactant micelles, whereas, acrylamide is solubilized in water. For neutral or anionically charged hydrophobic polymer, Sodium dodecyl sulfate/ethylene glycol is used as surfactant and for cationically charged polymers either cationic or nonionic surfactants are used [41, 43, 44, 52, 53].

The heterogeneity in the copolymer or the length of the block and blockiness of the copolymer can be controlled by the reactivity ratios (ratio of reactivity of a hydrophobic to hydrophilic monomer) and the micellar effect, i. e. by varying the concentration of surfactant or number of hydrophobic monomer per surfactant micelle (NH) during the synthesis [31,54]. It was observed that a low value of NH produces more random copolymer.

In another route for the synthesis of hydrophobically modified poly(acrylamide) by micellar polymerization, a polymerizable surfactant monomer or surfactant macromonomer (Surfmer) is used [55-57]. In the surfactant macromonomer route, a water-soluble polymerizable surfactant surfmer *n*-hexadecyldimethyl-4-vinylbenzyl ammonium chloride, which has both hydrophilic head and hydrophobic tail, is used (as shown in **Scheme 1.1**).

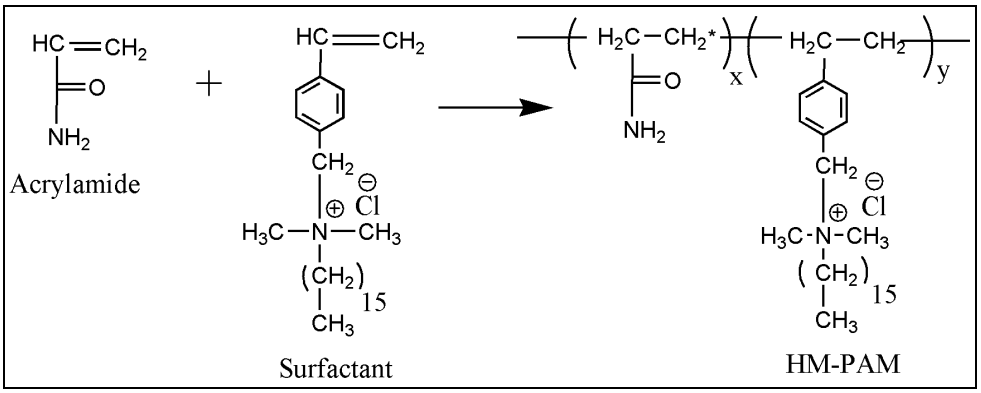

Scheme 1.1: *Micellar polymerization of acrylamide with polymerizable surfactant*

In this case the hydrophobic block length corresponds to the aggregation number (N_{agg}) of the surfactant. Therefore, the block length of copolymer obtained by using surfactant is much larger than obtained with hydrophilic monomer and surfactant.

1.1.2.2. Post-Polymerization Functionalization

Post-polymerization functionalization or chemical modifications of water-soluble polymers are the second way of obtaining APs/HMPs. The advantage with this method is that, due to post-functionalization, hydrophobic content can be easily controlled by keeping the parent polymer molecular weight and the distribution of hydrophobic groups constant. However, the chemical reactivity of functional groups on the polymer chains usually differs from the low molecular weight analogue and the degree of modification is often limited. The post-polymerization modification approach is simple and the easiest way to synthesize APs/HMPs.

A typical example of post polymerization modification is the preparation of polysoaps [7, 8, 58, 59]. The preparation of polysoap involves the chemical modification; particularly quaternization of poly(2-vinyl pyridine) with n-dodecyl bromide carried out by Strauss [7]. The reaction pathway is as shown **Scheme 1.2**.

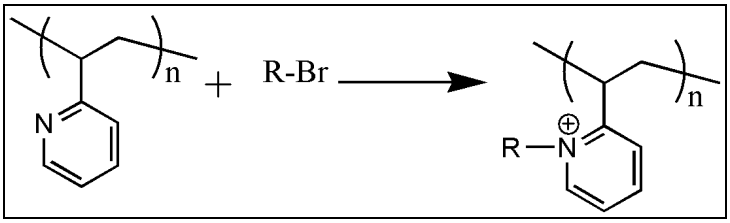

Scheme 1.2: *Chemical modification of poly(vinyl pyridine)*

Similarly, hydrophobic modification of poly(acrylic acid); PAA with alkylamine was carried out in an aprotic solvent (1-methyl-2-pyrrolidone;NMP) using dicyclohexylcarbodiimide (DCC) [60, 61]. Hydrophobically modified poly(acrylic acid) with up to 10 mol% hydrophobic content were prepared by Iliopoulos and coworkers, a

reaction scheme is shown in **Scheme 1.3**.

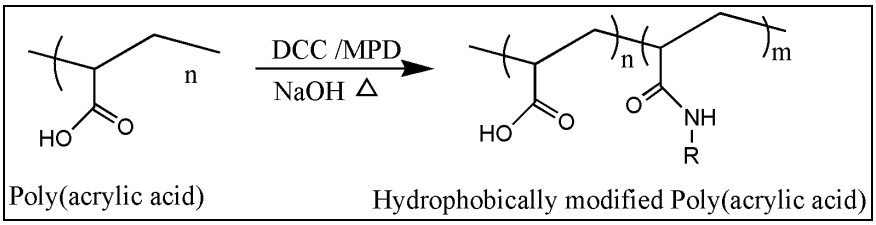

Scheme 1.3: *Post-polymerization modification of poly(acrylic acid)*

PAM was hydrophobically modified by several authors by incorporating hydrophobic groups onto poly(acrylamide) using anhydrous dimethyl sulfoxide (DMSO) as a solvent

for PAM and potassium *tert*-butoxide as a base [62, 63]. The synthetic route involves the reaction between amide group of PAM and alkyl bromide, a reaction pathway is shown in **Scheme 1.4**.

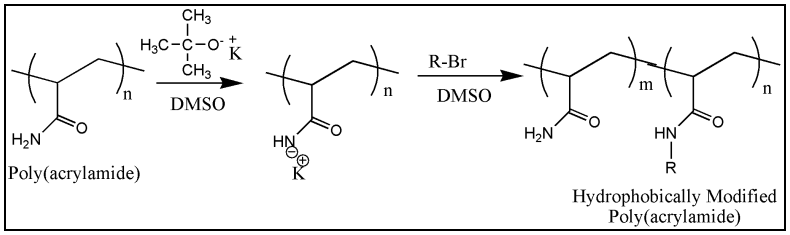

Scheme 1.4: *Post-polymerization modification of poly(acrylamide)*

The hydrophobic modification of PAM can also be performed by grafting reaction. For example, Bromberg prepared a novel HM-PAM by grafting PEO-*b*-PPO-*b*-PEO onto PAM [64]. Hydrophobically modified hydroxyethyl cellulose (HM-HEC) has also been prepared by post-polymerization modification by several researchers. In this methodology, the hydrophobic modification involves the reaction of hydroxyl group of HEC with various hydrophobes of long chain alkyl, aryl or alkyl aryl functional groups such as epoxyalkanes (C_{10}, C_{12}, C_{14} and $C_{20\text{-}24}$), alkyl and aryl halides, isocyantes and anhydrides [11, 65-68]. A general scheme of hydrophobic modification of HEC using various reactive functional groups is shown in **Scheme 1.5**.

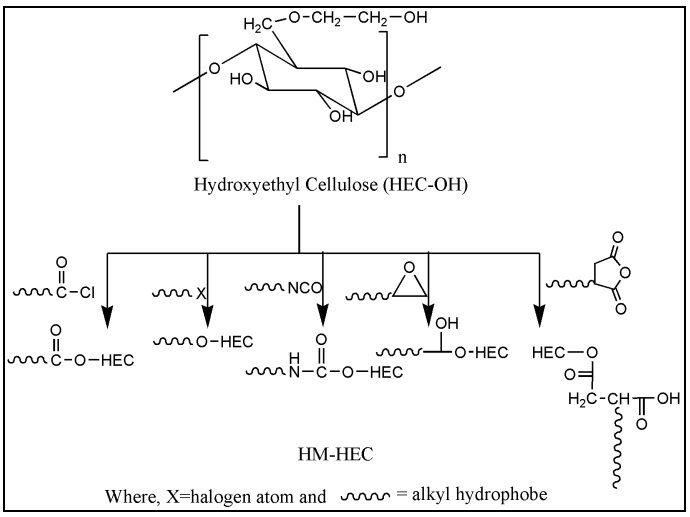

Scheme 1.5: *Post-polymerization modification of HEC*

Telechelic polymers such as HEUR or hydrophobically end-capped PEOs of various architectures like comb, block and star are mostly synthesized by the post-polymerization functionalisation approach [20, 22, 66, 69-73]. The simplest types of HEUR, with mono (α-) and di (α, ω-) end-capped polymers are synthesized by reacting the terminal hydroxyl groups with long chain alkyl or aryl hydrophobes with reactive functional groups, such as isocyanates or diisocyanates and acid chloride [66, 70, 71]. The comb type HEUR are prepared by reacting preformed polymer bearing isocyanate functionality with hydrophobe such as di-ethanol amine and mono methyl poly (ethylene glycol)s (Me-PEGs) [74].

1.1.3. Solution Properties of APs

It is well known that the unusual rheological properties of APs originate from the formation of a physically crosslinked network. The driving force for the association process is the interaction between the hydrophobic segments that arises in order to minimize their exposure to water. The resulting micellar associations give rise to both intra- and intermolecular temporary domains or junctions. The network is temporary in the sense that the junctions that hold the network together break and reform continuously due to thermal fluctuations

The solution rheology (i.e. η vs concentration) of APs can be interpreted based on the existence of three distinct concentration regimes (**See Figure 1.5**): (i) a dilute regime where the viscosity is essentially controlled by intramolecular interactions, (ii) a semidilute unentangled regime dominated by intermolecular hydrophobic associations and (iii) a semi-dilute entangled regime for which the viscoelastic behavior can be described by a sticky reptation mechanism.

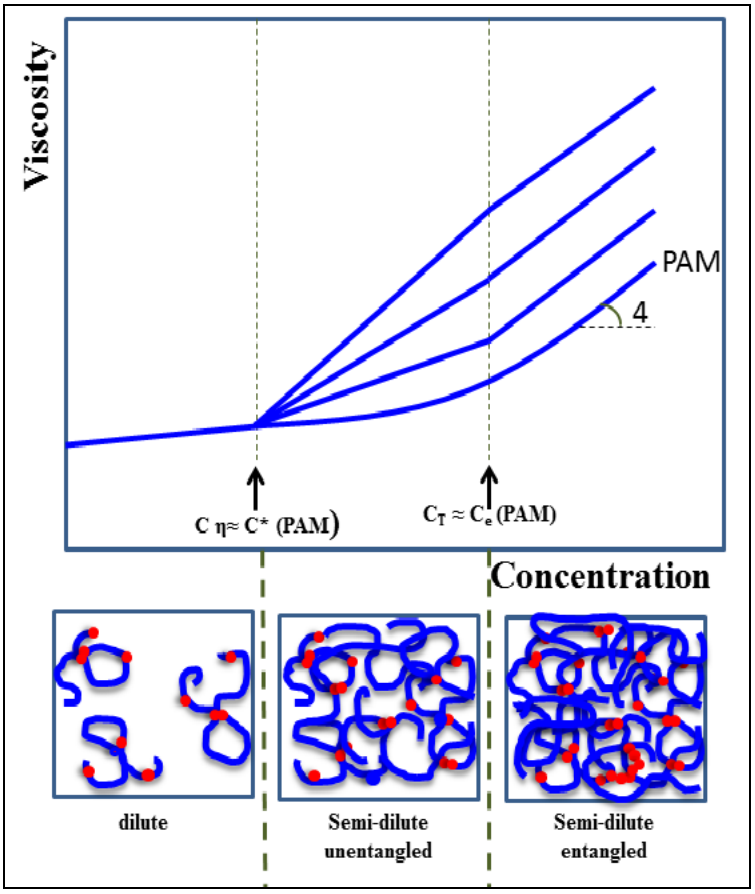

Figure 1.5: *Different regimes of concentrations in polymer solution*

(Courtesy: Enrique Jime´nez Regalado et al. Macromolecules, Vol. 32, No. 25, 1999)

Large numbers of research groups have investigated the association and rheology of these APs. A review article by Winnik and Yekta [3] and the text book of Larson [75] provide a detailed survey of this literature.

The solution properties of hydrophobically modified hydroxyl ethyl Cellulose (HM-HECs) were studied in water or dilute salt solutions or co-solvents. The enhanced viscosity of HM-HEC's compared to HEC is attributed to the hydrophobic associations of the side chains [76, 77].

The hydrophobic modification and the influence of hydrophobic comonomer on the solution behavior of polyacrylamides have been studied by several researchers [31, 42, 44, 45, 49, 78]. The incorporation of small amount of hydrophobe causes drastic changes in

the viscometric and rheological behavior. At low polymer concentrations, where intramolecular associations are predominant, the hydrophobic associations produce a decrease in the hydrodynamic radius of the polymer coil. In the semi-dilute regime, the hydrophobe can considerably enhance the solution viscosity and lead to interesting rheological properties such as, shear thinning, shear thickening, viscoelasticity etc.

The viscoelastic behavior can be strongly influenced by the physical crosslinks formed by hydrophobic associations. The viscoelastic properties of unmodified polyacrylamide above the critical overlap concentrations are governed by chain entanglements. However, in the case of modified Polyacrylamide, the hydrophobic associations play a major role in determining the viscoelastic properties. The HM-PAM shows a drastic increase in storage (G') and loss (G") moduli compared to the unmodified PAm. The high value of G' and the "entanglement coupling" (which cannot be ruled out) reflect the high elasticity of the associating polymer solution.

HASE polymers are becoming increasingly important because of their wide range of applications in water-borne paints and coatings. English et al. [79] have reported on the rheological studies of HASE polymers bearing n-alkyl hydrophobes.

Over the past few years, several studies on the HEUR polymers in aqueous solutions have been reported in the literature [22, 80-82]. The important findings of these studies indicate that the oscillatory shear data can be fitted to a simplest model of viscoelastic behavior, a Maxwell model consisting of a single elastic component with a single viscous element. This implies that the stress relaxation in these systems is characterized by a single relaxation time which depends on the length of the hydrophobe, concentration and molecular weight of the polymer. In HEUR polymers, depending on the relative locations of the two hydrophobic end groups, different

scenarios can be imagined. Loops are formed if the end groups of the chain are present in the same micelle. The hydrophobic end groups may be located in different micelles in which case, a bridge is established between two micelles. These bridging chains may be referred to as elastically active chains since they form part of the temporary elastic network (**See Figure 1.6**). Depending on the hydrophobicity of the end groups and the polymer concentration, one or both ends can also temporarily exist without any association. These molecules form dangling chains which can relax before being incorporated into the micellar network. The complex rheological behavior of these telechelic polymers originate from the dynamical interchange of these loops, bridges, and the dangling chains as a function of deformation imposed on the network.

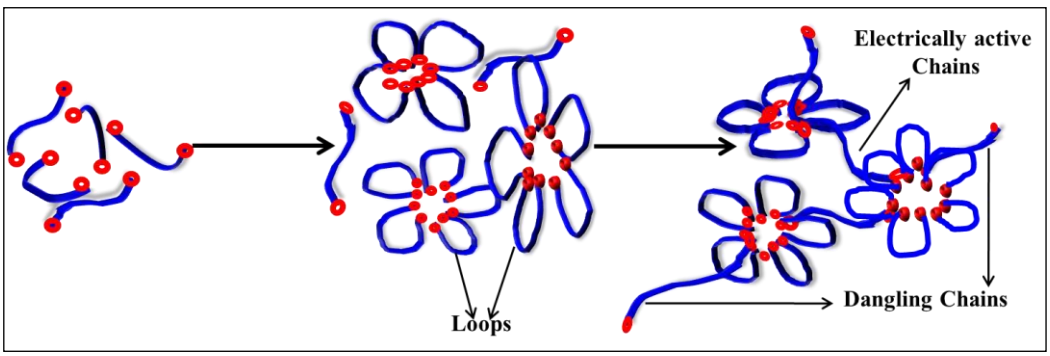

Figure 1.6: *Schematics of hydrophobic associations between end groups of the end-capped polymer*

The structure and dynamics of these telechelic polymers depends on numerous parameters such as polymer concentration, molecular weight, hydrophobe size and characteristic degree of hydrophobicity, temperature and the imposed shear deformation. The various rheological behavior exhibited by telechelic polymers include the ability to form high viscous solutions at low to moderate concentrations, a linear viscoelastic response that fits the Maxwell model with a single relaxation time [22,83]. Shear thickening at moderate shear rates and marked shear thinning at high shear

rates[69, 73, 84, 85], Arrhenius-like temperature dependence of the zero-shear rate viscosity [22, 86] and a decrease in the critical shear rate ($\dot{\Upsilon}_{crit}$) at which onset of shear thickening occurs as the concentrations of the polymer increases [87].

Several constitutive models have been developed to describe the rheological behavior of APs. Tanaka and Edwards [88-90] developed a temporary network model for telechelic polymers, by applying formulations given by Green & Tobolsky [91].

Tanaka and Edwards assumed that the chains obey Gaussian statistics and relax rapidly into their equilibrium state through Rouse dynamics upon detachment from each network point. This theory could explain the observation of single relaxation time but does not explain the shear thickening phenomenon at moderate shear rate.

1.1.4. Thermo-associating Polymers

Recently, the introduction of responsive stickers instead of just a hydrophobe ones into the macromolecular architecture has opened up the way of reversible associations and prompted the formation of physical networks using stimuli such as temperature, pH, light etc. For example, water-soluble polymers with stickers having LCST in water are able to undergo a sol-gel transition by increasing the temperature: they are called as thermo-associating/thermo-responsive polymers. Thermo-thickening behavior, based on the micro phase separation of LCST moieties grafted on water-soluble backbones, is a general concept and can be extended to a wide variety of copolymers. These thermo-associating polymers show potential applications as injectable in controlled drug delivery. Drugs, protein and cells can be easily incorporated into polymer solutions prior to administration into the body and rapidly gel inside where drugs can be releases at a controlled rate. Importantly, no surgical procedures are required for the insertion of liquid into the body and administration by simple injection is sufficient. These polymers can undergo self-assembly in response

to the body temperature and display sol-gel transition without marked, volume changes. The phenomenon of physical sol-gel transition w.r.t temperature is now well demonstrated in synthetic and modified natural polymers [92-94]. Significant progress has been achieved in the development of injectable biodegradable polymers, and each polymer-gel has special intrinsic properties (including gel strength, pH after degradation and degradation rate) that may be appropriate for a particular application. However, there are some challenges remaining in the improvement of applicability of these polymers. For example, the risk of syringe clogging, life time of the gel prior to degradation, inflammation of degraded products, cell adhesion to gel and tissue/polymer interface need to be addressed. Park et al have reported on a thermo sensitive chitosan –pluronic hydrogel as an injectable cell delivery carrier for cartilage regeneration [95]. An excellent review on the injectable biodegradable hydrogels is recently published in the literature [96].

1.1.5. Superabsorbent Polymers based on Polysaccharides

Superabsorbent Polymers (SAPs) based on natural polymers such as polysaccharides are becoming increasingly important due to their environmentally friendly nature and biodegradability. Most of the commercially available SAPs are based on partially crosslinked sodium polyacrylates and are not biodegradable. Further, the cost of basic raw material i.e. acrylic acid which is from petroleum origin keeps fluctuating depending on the oil price. Therefore, research efforts are being made to develop SAPs from renewable resource materials such as polysaccharides. Polysaccharides are the cheapest and most abundant renewable resource materials. Sources, structure and properties of some of the well known polysaccharides is given in **table 1.1**.

Table 1.1: *Source, structure and properties of some of the well-known polysaccharides*

Polysaccharide	Cellulose	Dextran	Starch	Guar Gum	Tamarind kernel powder	Chitosan	Hyaluronic acid	Xanthan	Pullulan	Carrageenan
Structure	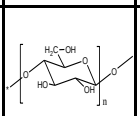	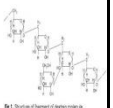	Amylose (20-25%) and amylopectin (75-80%)	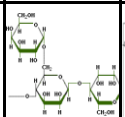	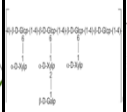	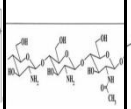	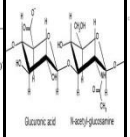	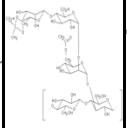	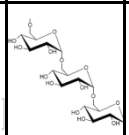	Kappa, Lamda, Iota
Functional grp	-OH	-OH	-OH	-OH	-OH	-OH, -NH_2, $NHCOCH_3$	-COOH, -OH -$NHCOCH_3$,	-OH, COOH, -$OCOCH_3$	-OH	-OH, -OSO_3^-
Derivative	MC, CMC, HEC, EHEC	CMDx, Dextran sulphate, cationic dextran	CMSt, cationic starch	CMG, HPG, HEG, CMHPG, cationic	CMT, HPT, HET	CMCs,	Benzyl, methyl, amine, NHS ester,	CMX, HPX	CMP, sulfo Propyl,	CMCrg, HPCrg
Solvents	Cupriethyl enediamine Cadmium methyl enediamine	water and electrolyte solutions	Hot water	Water	Water	AcCOOH	Water, mix alcohol-water (1:1)	Hot and cold	Water	Hot water all,
Non-solvents	N- methyl morpholine N-oxide , LiCl/DMF Water and organic solvents	monohydric alcohols, ketones	cold water or alcohol	Organic solvents	Organic solvents	Water, organic solvents	Organic solvents	Water , brine	Organic solvents	Water (λ), milk(λ), hot milk (K, I)
Mol. Wt (KDa)	570	1-2000	200-3000	50-8000	250-650	3.8-20	5-20000	2000-50000	5-5000	100- 600
Applicaations	Paper	Anti thrombotic	Filler, sizing, binder, food additive, paper	Thickener, stabilizer, emulsifier	Textile as starch, sizing agent, adhesives, thickener	Agriculture, water treatment, preservative, cosmetics	Cushion and lubricant in joints, healing wounds, moisturiser	Thickening, Stabilising and binding agent, pseudoplastic	**Superior to HPMC** films in food Packaging, coating, binder, flocculant	Weight loss, prevent ice crystalisation, thickner, stabiliser
Source	Wood pulp, cotton	sucrose by certain lactic-acid bacteria	All green plants	endosperm of the seed of guar plant, *Cyamopsis tetragonaloba*	plant Tamarindus Indica	Exoskeleton crusta cean(crab , shrimp)	Synovial fluid, Skin, cartilage	fermentation of glucose, sucrose, or lactose by	aerobically by growing a yeast like fungus *Aureobasidium pullulans*	Seaweeds

In this thesis work, we report on the design and synthesis of SAPs based on CMG and HPG and compared the properties with a commercial synthetic SAP based on polyacrylate. The details are given in Chapter V.

1.1.6. Characterization techniques used in this work

1.1.6.1. Rheology

For a perfectly elastic solid material, Hooke's law states that, the stress (σ) is related to the deformation (γ, strain) via a constant, elastic modulus (G), and is given as:

$$\sigma = G\gamma \qquad (1)$$

While for a perfectly viscous fluid, Newton's law states that, shear stress (σ) is related to the deformation (γ, strain) via a constant, viscosity coefficient (η), and is given as:

$$\sigma = \eta\gamma \qquad (2)$$

When a material exhibits both the properties, elastic as well as viscous behavior, the material is called as viscoelastic material. Many of the APs exhibit viscoelastic behavior and can be understood by rheological experiments. The influence of hydrophobic modification on the viscosity of solutions can be studied by viscometry (for dilute solutions) and rheometry (for concentrated solutions). The steady-state experiments such as flow curves give information on zero-shear viscosity; shear thinning/shear thickening behavior of APs.

In dynamic experiments, such as oscillatory shear flow, a sinusoidally varying strain of amplitude, γ_o is applies to the sample, which is explained with the equation:

$$\gamma(t) = \gamma_o \sin(\omega t) \qquad (3)$$

Where γ is the shear strain, γ_o is the amplitude, ω is the frequency of oscillation and *t* is time. When very small amplitude of strain is applied to the material or sample, it is possible to measure the viscoelastic properties of sample without destructing the

networks in sample; hence such a regime of measurement is called a linear viscoelastic regime (LVR). Then the stress generated due to sinusoidal shear will again be sinusoidal and expressed by:

$$\tau(t) = \tau_o \sin(\omega t + \delta) \qquad (4)$$

Where τ_o is the stress amplitude and δ is phase angle. For a perfectly elastic solid, both stress and strain will be in phase ($\delta = 0^o$), while for a perfectly viscous material, stress and strain will be completely out of phase ($\delta = 90^o$). When a viscoelastic material is subjected to sinusoidal oscillatory stress (eq. 5), there exist a phase lag between strain and stress wave, which is defined by a phase angle (δ) and it varies from 0 to 90 °. An oscillating stress and strain response for a viscoelastic material is as shown in **figure 1.7**.

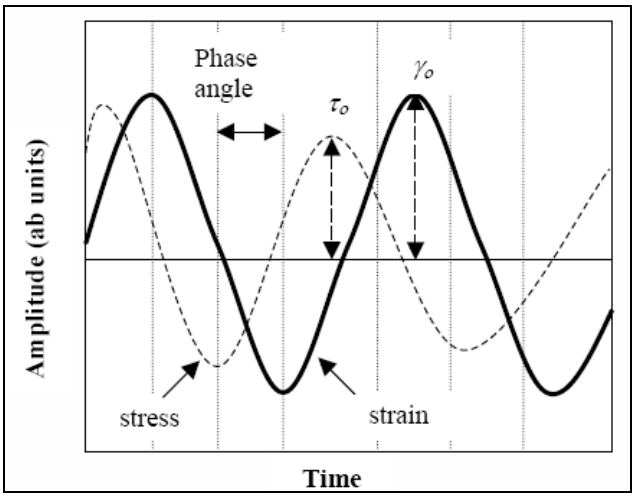

Figure 1.7: *An oscillating strain and stress response of a viscoelastic material*

Eq. 4 for the stress can be rearranged in the following alternative form [75].

$$\tau(t) = \gamma_o[G'(\omega)\sin\omega t + G''(\omega)\cos\omega t] \qquad (5)$$

Where, $$G' = \frac{\tau_0}{\gamma_0}\cos\delta \qquad (6)$$

$$G'' = \frac{\tau_0}{\gamma_0}\sin\delta \qquad (7)$$

Where *G′* is elastic or storage modulus and *G″* is loss modulus. These two moduli are material functions and are usually reported in the literature for characterizing the viscoelastic properties of polymer solutions. In the linear range of deformation, they are

frequency dependent only. But, outside the range of linear viscoelasticity, they depend on both strain and frequency. The complex viscosity (η*) can be defined as the ratio of

complex modulus ($G^* = \sqrt{G'^2 + G''^2}$) to frequency of deformation (ω).

$$\eta^*(\omega) = \frac{G^*}{\omega} = \sqrt{\left(\frac{G'}{\omega}\right)^2 + \left(\frac{G''}{\omega}\right)^2} \qquad (8)$$

An oscillatory response of viscoelastic material, like polymer gel/solution, or covalently

linked networks or elastic solid is shown in **figure 1.8**.

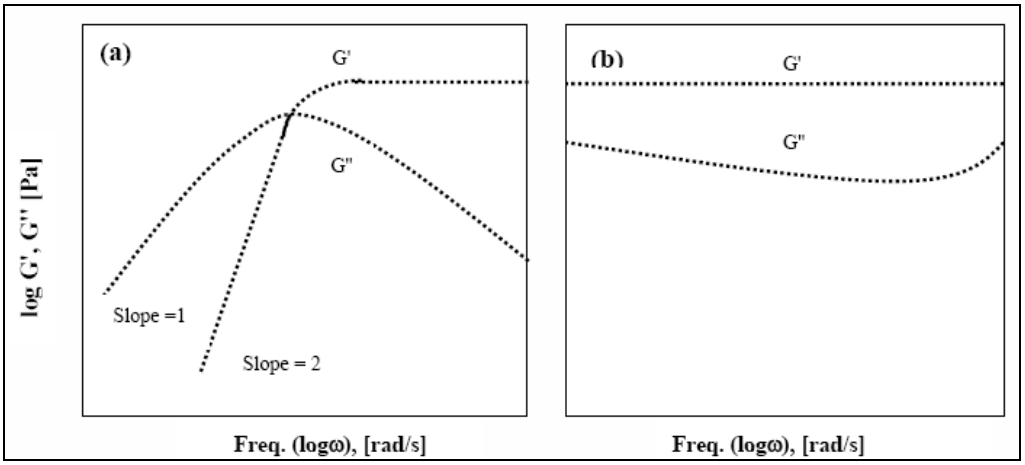

Figure 1.8: *Dynamic oscillatory response of viscoelastic material: (a) polymer gel formed through physical associations and (b) covalently cross-linked network or elastic solid*

From **Figure 1.8 (a),** one can notice two types of behaviors: in the high frequency region, an elastic behavior is observed for a short interval of time with almost

constant value of storage modulus, which corresponds to a plateau region. A frequency at which both moduli are equal [G' (ω) = G" (ω)] is referred to as a characteristic frequency and the reciprocal of this frequency corresponds to the relaxation time of the temporary polymer network. The relaxation time depends on concentration and temperature. For a longer interval of time, the flow behavior (i.e. viscous nature) is observed after a crossover frequency. For an elastic solid, only a elastic behavior can be seen for all frequencies (**Figure 1.8(b)).**

Linear viscoelastic properties can be explained by various transient experiments; stress relaxation or strain relaxation, stress growth, anti-thixotropic response and creep measurement. The transient experiments provide information corresponding to a very short time scale. For a wide range of time scale, one usually performs transient and sinusoidal experiments at various temperatures to obtain information related to molecular dynamics of polymer network. Since hydrophobically modified polymers form transient network due to physical associations between the hydrophobic groups, the viscoelastic properties of HMPs can provide valuable information about the nature and the rate of associations and dissociations of hydrophobes.

1.1.6.2. Fluorescence Spectroscopy

The fluorescence technique has been used in the past to study the aggregation behavior or micellar structure of low molecular weight surfactants [97-99]. This technique has been extended to HMPs to study the aggregation properties [73, 100, 101]. Particularly, the aggregation behavior of HEUR polymers has been extensively studied using, both static and dynamic methods.

In fluorescence technique, a probe molecule is used to obtain information on the micro-environment of the probe. The probe molecule can be either used externally in

which it can bind to the polymer through physical association or it can be linked covalently to the polymer chain. Various probe molecules used in fluorescence study are pyrene, pyrene-1-carboxyaldehyde (PcA), 1-pyrene sulfonic acid, Dipyme, 1-methylanthracene etc. Amongst these, pyrene is the most favorable probe molecule used for various fluorescence measurements. Pyrene has several interesting photophysical properties; notably, the long singlet lifetime (200-300 ns), it can readily form "excimer", a dimer formed by ground state and excited molecule through π-π stacking. Furthermore, pyrene acts as its own quencher and its vibronic bands are sensitive to the environment in its vicinity.

A typical steady-state fluorescence emission spectrum of pyrene consists of five vibronic bands (I_1 to I_5). The bands appearing in the range of 360-430 nm, corresponds to monomer and the broad structureless peak at 480 nm, corresponds to the excimer (**Figure 1.9 (a)).**

(a) 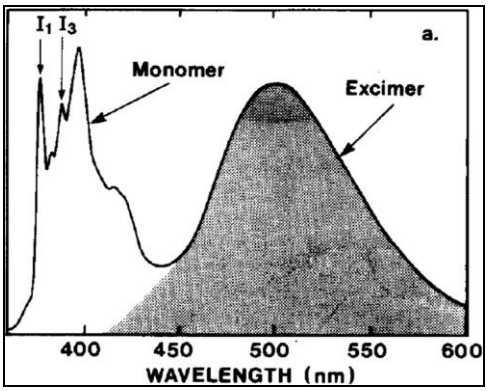

(b) 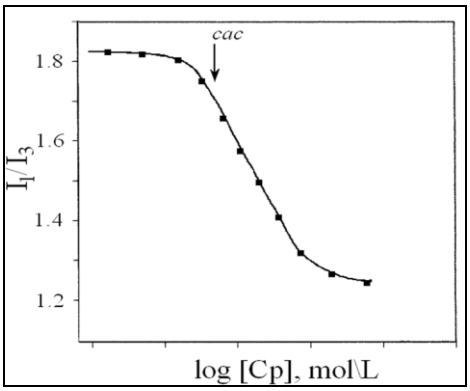

Figure 1.9: *(a) Steady-state fluorescence emission spectra of pyrene and (b) I_1/I_3 – polymer concentration profile for hydrophobically end-capped PEO*

The first vibronic band (I_1) related to the $S_1^{\nu=0} \rightarrow S_0^{\nu=0}$ (0-0) transition is symmetry forbidden. An important parameter drawn from the steady-state fluorescence spectrum, is the ratio of the intensity of first to third (I_3; $S_1^{\nu=0} \rightarrow S_0^{\nu=1}$ transition)

vibronic bands (I_1/I_3), and it is called as a polarity indicator. The ratio, I_1/I_3 depends on the solvent polarity. For example, the value of I_1/I_3 in polar medium such as water is ~ 1.9, while in non-polar medium (cyclohexane) the value decreases to 0.6. In aqueous associative thickeners, the value of I_1/I_3 ~ 1.17 [99, 102]. The I_1/I_3 – polymer concentration profile for hydrophobically end-capped PEO is shown in **figure 1.9(b)**.

1.1.6.3. X-Ray Diffraction (XRD)

X-Ray diffraction (XRD) is one of the most important characterization tools used in solid state chemistry and materials science. It represents a non-destructive analytical technique for identification and quantitative determination of crystalline compounds. The diffraction depends on the crystal structure and on the wavelength. Because the wavelength of X-rays is comparable to the size of atoms, they are ideally suited for probing the structural arrangement of atoms and molecules in a wide range of materials. In our study, we have used thermo-associating polymer to synthesize silver nanoparticles (AgNPs) and XRD technique was used to characterize the crystalline nature of AgNPs.

X-rays are electromagnetic radiation with typical photon energy. The energy of X-ray photon and its wavelength is related by the equation, which is

$$E = hc / \lambda, \qquad (9)$$

where h is Planck's constant [6.62 x 10^{-34} Js] and c is speed of light. X-ray used in diffraction has wavelengths lying approximately in the range 0.5-2.5 Å. X-rays are produced by collision of high speed electrons with a metal target. All X-ray tubes contain two electrodes, an anode (the metal target) and a cathode. The common targets

used in X-ray tube include copper (Cu) and molybdenum (Mo) which emit 8 and 14 KeV with corresponding wavelength 1.54 Å and 0.8 Å respectively. Copper makes a good target since it is an excellent heat conductor with a high melting point. X-rays primarily interact with electrons in atoms. If the atoms are arranged in a periodic fashion, as in crystals, the diffracted waves will consist of sharp interference maxima (peaks) with the same symmetry as in the distribution of atoms and hence this diffraction pattern allows to deduce the distribution of atoms in a material. XRD spectrum is usually obtained by measuring the diffracted intensity as a function of diffracted angles 2θ (angle between incident and diffracted beams) and orientation of specimen. The peaks in X-ray diffraction pattern are directly related to the atomic distance by Bragg's law.

$$n\lambda = 2d\sin\theta \qquad (10)$$

where, 'λ' is wavelength of X-rays and 'd' is d-spacing between atomic planes (interplaner distance) in the crystal, 'q' is the scattering angle and 'n' is an integral representing the order of diffraction peaks.

Bragg's equation can be utilized for the surface analysis by using X-rays of known wavelength and measuring theta, one can determine the d-spacing of various planes in a crystal.

1.1.6.4. X-ray Photoelectron Spectroscopy (XPS)

XPS is a surface sensitive technique which analyses the electronic structure, atomic compositions in the top (~50Å) surface. Each atom in the surface has core electrons with the distinct binding energy, which helps in the identification of all elements by XPS. Binding energy (BE) is a direct measure of the energy required to remove the electrons concerned from its initial state to vacuum level. Alternatively, it may be

called ionization energy also, which is nothing but the minimum energy required to remove an electron from a given orbital. Since the BE is a characteristic property of atoms and ions, XPS provides the direct information of chemical analysis such as, oxidation states and surface concentrations and hence also known as electron spectroscopy for chemical analysis (ESCA).

The principle of this technique is based on the photoelectric effect. When the X- ray beam bombards on the sample, the photon (energy, hn where, h = Planck's constant [6.62 X 10-34 Js] and ν = frequency [Hz]) is absorbed by an atom in a molecule or solid which leads to emission of electron from any orbital, provided the incident photon energy is higher than the binding energy of electron in that particular orbital. The emitted electrons with some kinetic energy are referred to as photoelectrons. The efficient ionization creates a hole in core shell. The hole near to nucleus is in a very unstable state. So, this hole is filled by the transition of electron from an outer level (L_1) and releases energy in the form of a photon, which is equal to the energy difference between E_K and E_{L1}. The above photon of energy ($h\nu = E_K - E_{L1}$) is known as X-ray fluorescence. Alternatively, this energy can be utilized for the ejection of second electron known as Auger electron and the process is known as Auger electron emission. In Auger process, the emitted energy is involved in ejecting another electron, whose binding energy is lower than the available energy from the relaxation process. These low energy Auger electrons can escape only from the first few molecular layers and hence more surface sensitive than photoemission. Also since the fluorescence yield of K shell is small, the KLL Auger transitions are used to locate and identify elements on the surface. Auger emission is normally indicated such as KL_1L_2. KLL indicates the photoelectron emission (and hence a hole) from K, electron

cascade from L_1-level (to K-level) and the level (L_2) from Auger electron got emitted. Such notations are used for Auger transitions.

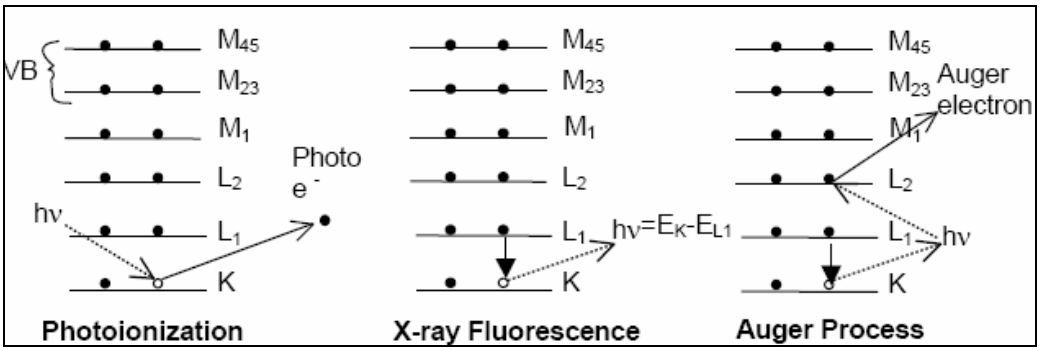

Figure 1.10: *Comparison between Photoionization, X-ray Fluoresecence and Auger process*

Figure 1.10 shows the comparison between processes such as photoionization, X-ray fluorescence and Auger process.

Although X-rays penetrates to a depth of several micrometers, the ejected electrons generally come from the first few nanometers of any material surface. Electron emitted from the bulk loses its energy in collision and does not reach detector or at the most contribute to background. Thus, the surface sensitivity is not dependent on the X-ray penetration depth but on the photoelectrons escape depth without losing energy. The binding energy of the photoelectrons can be calculated by Einstein relationship

$$E_b = h\nu - E_k - \Phi \qquad (11)$$

Where E_k is the kinetic energy of photoelectron, E_b is a binding energy of the photoelectron; F is a work function of the spectrometer.

The peaks observed in the XPS are of three basic types: Peaks due to photoemission from core level, valence level and peaks due to X-ray excited Auger process. In case of polymers, valence band reveal structural information, which is unobtainable from the core level studies. Valence levels are occupied by electrons of low binding energy, which are involved in delocalized or bonding orbitals.

The peak area with appropriate sensitivity factors can be used to determine the surface composition of the materials.

$$\frac{N_A}{N_B} = \frac{I_A}{I_B}\sqrt{KE_A / KE_B}\,\frac{\sigma_B}{\sigma_A} \qquad (12)$$

Where, N is number of atom, I is intensity, s is photo-ionization cross-section and KE is kinetic energy of the photoelectron.

On samples with poor conducting characteristics, like polymers, during photoionization process, a positive charge zone occurs and the intensity of this zone depends on the conducting nature of the material. As a result of the positive potential around the material, the kinetic energy of photoelectrons is reduced. Consequently, this surface charging results in the shift of all XPS peaks to higher binding energies. Therefore, the calibration is necessary and the binding energy has to be calibrated with

internal or external reference like adventitious carbon on any sample or depositing a thin layer of metal on the surface. In some cases, surface charging can be neutralized by using a low energy electron flood gun with appropriate energy. BE is very sensitive to the oxidation state and the chemical environment of the electron. Therefore, it shows chemical shift up to 10 eV when atom is linked to different species.

Consequently, this can be used to determine the chemical environment of the element. Change in binding energy is normally attributed to change in the oxidation state, effective charge as well as the bonding characteristics between atoms. Same elements with different environment give rise to different measurable binding energy. The chemical shift effect for most of the elements is well-studied and reported in the literature.

The X-ray instruments consist of X-ray source, an energy analyzer for emitted photoelectrons and a detector in an ultra-high vacuum chamber. Al Ka (1486.6eV /1 eV width) or Mg Ka (1253.6 ev energy/0.7 eV width) are generally used in soft x-ray sources. High vacuum is normally attained with a combination of several vacuum pumps. Generally, concentric hemispherical analyzer has been explored. Finally the image detector detects the spectra due to photoelectrons.

1.1.6.5. Surface Enhanced Raman Spectroscopy (SERS)

Raman Spectroscopy (RS) is a light scattering technique, and can be thought of in its simplest form as a process where a photon of light interacts with a sample to produce scattered radiation of different wavelengths. RS has become an important analytical and research tool and useful for chemical identification, characterization of molecular structures, effects of bonding, environment and stress on a sample, it is widely used in the analysis of pharmaceuticals, forensic science materials, polymers, thin films, semiconductors and even for the analysis of fullerene structures and carbon nanomaterials.

Surface Enhanced Raman Spectroscopy (SERS) is a RS technique that provides greatly enhanced Raman signal. The principle of the Raman spectroscopy is relatively simple.

The Raman phenomenon is a consequence of sample illumination with a monochromatic photon beam (laser), most of which are absorbed, reflected, or transmitted by the sample. However, a small fraction of photons interacts with the sample. During this interaction, some energy is transmitted to elementary particles of which materials are constituted (electrons, ions etc.). This causes their transition from ground energy levels to ‘virtual’ excited states. These excited states are highly

unstable and particles decay instantaneously to the ground state by one of the following three different processes: Rayleigh scattering: the emission of a photon of the same energy allows the molecule to relax to its ground vibrational state (elastic scattering). Rayleigh scattering, therefore, bears no information on vibrational energy levels of the sample. Stokes and anti-Stokes Raman photons (inelastic scattering): emission of a photon with energy either below or above that of Rayleigh photons, thereby generating a set of frequency-shifted 'Raman' photons. The energy differences of the Stokes and anti-Stokes Raman photons with respect to the excitation energy give information about molecular vibrational levels.

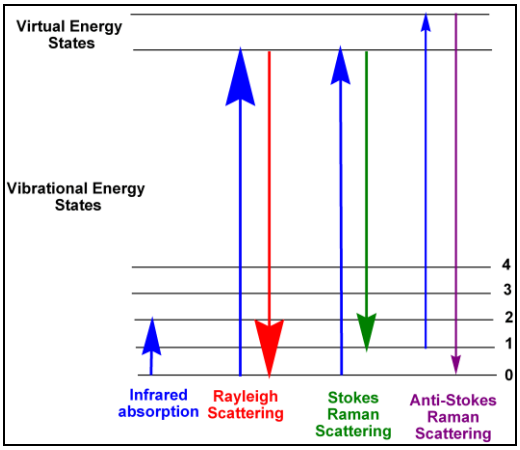

Figure 1.11: *Energy level diagram showing the states involved in Raman signal*

These photons are collected by a detector and transformed to electrical signals and finally to the corresponding Raman spectrum. Usually, Stokes bands which are more intense than anti-stokes bands are called "Raman spectrum" of the sample. The Rayleigh band is filtered out before the detector.

Raman spectroscopy, discovery by C.V. Raman in the 1920s, remained without interest for decades due to the lack of an efficient monochromatic source and appropriate detectors. Raman spectroscopy was born again with the invention and availability of lasers and CCD detectors.

One of the main uses is the characterization of the chemical composition of a material. Indeed, energies of vibration are characteristic not only of materials, but also of their crystal structure in the case of the solids.

1.2. Summary

This introductory Chapter-I gives a comprehensive review of the literature on Associating Polymers (APs) covering their genesis, types of APs, synthetic methods, rheological properties, mechanism of association and applications in various areas. Rheological behavior of different types of APs namely HASE, HEUR and amphiphilic polymers is discussed. The emphasis is given on thermo-associating polymers based on polysaccharides. Background on Superabsorbent Polymers (SAPs) and scope for developing SAPs based on polysaccharides is demonstrated.

The characterization techniques such as Rheology, Fluorescence spectroscopy, XRD, XPS, Raman Spectroscopy used in this work have been briefly described. Relevant references are given at the end of the chapter.

1.3. References

1. Alexandridis, P., Amphiphilic copolymers and their applications. *Current Opinion in Colloid & Interface Science* **1996,** 1, (4), 490-501.

2. Glass, J. E., *Polymers in aqueous media: performance through association*. American Chemical Society: 223, **1989**.

3. Winnik, M. A.; Yekta, A., Associative polymers in aqueous solution. *Current opinion in colloid & interface science* **1997,** 2, (4), 424-436.

4. Glass, J. E., Water Soluble Polymers: Beauty with performance. *Advances in chemistry series: 213*, American Chemical Society, **1986**.

5. Shalaby, S. W.; McCormick, C. L.; Butler, G. B., *Water-soluble polymers: synthesis, solution properties, and applications*. American Chemical Society: 467, **1991**.

6. Stahl, G. A.; Schulz, D. N., *Water-soluble polymers for petroleum recovery*. Springer: **1988**.

7. Strauss, U. P.; Jackson, E. G., Polysoaps. I. Viscosity and solubilization studies on an n-dodecyl bromide addition compound of poly-2-vinylpyridine. *Journal of Polymer Science* **1951,** 6, (5), 649-659.

8. Strauss, U. P.; Vesnaver, G., Optical probes in polyelectrolyte studies. I. Acid-base equilibriums of dansylated copolymers of maleic anhydride and alkyl vinyl ethers. *The Journal of Physical Chemistry* **1975,** 79, (15), 1558-1561.

9. Schulz, D. N.; Bock, J.; Valint Jr, P. L., Synthesis and characterization of hydrophobically associating water-soluble polymers. In *Macromolecular complexes in chemistry and biology*, Springer: **1994**; 3-13.

10. Hester, R. D.; Squire, D. R., Rheology of waterborne coatings. *Journal of Coatings Technology* **1997,** 69, (864), 109-114.

11. Landoll, L. M., Nonionic polymer surfactants. *Journal of Polymer Science: Polymer Chemistry Edition* **1982,** 20, (2), 443-455.

12. Nystroem, B.; Thuresson, K.; Lindman, B., Rheological and dynamic light-scattering studies on aqueous solutions of a hydrophobically modified nonionic cellulose ether and its unmodified analog. *Langmuir* **1995,** 11, (6), 1994-2002.

13. Rosén, O.; Sjöström, J.; Piculell, L., Responsive polymer gels based on hydrophobically modified cellulose ethers and their interactions with ionic surfactants. *Langmuir* **1998,** 14, (20), 5795-5801.

14. Aubry, T.; Moan, M., Rheological behavior of a hydrophobically associating water soluble polymer. *Journal of rheology* **1994,** 38, (6), 1681-1692.

15. Kjøniksen, A.-L.; Nyström, B.; Lindman, B., Dynamic viscoelasticity of gelling and nongelling aqueous mixtures of ethyl (hydroxyethyl) cellulose and an ionic surfactant. *Macromolecules* **1998,** 31, (6), 1852-1858.

16. Thuresson, K.; Nilsson, S.; Lindman, B. R., Influence of cosolutes on phase behavior and viscosity of a nonionic cellulose ether. The effect of hydrophobic modification. *Langmuir* **1996,** 12, (10), 2412-2417.

17. Thuresson, K.; Nilsson, S.; Lindman, B. r., Effect of hydrophobic modification on phase behavior and rheology in mixtures of oppositely charged polyelectrolytes. *Langmuir* **1996,** 12, (2), 530-537.

18. Fernando, R. H.; Glass, J. E., The influence of associative thickeners on coatings performance. II: Heterodispersed, hydroxyethyl cellulose-stabilized vinyl-acrylic latex studies. *Journal of the Oil and Colour Chemists' Association* **1984,** 67, (11), 279-283.

19. Glass, J. E.; Fernando, R. H.; Egland-Jongewaard, S. K.; Brown, R. G., The influence of associative thickeners on coatings performance. I: Small particle, all-

acrylic latex studies. *Journal of the Oil and Colour Chemists' Association* **1984,** 67, (10), 256-261.

20. Karunasena, A.; Brown, G.; Glass, J. E., Hydrophobically modified ethoxylated urethane architecture. Importance for aqueous-and dispersed-phase properties. *Adv. Chem. Ser* **1989,** 223, 495-525.

21. Tam, K. C.; Jenkins, R. D.; Winnik, M. A.; Bassett, D. R., A structural model of hydrophobically modified urethane-ethoxylate (HEUR) associative polymers in shear flows. *Macromolecules* **1998,** 31, (13), 4149-4159.

22. Annable, T.; Buscall, R.; Ettelaie, R.; Whittlestone, D., The rheology of solutions of associating polymers: Comparison of experimental behavior with transient network theory. *Journal of rheology* **1993,** 37, (4), 695-726.

23. Kenneth L. Hoy, R. C. H. Polymers with hydrophobe bunches. USP 4426485, **1984**.

24. William D. Emmons, T. E. S. Polyurethane thickeners in latex compositions. USP 4079028, **1978**.

25. Kramer, M. C.; Steger, J. R.; Hu, Y.; McCormick, C. L., Water-soluble copolymers. 65. Environmentally responsive associations probed by nonradiative energy transfer studies of naphthalene and pyrene-labeled poly (acrylamide-co-sodium 11-(acrylamido) undecanoate). *Macromolecules* **1996,** 29, (6), 1992-1997.

26. Selb, J.; Biggs, S.; Renoux, D.; Candau, F., Hydrophobic and electrostatic interactions in water-soluble associating copolymers. *ACS Advances in Chemistry Series* **1996,** 248, 251-278.

27. Hogen-Esch, T. E.; Amis, E., Hydrophobic association in perfluorocarbon-containing water-soluble polymers. *Trends in polymer science* **1995,** 3, (3), 98-104.

28. Xie, X.; Hogen-Esch, T. E., Copolymers of N, N-Dimethylacrylamide and 2-(N-ethylperfluorooctanesulfonamido) ethyl Acrylate in Aqueous Media and in Bulk. Synthesis and Properties. *Macromolecules* **1996,** 29, (5), 1734-1745.

29. Biggs, S.; Selb, J.; Candau, F., Copolymers of acrylamideN-alkylacrylamide in aqueous solution: the effects of hydrolysis on hydrophobic interactions. *Polymer* **1993,** 34, (3), 580-591.

30. Bock, J.; Valint, P. L.; Pace, S. J.; Siano, D. B.; Shulz, D. N.; Turner, S. R., *Hydrophobically associating polymers*. Plenum Press. NY: **1988**.

31. Hill, A.; Candau, F.; Selb, J., Properties of hydrophobically associating polyacrylamides: influence of the method of synthesis. *Macromolecules* **1993,** 26, (17), 4521-4532.

32. McCormick, C.L; Johnson, C.B., *Polym. Mater. Sci. Eng.* **1986,** 55. 366.

33. McCormick, C. L.; Nonaka, T.; Johnson, C. B., Water-soluble copolymers: 27. Synthesis and aqueous solution behaviour of associative acrylamideN-alkylacrylamide copolymers. *Polymer* **1988,** 29, (4), 731-739.

34. Wanka, G.; Hoffmann, H.; Ulbricht, W., Phase diagrams and aggregation behavior of poly (oxyethylene)-poly (oxypropylene)-poly (oxyethylene) triblock copolymers in aqueous solutions. *Macromolecules* **1994,** 27, (15), 4145-4159.

35. Wu, G.; Zhou, Z.; Chu, B., Water-induced micelle formation of block copoly (oxyethylene-oxypropylene-oxyethylene) in o-xylene. *Macromolecules* **1993,** 26, (8), 2117-2125.

36. Magny, B.; Iliopoulos, I.; Audebert, R., Aggregation of hydrophobically modified polyelectrolytes in dilute solutions: ionic strength effects. *Macromolecular Complexes in Chemistry and Biology. Berlin: Springer Verlag* **1994**, 51-62.

37. Petit, F.; Iliopoulos, I.; Audebert, R., Hydrophobically modified polyelectrolytes with perfluorinated or hydrogenated side alkyl chains. Comparison of the associating behavior. *Journal de chimie physique* **1996,** 93, (5), 887-898.

38. McConnell, G. A.; Gast, A. P.; Huang, J. S.; Smith, S. D., Disorder-order transitions in soft sphere polymer micelles. *Physical review letters* **1993,** 71, (13), 2102-2105.

39. Alexandridis, P.; Lindman, B., *Amphiphilic block copolymers: self-assembly and applications*. Elsevier Science: **2000**.

40. Emmons; William D. (Huntingdon Valley, P., Stevens; Travis E. (Ambler, PA) Acrylamide copolymer thickener for aqueous systems 4,395,524, July 26,**1983**.

41. Evani; Syamalarao (Midland, M. Water-dispersible hydrophobic thickening agent. USP 4,432,881, February 21, **1984**.

42. Turner; S. Richard (Rochester, N., Siano; Donald B. (Fanwood, NJ), Bock; Jan (Bridgewater, NJ) Acrylamide-alkylacrylamide copolymers. USP 4,520,182, May 28, **1985**.

43. Turner; S. Richard (Rochester, N., Siano; Donald B. (Fanwood, NJ), Bock; Jan (Bridgewater, NJ) Micellar process for the production of acrylamide-alkyl acrylamide copolymers. USP 4,528,348, July 9, **1985**.

44. Turner; S. Richard (Rochester, N., Siano; Donald B. (Fanwood, NJ), Bock; Jan (Bridgewater, NJ) Microemulsion process for producing acrylamide-alkyl acrylamide copolymers 4,521,580, June 4, 1985, **1985**.

45. Bock J, S. D., Valint PL Jr, Pace SJ *Polym Mater Sci Eng* **1987,** 57, 487-491.

46. Lacík, I.; Selb, J.; Candau, F., Compositional heterogeneity effects in hydrophobically associating water-soluble polymers prepared by micellar copolymerization. *Polymer* **1995,** 36, (16), 3197-3211.

47. Volpert, E.; Selb, J.; Candau, F. o., Influence of the Hydrophobe Structure on Composition, Microstructure, and Rheology in Associating Polyacrylamides Prepared by Micellar Copolymerization. *Macromolecules* **1996,** 29, (5), 1452-1463.

48. Ezzell, S. A.; Hoyle, C. E.; Creed, D.; McCormick, C. L., Water-soluble copolymers. 40. Photophysical studies of the solution behavior of associative pyrenesulfonamide-labeled polyacrylamides. *Macromolecules* **1992,** 25, (7), 1887-1895.

49. Ezzell, S. A.; McCormick, C. L., Water-soluble copolymers. 39. Synthesis and solution properties of associative acrylamido copolymers with pyrenesulfonamide fluorescence labels. *Macromolecules* **1992,** 25, (7), 1881-1886.

50. Peer William, J., Polymerization of Hydrophobically Modified Polyacrylamide. In *Polymers in Aqueous Media*, American Chemical Society: **1989**; 223, 381-397.

51. Peiffer, D. G., Hydrophobically associating polymers and their interactions with rod-like micelles. *Polymer* **1990,** 31, (12), 2353-2360.

52. McCormick, C. L.; Middleton, J. C.; Cummins, D. F., Water-soluble copolymers. 37. Synthesis and characterization of responsive hydrophobically modified polyelectrolytes. *Macromolecules* **1992,** 25, (4), 1201-1206.

53. Schulz, D. N.; Kaladas, J. J.; Maurer, J. J.; Bock, J.; Pace, S. J.; Schulz, W. W., Copolymers of acrylamide and surfactant macromonomers: synthesis and solution properties. *Polymer* **1987,** 28, (12), 2110-2115.

54. Branham, K. D.; Davis, D. L.; Middleton, J. C.; McCormick, C. L., Water-soluble polymers: 59. Investigation of the effects of polymer microstructure on the associative behaviour of amphiphilic terpolymers of acrylamide, acrylic acid and *N*-[(4-decyl) phenyl] acrylamide. *Polymer* **1994,** 35, (20), 4429-4436.

55. Schulz; Donald N. (Annandale, N., Maurer; John J. (New Providence, NJ), Bock; Jan (Bridgewater, NJ) Process for the formation of novel acrylamide acrylate copolymers. USP 4,463,151, July 31, 1984, **1984**.

56. Schulz; Donald N. (Annandale, N., Maurer; John J. (New Providence, NJ), Bock; Jan (Bridgewater, NJ) Acrylamide acrylate copolymers. 4,463,152, July 31, **1984**.

57. Scully; John W. (Raynham, M. Apparatus for forming, filling and depositing filled bags into cartons. *USP 4,571,926*, February 25, **1986**.

58. Strauss, U. P.; Gershfeld, N. L., The Transition from Typical Polyelectrolyte to Polysoap. I. Viscosity and Solubilization Studies on Copolymers of 4-Vinyl-N-ethylpyridinium Bromide and 4-Vinyl-N-dodecylpyridinium Bromide. *The Journal of Physical Chemistry* **1954,** 58, (9), 747-753.

59. Strauss, U. P.; Gershfeld, N. L.; Crook, E. H., The Transition from Typical Polyelectrolyte to Polysoap. II. Viscosity Studies of Poly-4-vinylpyridine Derivatives in Aqueous KBr Solutions. *The Journal of Physical Chemistry* **1956,** 60, (5), 577-584.

60. Perrin, P.; Lafuma, F. o., Low hydrophobically modified poly (acrylic acid) stabilizing macroemulsions: Relationship between copolymer structure and emulsions properties. *Journal of colloid and interface science* **1998,** 197, (2), 317-326.

61. Shedge, A. S.; Lele, A. K.; Wadgaonkar, P. P.; Hourdet, D.; Perrin, P.; Chassenieux, C.; Badiger, M. V., Hydrophobically Modified Poly (acrylic acid) Using 3-Pentadecylcyclohexylamine: Synthesis and Rheology. *Macromolecular Chemistry and Physics* **2005,** 206, (4), 464-472.

62. Deguchi, S.; Lindman, B., Novel approach for the synthesis of hydrophobe modified polyacrylamide. Direct N-alkylation of polyacrylamide in dimethyl sulfoxide. *Polymer* **1999,** 40, (25), 7163-7165.

63. Feng, Y.; Billon, L.; Grassl, B.; Khoukh, A.; FranÃ§ois, J., Hydrophobically associating polyacrylamides and their partially hydrolyzed derivatives prepared by post-modification. 1. Synthesis and characterization. *Polymer* **2002,** 43, (7), 2055-2064.

64. Bromberg, L., Properties of aqueous solutions and gels of poly (ethylene oxide)-b-poly (propylene oxide)-b-poly (ethylene oxide)-g-poly (acrylic acid). *The Journal of Physical Chemistry B* **1998,** 102, (52), 10736-10744.

65. Freitas, R. F. S.; Cussler, E. L., Temperature sensitive gels as extraction solvents. *Chemical Engineering Science* **1987,** 42, (1), 97-103.

66. Hoy; Kenneth L. (St. Albans, W., Hoy; Richard C. (South Charleston, WV) Polymers with hydrophobe bunches. USP 4,426,485, January 17, **1984**.

67. Landoll, L. M. Modified nonionic cellulose ethers. *USP 4,228,277*, **1980**.

68. Ye, L.; Li, Q.; Huang, R., Study on the rheological behavior of the hydrophobically modified hydroxyethyl cellulose with 1, 2-epoxyhexadecane. *Journal of applied polymer science* **2006,** 101, (5), 2953-2959.

69. Cathbras, N.; Collet, A.; Viguier, M.; Berret, J.-F. o., Synthesis and linear viscoelasticity of fluorinated hydrophobically modified ethoxylated urethanes (F-HEUR). *Macromolecules* **1998,** 31, (4), 1305-1311.

70. Emmons; William D. (Huntingdon Valley, P., Stevens; Travis E. (Ambler, PA) Polyurethane thickeners in latex compositions. *USP 4,079,028*, March 14, **1978**.

71. Jenkins, R. D. *The fundamental thickening mechanism of associative polymers in latex systems: A rheological study*. Lehigh University, Ph.D. Dissertation, **1990**.

72. Wang, Y.; Winnik, M. A., Onset of aggregation for water-soluble polymeric associative thickeners: a fluorescence study. *Langmuir* **1990,** 6, (9), 1437-1439.

73. Yekta, A.; Xu, B.; Duhamel, J.; Adiwidjaja, H.; Winnik, M. A., Fluorescence studies of associating polymers in water: Determination of the chain end aggregation number and a model for the association process. *Macromolecules* **1995,** 28, (4), 956-966.

74. Brown, R. G. Synthesis and characterization of HEUR polymers. North Dakota State University, Ph.D. Dissertation, **199**1.

75. Larson, R. G., *The structure and rheology of complex fluids*. Oxford university press, **1999**, Vol. 1.

76. Gelman, R. A., Characterization of carboxymethylcellulose: Distribution of substituent groups along the chain. *Journal of applied polymer science* **1982,** 27, (8), 2957-2964.

77. Wirick, M. G.; Elliott, J. H., A one point intrinsic viscosity method for hydroxyethylcellulose, hydroxypropylcellulose, and sodium carboxymethylcellulose. *Journal of Applied Polymer Science* **1973,** 17, (9), 2867-2875.

78. Gonzaez Coronel, V. J.; Jimenez-Regalado, E. J., Rheological properties of three different microstructures of water-soluble polymers prepared by solution polymerization. *Polymer bulletin* **2011**, 67, (2), 251-262.

79. English, R. J.; Raghavan, S. R.; Jenkins, R. D.; Khan, S. A., Associative polymers bearing n-alkyl hydrophobes: Rheological evidence for microgel-like behavior. *Journal of rheology* **1999,** 43, (5), 1175-1194.

80. Fonnum, G.; Bakke, J.; Hansen, F. K., Associative thickeners. Part I: Synthesis, rheology and aggregation behavior. *Colloid & Polymer Science* **1993,** 271, (4), 380-389.

81. Hulden, M., Hydrophobically modified urethane ethoxylate (HEUR) associative thickeners 1. Rheology of aqueous solutions and interactions with

surfactants. *Colloids and Surfaces A: Physicochemical and Engineering Aspects* **1994,** 82, (3), 263-277.

82. Jenkins, R. D., CA Silebi, and MS El-Aasser,, Steady shear and linear viscoelasticity material properties of associative thickener solutions. *Polym. Mater. Sci. Eng* **1989,** 61, 629-633.

83. Annable, T.; Buscall, R.; Ettelaie, R., Network formation and its consequences for the physical behaviour of associating polymers in solution. *Colloids and Surfaces A: Physicochemical and Engineering Aspects* **1996,** 112, (2-3), 97-116.

84. Duhamel, J.; Yekta, A.; Hu, Y. Z.; Winnik, M. A., Evidence for intramolecular hydrophobic association in aqueous solution for pyrene-end-capped poly (ethylene oxide). *Macromolecules* **1992,** 25, (25), 7024-7030.

85. Yekta, A.; Duhamel, J.; Adiwidjaja, H.; Brochard, P.; Winnik, M. A., Association structure of telechelic associative thickeners in water. *Langmuir* **1993,** 9, (4), 881-883.

86. Ng, W. K.; Tam, K. C.; Jenkins, R. D., Lifetime and network relaxation time of a HEUR-C20 associative polymer system. *Journal of rheology* **2000,** 44, 137-156.

87. Ma, S. X.; Cooper, S. L., Shear thickening in aqueous solutions of hydrocarbon end-capped poly (ethylene oxide). *Macromolecules* **2001,** 34, (10), 3294-3301.

88. Tanaka, F.; Edwards, S. F., Viscoelastic properties of physically crosslinked networks: Part 3. Time-dependent phenomena. *Journal of non-newtonian fluid mechanics* **1992,** 43, (2), 289-309.

89. Tanaka, F.; Edwards, S. F., Viscoelastic properties of physically crosslinked networks: Part 1. Non-linear stationary viscoelasticity. *Journal of Non-Newtonian Fluid Mechanics* **1992,** 43, (2-3), 247-271.

90. Tanaka, F.; Edwards, S. F., Viscoelastic properties of physically crosslinked networks: Part 2. Dynamic mechanical moduli. *Journal of Non-Newtonian Fluid Mechanics* **1992,** 43, (2-3), 273-288.

91. Green, M. S.; Tobolsky, A. V., A new approach to the theory of relaxing polymeric media. *The Journal of Chemical Physics* **1946,** 14, 80-92.

92. Roy, D.; Brooks, W. L. A.; Sumerlin, B. S., New directions in thermoresponsive polymers. *Chemical Society Reviews* **2013,** **DOI:** 10.1039/C3CS35499G.

93. Seuring, J.; Agarwal, S., Polymers with Upper Critical Solution Temperature in Aqueous Solution. *Macromolecular Rapid Communications* **2012**, 33(22), 1898-1920

94. Ward, M. A.; Georgiou, T. K., Thermoresponsive polymers for biomedical applications. *Polymers* **2011**, 3, (3), 1215-1242.

95. Park, K. M.; Lee, S. Y.; Joung, Y. K.; Na, J. S.; Lee, M. C.; Park, K. D., Thermosensitive chitosan Pluronic hydrogel as an injectable cell delivery carrier for cartilage regeneration. *Acta biomaterialia* **2009,** 5, (6), 1956-1965.

96. Nguyen, M. K.; Lee, D. S., Injectable biodegradable hydrogels. *Macromolecular bioscience* **2010,** 10, (6), 563-579.

97. Hautala, R. R.; Schore, N. E.; Turro, N. J., Novel fluorescent probe. Use of time-correlated fluorescence to explore the properties of micelle-forming detergent. *Journal of the American Chemical Society* **1973,** 95, (17), 5508-5514.

98. Schore, N. E.; Turro, N. J., Novel and versatile fluorescence probe for the structure of micelles. 11-[3-Hexyl-1-indolyl] undecyltrimethylammonium bromide. *Journal of the American Chemical Society* **1974,** 96, (1), 306-308.

99. Turro, N. J.; Grätzel, M.; Braun, A. M., Photophysical and Photochemical Processes in Micellar Systems. *Angewandte Chemie International Edition in English* **1980,** 19, (9), 675-696.

100. Vorobyova, O.; Yekta, A.; Winnik, M. A.; Lau, W., Fluorescent probe studies of the association in an aqueous solution of a hydrophobically modified poly (ethylene oxide). *Macromolecules* **1998,** 31, (25), 8998-9007.

101. Yekta, A.; Duhamel, J.; Brochard, P.; Adiwidjaja, H.; Winnik, M. A., A fluorescent probe study of micelle-like cluster formation in aqueous solutions of hydrophobically modified poly (ethylene oxide). *Macromolecules* **1993,** 26, (8), 1829-1836.

102. Dong, D. C.; Winnik, M. A., The Py scale of solvent polarities. *Canadian journal of chemistry* **1984,** 62, (11), 2560-2565.

Scope and Objectives

Chapter - II

Associating Polymers (APs) or hydrophobically modified polymers (HMPs) have attracted increasing attention lately because of their unique rheological properties such as super–viscosifying, shear thickening / shear thinning, strain- hardening etc [1,2]. They find a large number of applications in various technological areas such as, thickeners for cosmetic lotions, creams, pharmaceuticals, paints, oil-recovery, paper, textile and other industrial products [3, 4]. APs are typically made up of water-soluble polymer backbone bearing a small number of hydrophobic stickers either dispersed along the polymer chain (grafts) or specifically located at the ends of the polymer chain (telechelic). Their thickening ability in aqueous solution arises through reversible intermolecular associations caused by the unfavorable interactions between water molecules and hydrophobic groups/ stickers [5, 6]. The synthesis of graft and telechelic APs, together with their self-assembling properties in semi dilute aqueous solutions, have been widely reported during the 90's and have found industrial developments with Hydrophobic Ethoxylated Urethane (HEUR) [7] and Hydrophobically modified Alkali Swellable Emulsions (HASE) [8].

More recently, the introduction of responsive stickers in macromolecular chain architecture has opened up the way of reversible associations and promoted the formation of physical networks using various stimuli such as temperature, pH, ionic-strength, shear stress, light etc [9]. For example, water-soluble polymers with 'stickers' characterized by a Lower Critical Solution Temperature (LCST) in water are able to undergo a sol/gel transition by increasing/decreasing the temperature. They are called as thermo-associating/thermo-thickening/thermo gelling polymers and show promising applications as injectables in controlled release technology.

Amongst the APs, hydrophobically modified polysaccharides are becoming more prominent recently because of their non-toxicity, biocompatibility and biodegradability. The main micro structural characteristic of such polymer systems is their ability to give rise to weak intra and intermolecular interactions in aqueous solutions. Studies on some of the hydrophobically modified polysaccharides such as, hydrophobically modified hydroxyethyl cellulose (HM-EHEC) and hydroxypropyl guar gum (HM-HPG), hydrophobically modified carboxymethyl cellulose (HM-CMC) with 1-2% dodecyl groups have been reported [10].

Polysaccharides are available in a variety of structures with different properties. Since they contain reactive functional groups, they can be easily modified chemically. Furthermore, their high stability and gel forming property lead their applications in food and pharmaceuticals. The commercial production of polysaccharides has expanded steadily over the last 20-30 years. Therefore, there is a great scope for these 'environmentally friendly', renewable resource materials and their practical applications.

Although there are several reports on hydrophobically modified Polysaccharides such as Carboxymethyl Cellulose (CMC), Hydroxyethyl Cellulose (HEC), Dextran, Alginates etc., the polysaccharides namely, Carboxymethyl Guar (CMG) and Carboxymethyl Tamarind (CMT) have not been fully explored in terms of their value addition.

In this thesis, we have worked on the synthesis and rheological properties of graft copolymers based on CMG and CMT backbone bearing thermo-sensitive polymers such as Poly (N-isopropylacrylamide) (PNIPAm) and Polyethylene oxide-Polypropylene oxide (PEO-PPO) (PEPO) as side chains. These thermo-associating

polymers are biodegradable in nature and can have potential applications as injectables in controlled release technology (CRT). They can also be used as thickeners in cosmetics and pharmaceutical formulations.

Highly swelling hydrogels or superabsorbing polymers (SAPs) based on natural polymers such as polysaccharides are in great demand due to their environmentally friendly nature, biodegradable and biocompatible. Therefore, we have worked on the design and development of new SAPs based on CMG and Hydroxypropyl Guar gum (HPG). Different crosslinking agents with reaction mechanism have been investigated along with swelling characterization of hydrogels. Besides the above studies, we also demonstrated the use of CMG-g-PEPO in the synthesis of Silver (Ag) nanoparticles (AgNPs) as an efficient reducing agent and capping agent. Conventional reducing agents such as borohydrides, phosphines have some disadvantages like toxicity and stability of the obtained nanoparticles. The obtained nanoparticles have a layer of polysaccharide encapped with reactive functional groups which can be linked to various APIs. These nanoparticles have been characterized using UV, XRD, TEM, XPS and Raman Spectroscopy. The nanoparticles with API have potential applications in targeted drug delivery and other clinical treatments.

Finally, we have made an attempt to synthesize APs and hydrogels based on Hyaluronic Acid (HA) using "Click Chemistry" approach. At present "Click Chemistry" has attracted major attention because of high specificity, quantitative yields and moderate reaction conditions. The scope and objectives of the thesis work are as follows:

- To design and synthesize new APs based on Guar Gum (GG), Tamarind Kernel Powder (TKP) and their derivatives

- To synthesize new thermo associating polymers based on CMG-g-PNIPAm and CMG-g-PEPO, CMT-g-PEPO which have potential applications as injectables in controlled release technology
- Characterization of thermo-associating polymers by Rheology and Fluorescence Spectroscopy
- To demonstrate the use of above synthesized thermo-associating polymers as a reducing and stabilizing agents for green synthesis of silver nanoparticles and the application of nanoparticles in controlled drug delivery
- To synthesize hydrogels and Superabsorbent polymers using environmentally friendly polysaccharides namely, CMG and HPG
- To understand and correlate the structural attributes of SAPs & hydrogels which influence the swelling behavior and mechanical strength
- To apply “Click chemistry” approach to synthesize Hydrogels

References

1. Glass, J. E., Polymers in aqueous media: performance through association. *Advances in chemistry series: 223*, American Chemical Society, Washington, **1989**.

2. Glass, J. E., Hydrophilic polymers: performance with environmental acceptability *Advances in chemistry series: 248*, American Chemical Society, Washington, **1996**.

3. Taylor, K.; Nasr-El-Din, H. Hydrophobically Associating Polymers for Oil Field Applications, *Canadian International Petroleum Conference, 2007*; **2007**.

4. Tonge, S. R.; Tighe, B. J., Responsive hydrophobically associating polymers: a review of structure and properties. *Advanced drug delivery reviews* **2001,** 53, (1), 109-122.

5. Kumar, S. K.; Douglas, J. F., Gelation in physically associating polymer *Physical Review Letters* **2001,** 87, (18), 188301.

6. Petit-Agnely, F.; Iliopoulos, I., Aggregation mechanism of amphiphilic associating polymers solutions studied by ^{19}F and ^{13}C nuclear magnetic resonance. *The Journal of Physical Chemistry B* **1999,** 103, (23), 4803-4808.

7. Annable, T.; Buscall, R.; Ettelaie, R.; Whittlestone, D., The rheology of solutions of associating polymers: Comparison of experimental behavior with transient network theory. *Journal of rheology* **1993,** 37, (4), 695-726.

8. Seng, W. P.; Tam, K. C.; Jenkins, R. D.; Bassett, D. R., Calorimetric studies of model hydrophobically modified alkali-soluble emulsion polymers with varying spacer chain length in ionic surfactant solutions. *Macromolecules* **2000,** 33, (5), 1727-1733.

9. Stuart, M. A. C.; Huck, W. T. S.; Genzer, J.; Muller, M.; Ober, C.; Stamm, M.; Sukhorukov, G. B.; Szleifer, I.; Tsukruk, V. V.; Urban, M., Emerging applications of stimuli-responsive polymer materials. *Nature materials* **2010,** 9, (2), 101-113.

10. Zhang, L. M., Cellulosic associative thickeners. *Carbohydrate polymers* **2001,** 45, (1), 1-10.

Synthesis and Characterization of Thermo-associating polymers based on Polysaccharides

Chapter - III

3.1. Introduction

Over the past decade, thermo-associating polymers have gained considerable attention and are being widely investigated due to their interesting properties in response to temperature as a stimulus [1, 2]. Contrary to the conventional water-soluble polymers, thermo-associating polymers in aqueous solution exhibit opposite behavior to the Arrhenius law in which their rheological properties increase with increase in temperature. In most cases, the thermo-associating behavior is characterized by the presence of a polymer exhibiting an interesting thermodynamic property of Lower critical solution temperature (LCST) [3]. Therefore, if a polyelectrolyte chain is grafted with small chains of polymer having an LCST, the grafts start to become incompatible with water and the hydrophobic character induces an association which manifests into transient network formation leading to increase in viscosity. Various combinations of synthetic water-soluble polymers and polymers with characteristic LCSTs have been shown to exhibit thermo-associating behavior. For example, poly(N-isopropylacrylamide) [PNIPAm], poly(acrylic acid)-g-poly(ethylene oxide) [PAA-g-PEO] or poly(acrylic acid)-g-poly(N-isopropylacrylamide) [PAA-g-PNIPAm] have been shown to display thermo-associating behavior [4, 5]. The thermo-associating behavior of these polymers can be easily controlled by external parameters such as polymer concentration, nature and amount of added salt, pH and temperature. Nevertheless, the nature of both components (backbone and the polymer with LCST) is expected to play an important role in the macroscopic properties. Hourdet et al.[4] have developed a whole family of thermo-associating polymers by grafting side chains like PEO, PNIPAm, PEPO onto a hydrophilic polymer namely, sodium poly(acrylate) [PAA-Na]. Bokias et al [3], have reported on the synthesis and aqueous

solution properties of thermo-associating graft copolymers based on Carboxymethyl Cellulose [CMC] bearing PNIPAm side chains, CMC-g-PNIPAm.

Besides totally synthetic polymers, polysaccharide based thermo-responsive polymers are attracting increasing attention recently in biomedical applications. Polysaccharides are available in a variety of structure with different properties. Since they contain reactive functional groups, they can be easily modified chemically. Furthermore, their high stability, non-toxicity and biodegradability with gel forming property lead their applications in food and pharmaceuticals. In the recent past, many studies have been devoted to hydrophobically modified polysaccharides.

For example, hydrophobically modified chitosan polymers [3, 5, 6], thermo-responsive graft copolymers of carboxymethyl cellulose (CMC) have been reported in the literature. An interpenetrating networks (IPNs) based on guar gum and poly(N-isopropylacrylamide) PNIPAm, with a major focus on swelling kinetics has been reported [7]. Recently, Zhang et al. [8] have reported on the synthesis and characterization of thermo-sensitive graft copolymer of poly(N-isopropylacrylamide) and carboxymethyl chitosan. Similarly, Shi and Zhang [8, 9] studied the grafting of poly(N-isopropylacrylamide) onto carboxymethyl hydroxypropyl guar (CMHPG). However, it was intriguing to note from their study that, they did not observe the formation of hydrogel in their system but obtained thermo-sensitive polymer solutions. Furthermore, the polymer solutions did not exhibit thermo-thickening behavior as observed by Bokias et al [3] in a similar thermo-associating polymer system. Huh et al.[10] reported on the synthesis and characterization of carboxymethyl dextran and poly(N-isopropylacrylamide-co-N, N-dimethylacrylamide).

Most of the thermo-associating polymers based on synthetic and natural polymers, exhibit either phase separation or decrease in viscosity upon heating. The true

thermothickening (viscosity increase with temperature without undergoing macrophase separation) behavior is observed in a few cases which strongly depends on the balance of hydrophilic / hydrophobic components, concentrations and molecular weight of LCST side chains, pH and presence of salts in aqueous solutions.

Some of the polysaccharides used in the design and synthesis of thermo-associating polymers include Chitosan [8, 11-13], Hyaluronic acid [14], Carboxymethyl Cellulose [3, 15] alginates [15, 16], Pullulan [17-20] and Dextran [10, 15, 21]. However, polysaccharides namely, Guar Gum (GG) and Tamarind Kernel Powder (TKP) are not fully explored in synthesizing thermo-associating polymers based on them. Guar Gum is a water-soluble nonionic polysaccharide extracted from the seeds of Cyanopsis tetragonoloba, constituted by a β-1, 4- mannose backbone with randomLy distributed α-1, 6 - galactose side chains. The mannose/galactose ratio is generally 2:1 [22]. Tamarind Kernel Powder (TKP) is derived from the seeds of the tree Tamarindus indica. TKP is composed of (1→4)-β- D- glucan backbone substituted with side chains of α, D-xylopyranose and β -D- galactopyranosyl. It is a non-ionic, neutral, branched polysaccharide in which glucose, xylose and galactose units are present in the ratio of ~3:2:1 [22] because of which it is widely known as Xyloglucan.

Because GG and TKP are non-ionic in nature their solubility in water is poor and hence the commercial grades of carboxymethyl derivatives of these polysaccharides are more useful and improve the aqueous solubility significantly.

In this chapter, we report on the synthesis and solution properties of three graft copolymers namely (i) Carboxymethylguar-g-PNIPAm, CMG-g-PNIPAm (ii) Carboxymethylguar-g-Pluronics, CMG-g-PEPO and (iii) CarboxymethylTamarind-g-PEPO, CMT-g-PEPO. The grafting was performed by coupling reaction between amino terminated thermoresponsive PNIPAm and PEPO with CMG and CMT using

water-soluble EDC as a coupling agent. The aim of the work was to examine a structure-property relationship in terms of thermoresponsive rheological behavior and to investigate the influence of external parameters on the process of association. The structural characteristics of all the graft copolymers were performed using FT-IR and NMR spectroscopy. The solution behavior of graft copolymers was studied using fluorescence spectroscopy and rheometry.

3.2. Experimental Part

3.2.1. Materials

Carboxymethyl Guar (CMG) and Carboxymethyl Tamarind (CMT) were commercial products and were kindly provided by Dabur, Haryana, India; *N*-isopropylacrylamide (NIPAm) monomer was obtained from Acros, USA; 2-amino ethane thiol hydrochloride (AET·HCl) and *N*-hydroxysuccinimide (NHS) were purchased from Aldrich Chemical Company, USA; Jeffamine M-2005, an amino terminated poly (ethylene oxide-co-propylene oxide) (PEPO) with 84 mol % of propylene oxide, was kindly supplied by Huntsman, Belgium. The coupling agent, 1-(3-(dimethylamino) propyl)-3-ethyl carbodiimide hydrochloride (EDC) was obtained from Fluka, USA; Potassium persulphate (KPS), Azobisisobutyronitrile (AIBN) along with other solvents were of analytical grade and obtained from S.D Fine Chemicals, India. Except CMG and CMT, all the other chemicals were used as received. Water used for the experiments was purified using a Millipore laboratory unit (Q-Millipore, 18.2MΩ).

3.2.2. Purification of Polysaccharides (CMG and CMT)

The commercial CMG/CMT obtained from an industry was purified using the following procedure:

10g of CMG / CMT was taken in a 1L conical flask and 500 mL acetone was added. The entire mass was stirred with a magnetic needle on a magnetic stirrer for 12h at room temperature (25 ^{o}C). Then it was filtered and dried. The dried CMG / CMT was dissolved in 1L distilled/ deionised water and centrifuged at 8,000 rpm for 40 min. The supernatant liquid was dialyzed against water using a dialysis membrane with MWCO of 12 kDa. The dialysis was carried out for 24h by frequently changing the external water. The dialyzed solution was then freeze-dried to obtain white cotton like material. The purified CMG / CMT were used for all the experiments.

3.2.3. Synthesis of amino terminated PNIPAm [PNIPAm-NH_2]

PNIPAm-NH_2 were prepared in two molecular weight ranges i.e. higher (MW 6000-10500 g/mol) and lower (MW 1200- 2300 g/mol)

3.2.3.1. Higher Molecular weight (MW) PNIPAm-NH_2

These were prepared by free radical polymerization of NIPAm monomer in aqueous solution by using a redox initiator pair, KPS/AET.HCl [4]. The polymerization was carried out in a three necked flask equipped with a reflux condenser, a magnetic stirrer and a nitrogen inlet. The monomer was dissolved in water and the solution was deaerated with nitrogen gas. The temperature was maintained at 30 ˚C using a water circulating system. The initiator, KPS and the chain transfer agent, AET.HCl were separately dissolved in water (10 mL each) and added to the monomer solution. The reaction was continued for 18 h and the polymer was recovered by dialyzing against water using a membrane (MWCO of 3.5 kDa). Finally, the dialyzed solution was freeze-dried. The product was redissolved in minimum amount of methanol and the hydrochloride ions were neutralized using NaOH and solution was concentrated to

remove traces of methanol. The polymer was precipitated in excess of diethyl ether, decanted and vacuum dried. To this, chloroform was added and the solution was filtered to remove NaCl, and NaOH. The polymer was concentrated and vacuum dried. The stoichiometry of reactants used for the preparation of PNIPAm-NH_2 is shown in **Table 3.1.**

Table 3.1: *Stoichiometry for the synthesis of Higher MW PNIPAm-NH_2 along with the molecular weight and PDI for PNIPAm-NH_2*

	NIPAm (mol/L)	**AET.HCl (mol/L)**	**KPS (mol/L)**	**Mn [a]**	**Mw [a]**	**P.D.I [a]**	**Mn [b]**
PNIPAm06	1.28	0.026	0.013	$6.67x10^3$	$1.17x10^4$	1.75	$6.50x10^3$
PNIPAm10	1.24	0.025	0.025	$1.12x10^4$	$1.90x10^4$	1.697	$1.05x10^4$

[a] Gel permeation chromatography (in $CHCl_3$)
[b] pH titration method

3.2.3.2. Low MW PNIPAm-NH_2

Low MW PNIPAm-NH_2 was prepared by radical polymerization in the presence of a chain transfer agent, 2-aminoethanethiol hydrochloride (AET.HCl). NIPAm (50mmol), AET.HCl (4.1mmol), AIBN (5mmol) were dissolved in CH_3OH (20mL). The solution was bubbled with nitrogen at 25 °C for 1 hour. The reaction was carried out at 65 °C for 22 hours. After the reaction, KOH- methanol was added to remove HCl from AET.HCl. The reaction mixture was concentrated to 2-3 mL and precipitated in diethyl ether (800mL). Then it was washed thrice with diethyl ether and dried under vacuum. The dried product was redissolved in chloroform and for 2 hours. Then the solution was filtered and concentrated to get dry powder.

Table 3.2: *Stoichiometry for the synthesis of Low MW PNIPAm-NH_2*

	Monomer NIPAm moles	**Initiator AIBN moles**	**Solvent Methanol moles**	**CTA** AET.HCl **moles**	**M_n**
PNIPAm01	0.099	0.00101	20mL	0.0120	1.19×10^3
PNIPAm02	0.05	0.005	20mL	0.0041	2.27×10^3

PNIPAm01, PNIPAm02, PNIPAm06 and PNIPAm10 represent PNIPAm with a MW of1.2 Kg/mol, 2.2 Kg/mol, 6.5 Kg/mol and 10.5 kg/mol respectively.

3.2.4. Synthesis of Graft copolymers based on polysaccharides

3.2.4.1. Synthesis of CMG-g-PNIPAm (CMP06 and CMP10)

The CMG-g-PNIPAm copolymers were prepared by a coupling reaction between CMG and PNIPAm-NH_2 using water soluble EDC as a coupling agent. Totally, six graft copolymers were prepared with different contents of PNIPAm-NH_2 having molecular weights in the range of 6500-10500 g/mol. Stoichiometry of the reactants and the nomenclature of the samples are shown in **Table 3.3.**

In a typical procedure, 10g of CMG and 1.85g PNIPAm-NH_2 were dissolved separately in 980 mL and 20 mL water respectively under stirring for 15h. The two solutions were then mixed at room temperature and pH was adjusted to 8.0 by adding 1M NaOH solution. To the above mixture, 0.274g of EDC dissolved 5 mL of water was added and stirred for 8h at room temperature. After the reaction the mixture was dialyzed against distilled water and further extracted with chloroform for 6-8 h to remove unreacted PNIPAm. Finally, the product was freeze dried to obtain pure graft copolymer.

3.2.4.2. Synthesis of CMG-g-PNIPAm (CMP01 and CMP02)

For the synthesis of graft copolymers with lower MW PNIPAm-NH_2, a slightly different procedure is used which is given in the following: In a reaction vessel

equipped with a magnetic stirrer, 2 g of CMG was dissolved under stirring in 100 mL of water for at least 24 h at room temperature. Then 2 g of PNIPAm-NH_2 (1 mmol) was separately dissolved in 50 mL of cold water to get a homogeneous solution and the pH was adjusted around 5-6 with hydrogen chloride (1 mol/L). After cooling the CMG solution to 6 °C, the solution of PNIPAm-NH_2 was slowly added, and the pH was controlled again to 5-6. To this homogeneous mixture, 0.092 g of NHS (0.07 mmol) and 0.488 g of EDC (3.1 mmol) separately dissolved in 2 mL of water, were slowly added and the reaction was allowed to proceed over a period of 16 h at 8 °C. Then, the copolymer was progressively precipitated under vigorous stirring in ethanol at room temperature. The precipitate was washed several times with ethanol to remove unreacted reagents and carbodiimide byproduct, filtered off, and finally dried under vacuum.

Table 3.3: *Stoichiometry for the synthesis of CMG-g-PNIPAm*

Samples (with code)	**CMG (g)**	**PNIPAm (g)**	**EDC (g)**
CMG-g-PNIPAm06-5 (**CMP06-5**)	10	0.925	0.137
CMG-g-PNIPAm06-10 (**CMP06-10**)	10	1.85	0.274
CMG-g-PNIPAm06-27 (**CMP06-27**)	10	5	0.740
CMG-g-PNIPAm10-5 (**CMP10-5**)	10	0.925	0.137
CMG-g-PNIPAm 10-10 (**CMP10-10**)	10	1.85	0.274
CMG-g-PNIPAm 10-27 (**CMP10-27**)	10	5	0.740
CMG-g-PNIPAm01 (**CMP01**)	10	10	2.44
CMG-g-PNIPAm02 (**CMP02**)	10	10	2.44

Code: For example, CMP10-5 corresponds to a copolymer of CMG and PNIPAm containing 5 mol% of PNIPAm with a MW of PNIPAm 10.5 kg/mol and CMP01 corresponds to a copolymer of CMG and PNIPAm containing equal weights of CMG and PNIPAm and MW of PNIPAm 1.2 kg/mol

3.2.4.3. Synthesis of graft copolymers: CMG-g-PEPO and CMT-g-PEPO

The coupling reaction between carboxyl groups of polysaccharides and terminal amine of PEPO was carried out in cold water using EDC/NHS as coupling reagents (**Scheme 3.1**). The stoichiometry of reaction is given in **Table 3.4**. A typical reaction can be summarized as follows: In a reaction vessel equipped with a magnetic stirrer, 2 g of polysaccharide was dissolved under stirring in 100 mL of water for at least 24 h at room temperature. A total of 2 g of PEPO-NH_2 (1 mmol of NH_2) was separately dissolved in 50 mL of cold water to get a homogeneous solution and the pH was adjusted around 5-6 with hydrogen chloride (1 mol/L). After cooling, the polysaccharide solution at T=6 °C, the solution of PEPO-NH_2 was slowly added, and the pH was adjusted to 5-6. After 1 h of mixing, 0.092 g of NHS (0.07 mmol) and 0.488 g of EDC (3.1 mmol) were separately dissolved in 2 mL of water, slowly added into the reaction vessel, and the reaction was allowed to proceed over a period of 16 h at 8 °C. Then the copolymer was progressively precipitated under vigorous stirring in ethanol at room temperature. The precipitate was washed several times with ethanol to remove unreacted reagents and carbodiimide byproduct, filtered off, and finally dried under vacuum.

Table 3.4: *Stoichiometry for the synthesis of CMG-g-PEPO and CMT-g-PEPO*

CMG or CMT (g)	**PEPO-NH_2 (g)**	**CMG or CMT:PEPO ratio**	**% Grafting CMG-g-PEPO by ^{1}H NMR**	**% Grafting CMT-g-PEPO by ^{1}H NMR**
2	0.1	1:0.05	3	0.6
2	0.5	1:0.25	5	4.5
2	1	1:0.50	18	7.5
2	1.5	1:0.75	29	11.5
2	2	1:1	21	22

3.3. Characterization

3.3.1. Molecular Weight

3.3.1.1. Characterization of PNIPAm-NH_2

The average molecular weight and polydispersity of PNIPAm-NH_2 were measured by size exclusion chromatography (SEC) using polystyrene gel columns 1_60cm 100Å and 1_60 100Å from PSS GmbH standards. The solvent, chloroform was used as an eluent at a flow rate of 1mL/min. The molecular weight by end group analysis was performed by pH titration where in, the PNIPAm-NH_2 was titrated with standardized 0.01N HCl using a pH meter. This uses an electrode whose potential depends on the amount of H^+ ion present in the solution. At the endpoint, there will be a sudden change in the measured pH to calculate the moles of acid taken to neutralize the PNIPAm base (NH_2). From this data, the MW of PNIPAm-NH_2 could be calculated.

3.3.1.2. Characterization of CMG and CMT

The average molecular weight and polydispersity of CMG and CMT were measured by size exclusion chromatography (SEC) using OHpak SB-804HQ and Pullulan Standards from Shodex. The solvent, 0.1N $NaNO_3$ was used as an eluent at a flow rate of 0.3mL/min.

3.3.1.3. FT-IR spectroscopy

The FT-IR spectra of all the samples were recorded on a FT-IR spectrum-1 Perkin Elmer Spectrometer, UK in a diffused reflectance mode. The samples were mulled with KBr and the frequency range used was from 400 to 4000cm^{-1}.

3.3.1.4. NMR spectroscopy

The ^{1}H-NMR and ^{13}C-NMR spectra of CMG, PNIPAm-NH_2, PEPO and graft copolymers were recorded using a 5 mm QNP probe in a using Bruker DRX-500

spectrometer operating at a proton frequency of 500.13 MHz. The samples were made in D_2O and TMS was used as a reference for chemical shifts (0 ppm).

For high temperature measurements, the tubes were left to stabilize for 15 min at the desired temperature before recording the spectrum.

3.3.1.5. Fluorescence spectroscopy

Steady state fluorescence spectra were recorded on a Fluorolog spectrofluorometer (JY Horiba Inc.) equipped with a peltier plate to control the temperature of the measuring cell. Pyrene solution in acetone (1×10^{-3}M) was used as an external probe in a final concentration of 6×10^{-7}M. The excitation wavelength was 339 nm. The change in the intensity ratio (I_1/I_3) of the first and the third vibronic bands at 373nm and 384nm for I_1 and I_3 respectively in the emission spectra, were used to detect the hydrophobic micro domains.

3.3.1.6. Viscometry

Reduced viscosity measurements for PNIPAm-NH_2 and copolymers were carried out using an automated capillary viscometer system, SCHOTT-GERATE AVS-470, viscometer, Germany with a capillary diameter of 0.64mm and a temperature controller circulating bath with an accuracy of ±0.01 ◦C. The reduced viscosity was calculated as a ratio of $[(t–t_o)/t_o]/C_p$, where 't_o' and't' are the flow times of solvent and the polymer solution of concentration 'C_p'. The intrinsic viscosity, [η] was determined from the extrapolation of the reduced viscosity curve to zero concentration.

3.3.1.7. Steady Shear and Oscillatory Rheological Measurements

The viscoelastic properties of aqueous solutions of CMG and CMT copolymer solutions were performed on an Anton Paar MCR-301, controlled stress rheometer by using a cone-and-plate geometry (diameter = 50mm, angle = 1°) for highly viscous

gel samples. For low viscosity samples, cuvette (coaxial cylinder) geometry was used to measure viscosity, operating in flow or dynamic mode, respectively. The dynamic data was obtained as a function of strain amplitude first at a fixed frequency of 1Hz to ensure that the measurements were performed in a linear viscoelastic region. The frequency sweep experiments were then performed in the linear regime to determine storage (G') and loss (G") moduli in the frequency range of 0.01–100 Hz (rad/s).

A particular care was taken to prevent water evaporation during measurements at high temperature using a homemade cover combined with the deposition of a film of silicone oil on the edges of the sample.

3.3.2. Sample preparation

All the solutions were prepared using pure deionized water. Very gentle stirring was employed to get homogeneity of the sample before taking them for experiments.

3.4. Results and Discussion

3.4.1. Synthesis of PNIPAm-NH_2, graft copolymers CMG-g-PNIPAm

Semitelechelic, PNIPAm-NH_2 homopolymers containing reactive group at one end of the polymer chain were prepared by free radical polymerization in aqueous solution using 2-aminoethane thiol hydrochloride as a chain transfer agent. In order to avoid the phase separation of PNIPAm during the polymerization, the reaction temperature was maintained at 25 ˚C, which is below the LCST of PNIPAm (32 ˚C). This ensured the homogenous polymerization of NIPAm monomer. We show in **Table 3.1** the results of molecular weights obtained by both GPC and end group analysis using pH titration methods. It can be readily seen from the table that the M_n obtained by GPC matches reasonably well with the pH titration method. The polydispersity index shows that the distribution of molecular weights is not too broad. Use of carbodiimide

chemistry has been widely reported in the literature and practiced in peptide synthesis for the coupling reaction between amino groups and carboxyl groups. The pathway for coupling reaction is shown in **scheme 3.1**. For an amide formation between COOH and NH_2 groups, an excess of dicyclohexylcarbodiimde (DCCI) is used as a catalyst. The reactants and reagent are soluble in an organic solvent under moderate conditions with quantitative yields. Similar reaction can be carried out in aqueous media using water-soluble carbodiimide, 1-ethyl-3-(3-dimethylaminopropyl) carbodiimide) (EDC) as a coupling agent that can react with carboxyl groups at low pH (3.5-5) so as to form the *O*-acylisourea intermediate which is not very stable and therefore N-hydroxysuccinimide (NHS) is added with EDC to form a more stable activated ester. EDC alone is limited by low coupling yields and it is known that addition of NHS to such reactions can greatly enhance the coupling efficiency [22].

Lower pH also favors the formation of anhydride intermediates [23], which play an important role in the amide formation. On the other hand, the amide formation involves the reaction between previous intermediates (*O*-acylisourea, NHS-activated, or anhydride) and nonionized amines, which prevail at high pH. The ionization equilibrium depends on the p*K*a of the amine but, generally, pH > 5 is a good compromise between the above mentioned requirements [15].

In order to facilitate the random distribution of thermo-responsive side chains in the graft copolymer, the homogeneity of the reaction medium is maintained by doing the reaction in an aqueous medium at a temperature below the LCST of the thermo-responsive polymer.

Eight different graft copolymers were prepared with different contents of PNIPAm-NH_2 with four different molecular weights PNIPAm-NH_2 1190, 2275, 6500 and 10,500 g/mol.

Samples CMP01, CMP02 and CMP10 which showed thermo-responsive behavior were taken for measurements.

a

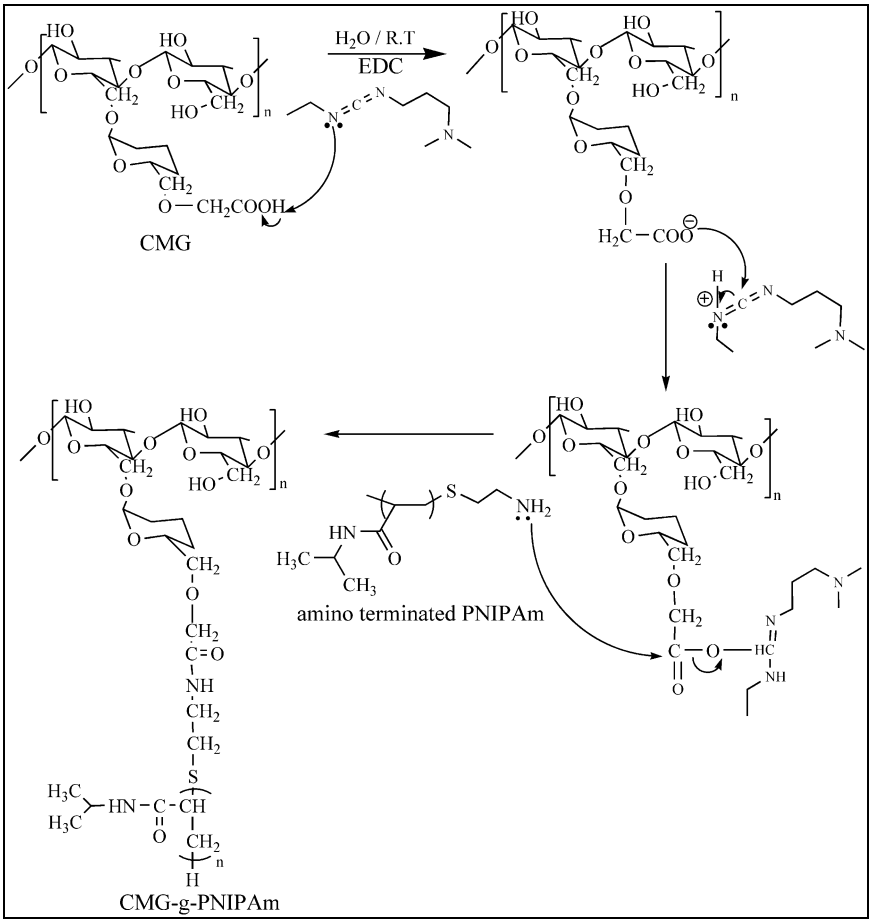

b

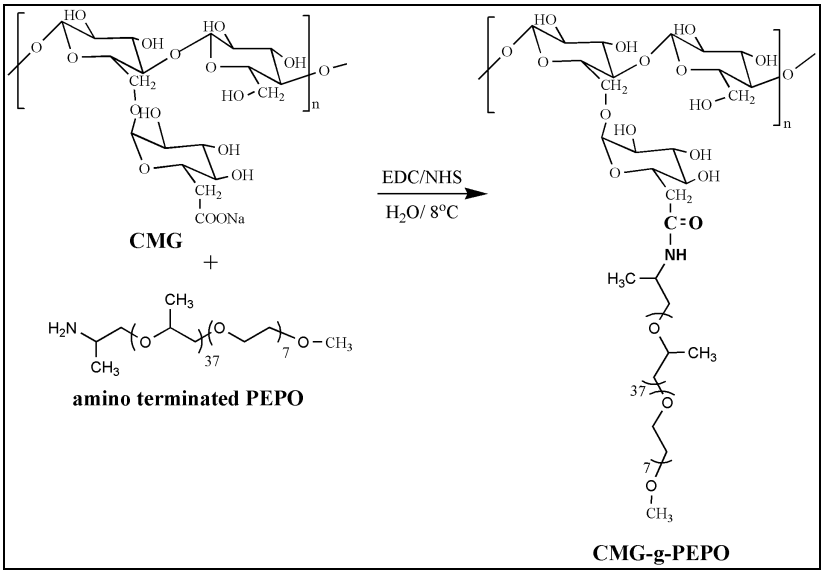

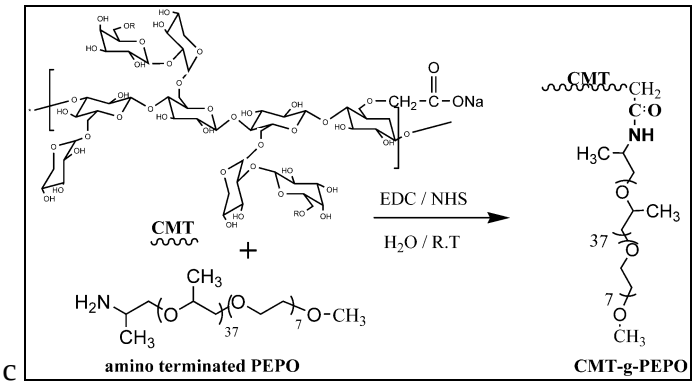

C

Scheme 3.1: *Synthesis of Thermo sensitive (a) CMG-g-PNIPAm copolymer and the grafting of PEPO onto (b) CMG and (c) CMT*

The coupling reaction in CMG-g-PNIPAm, CMG-g-PEPO and CMT-g-PEPO is shown in **Scheme 3.1 (a), (b) and (c)** and **Table 3.4** shows the various weight ratios of PEPO grafted onto CMG and CMT in this study. The PEPO was selected according to its relative hydrophobicity, and molecular weight (MW=2000). The hydrophobicity of PEPO is controlled by the ratio of ethylene oxide to propylene oxide units (6/29 mol ratio) in the oligomer. In both the CMG and CMT systems PEPO was added in the weight ratio of 1:0.05,1:0.25,1:0.5, 1:0.75 and 1:1 respectively.

The reaction was conducted in water and at a temperature lower than 18 °C to avoid phase separation of PEPO chains and to ensure that the reaction mixture is homogeneous. All the characterizations were done using CMG-g-PEPO 1:1 and CMT-g-PEPO 1:1, samples and will be reported as CMG-g-PEPO and CMT-g-PEPO.

3.4.2. FT-IR spectroscopy

We show in **figure 3.1 (a),** the IR spectra of CMG, PNIPAm-NH_2 and the graft copolymer CMP10-10. Compared to the homopolymers, CMG and PNIPAm-NH_2, the graft copolymer shows characteristic peaks around 3500-3200 cm^{-1} which can be attributed to the stretching of –OH from CMG and –NH from PNIPAm chains.

Further, the bands at 1652 cm^{-1} and 1541 cm^{-1} corresponds to the C=O stretching of amide I and –NH stretching of the amide II of PNIPAm. These results clearly indicate the incorporation of PNIPAm into CMG.

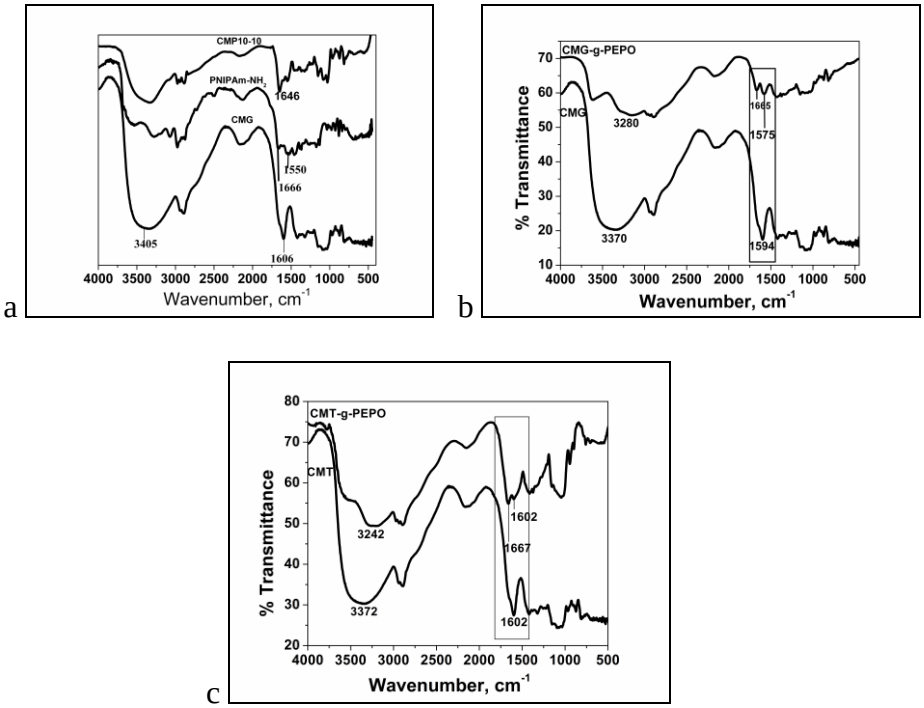

Figure 3.1: *The IR spectra of (a) CMG, PNIPAm-NH_2 and the graft copolymer CMP10-10 (b) CMG and CMG-g-PEPO (c) CMT and CMT-g-PEPO*

In **figure 3.1(b)** the IR spectra of CMG and the graft copolymer CMG-g-PEPO and **figure 3.1 (c)** the IR spectra of CMT and CMT-g-PEPO are shown. It was observed that, the graft copolymers show characteristic peaks around 3500–3200cm^{-1} which can be attributed to the stretching of –OH from CMG and –NH from PEPO chains. Further, the bands at 1665 cm^{-1} and 1575 cm^{-1} corresponds to the C=O stretching of amide. These results clearly indicate the incorporation of PEPO onto CMG and CMT.

3.4.3. ^{1}H-NMR Spectroscopy

3.4.3.1. ^{1}H NMR Spectra of homopolymers and graft copolymers

In order to further confirm the presence of PNIPAm in the graft copolymer, we performed ^{1}H NMR spectroscopy. We show in **figure 3.2 (a)** the ^{1}H NMR spectra of CMG, PNIPAm-NH_2 and the graft copolymer, CMP10-10.

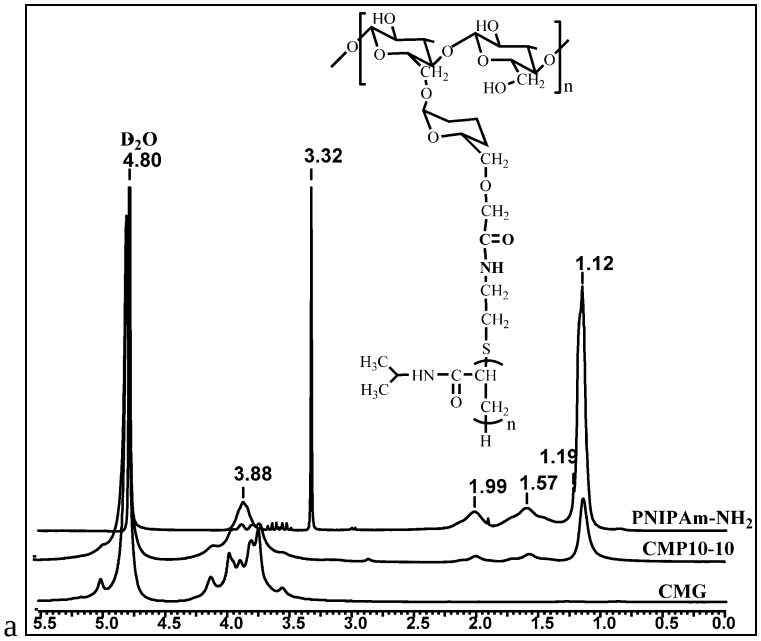

a

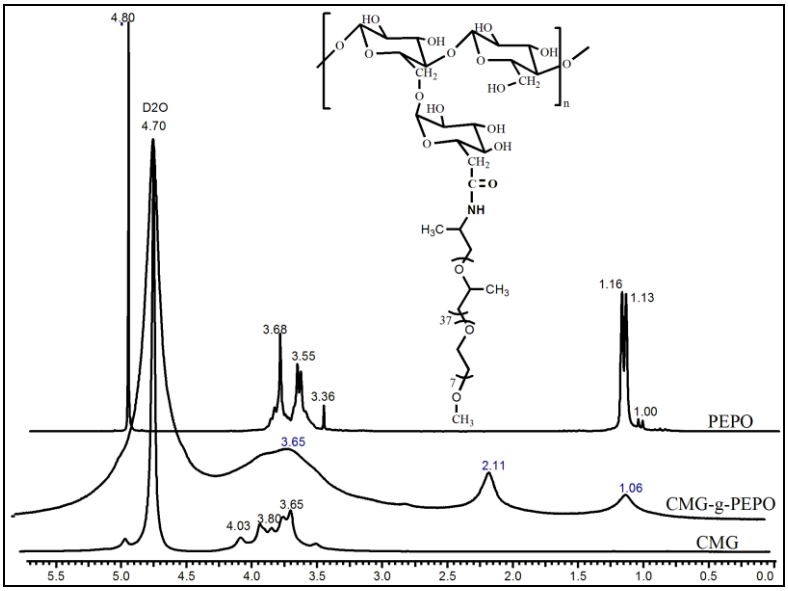

b

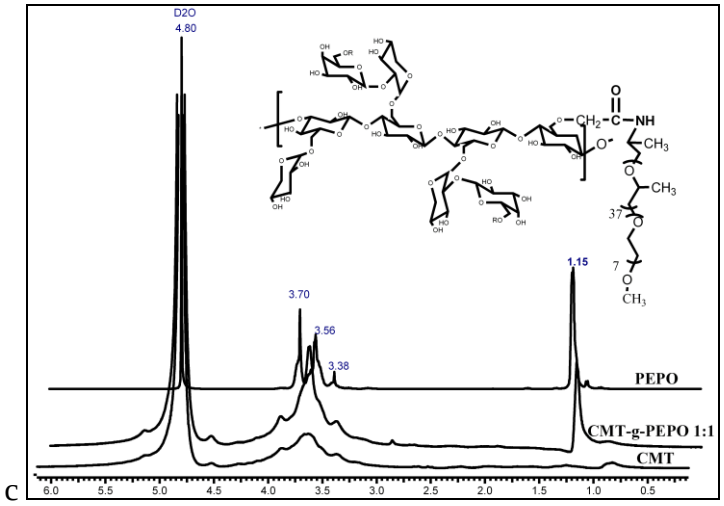

c

Figure 3.2: *^{1}H NMR spectra of (a) CMG, PNIPAm-NH_2 and CMP10-10 graft copolymer, (b) CMG, PEPO-NH_2 and the graft copolymer, CMG-g-PEPO and (c) CMT, PEPO and CMT-g-PEPO*

It can be readily seen from the figure that, the graft copolymer, CMP10-10 showed the characteristic peaks of both CMG and PNIPAm protons. The $–CH_3$ proton of PNIPAm-NH_2 and the graft copolymer appeared at 1.12 ppm which is completely absent in the homopolymer of CMG. Similarly, the –OH proton peak of CMG and CMG-g-PNIPAm appeared in the region of 3.5-4.5 ppm. The observation of characteristic proton peaks arising from both PNIPAm and CMG in the graft copolymer confirmed the structure of the graft copolymer.

Similarly, the ^{1}H NMR spectra of CMG, PEPO-NH_2 and the graft copolymer, CMG-g-PEPO are shown in **figure 3.2 (b)**. The graft copolymer, showed the characteristic peaks of both CMG and PEPO protons. The $–CH_3$ proton of PEPO-NH_2 and the graft copolymer appeared at 1.13 ppm which is completely absent in the homopolymer of CMG. The –OH proton peak of CMG and CMG-g-PEPO appeared in the region of 3.5–4.5 ppm. The observation of characteristic proton peaks arising from both PEPO

and CMG in the graft copolymer confirmed the structure of the graft copolymer. We also show in **figure 3.2 (c)** the ^{1}H NMR spectra of CMT, PEPO-NH_2 and CMT-g-PEPO graft copolymer. It can be seen from the figure that, the graft copolymer showed characteristic peaks of both CMT and PEPO protons. The $–CH_3$ proton of PEPO-NH_2 and the graft copolymer appeared at 1.13 ppm which is completely absent in the homopolymer of CMT. The –OH proton peak of CMT and CMT-g-PEPO 1:1 appeared in the region of 3.5–4.5 ppm. The observation of characteristic proton peaks arising from both PEPO and CMT in the graft copolymer confirmed the structure of the graft copolymer.

Further, we also attempted to study the quantitative composition of the graft copolymer, CMG-g-PEPO by ^{1}H NMR spectroscopy and show the stack plots of ^{1}H NMR spectra of CMG-g-PEPO with varying PEPO content in **figure 3.3 (a).** It is seen that as the PEPO content increases the$–CH_3$ peak height at 1.18 ppm increases indicating an increase in PEPO grafting. The results of the amount of grafted PEPO are reported in **Table 3.4**.

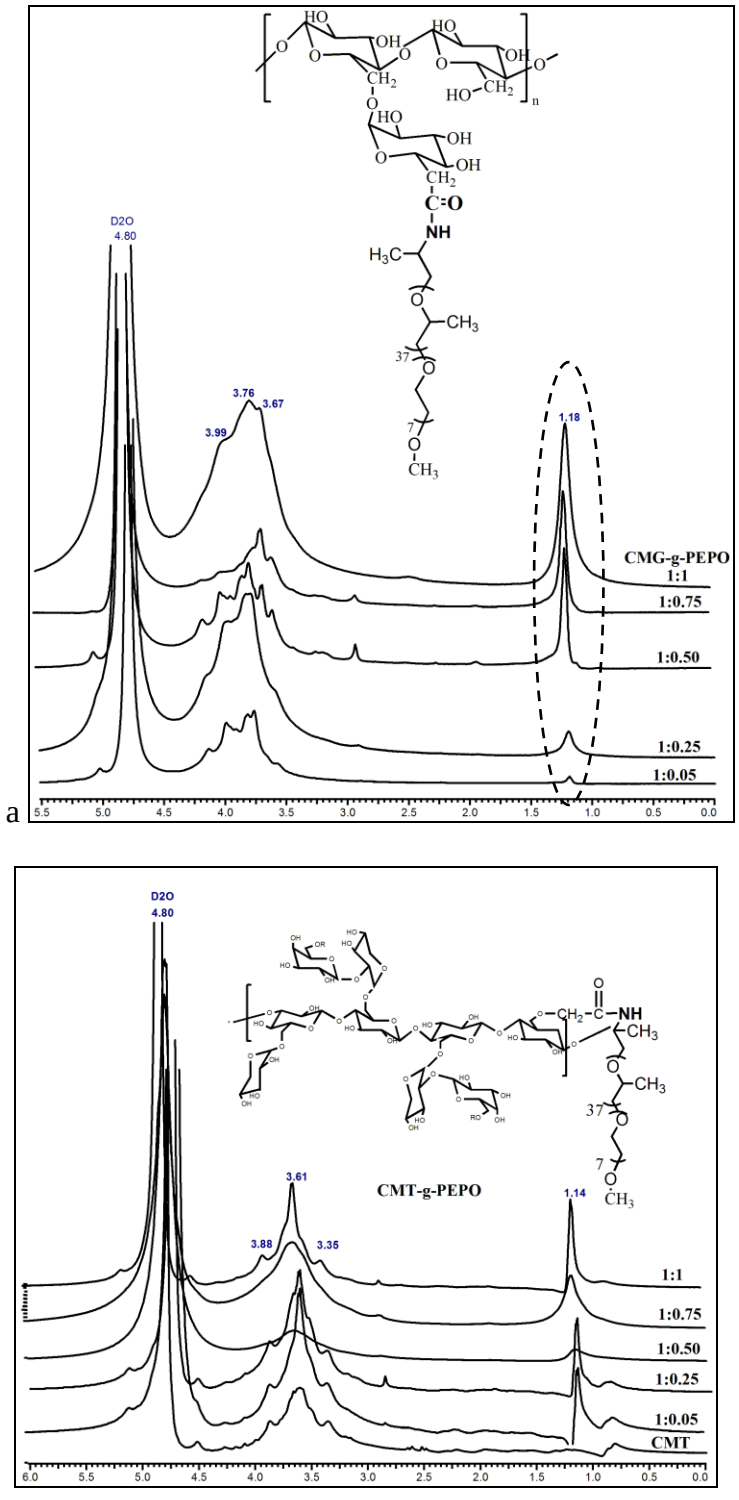

Figure 3.3: *^{1}H NMR spectra of different ratios of (a) CMG-g-PEPO and (b) CMT-g-PEPO*

The percentage grafting was found to be between 3-29% indicating that the grafting reaction does not undergo complete conversion as the number of carboxylate groups

are low and are noncyclizable which prevents the formation of anhydride intermediates [15].

Figure 3.3(b) shows the stack plots of CMT-g-PEPO with varying PEPO content. It is seen that as the PEPO content increase the–CH_3 peak height at 1.14 ppm increases indicating an increase in PEPO grafting and the amount of grafted PEPO was calculated by ^{1}H-NMR as reported in **Table 3.4**. Similarly, for CMT-g-PEPO a maximum grafting of 22% only could be achieved again and this depends on the number of carboxylate groups available for PEPO to react.

3.4.3.2. Temperature of Thermoassociation by NMR Spectroscopy

Above the overlap concentration (C^*), the thermoassociation occurs at a critical temperature which is termed as a temperature of association, T_{ass}. At T_{ass}, the LCST side chain stickers self-assemble and give rise to an enhancement of viscosity in the solution.

Interestingly, at T_{ass}, one can observe a deviation of line width of certain peaks in the NMR spectroscopy. This line width transition indeed mirrors the actual sol-gel transition occurring in a macroscopic way through the associated molecular motions. We show in **figure 3.4 (a)** the stacked plots of static proton spectra of CMG-g-PEPO at different temperatures ranging from 10-70 ^oC. The line width of the CH_3 peak of the PEPO chain was measured at each temperature and plotted against the temperature (**see Figure 3.4(b)**). It can be readily seen that, the ^{1}H static line width of the CH_3 peak of the PEPO chain showed a small gradual increase between 10-41 ^oC and exhibits an inflection point at 41.1 ^oC. Above this temperature, the line width increases sharply indicating the formation of gel as a result of thermoassociation.

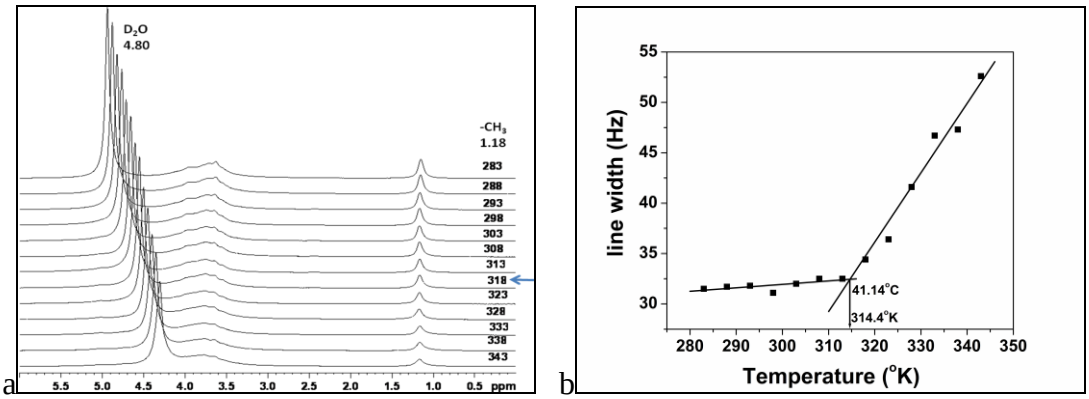

Figure 3.4: *(a) Stack plots of static proton spectra of CMG-g-PEPO at different temperatures (10-70 ºC); (b) Plot of proton line width of –CH_3 peak w.r.t. temperature*

The inflection point in the figure can be considered as T_{ass}. The T_{ass} obtained from the NMR experiments corresponds very well with the observed associating behavior investigated by rheological measurements on the same samples (which are discussed in the later sections). Therefore, the NMR technique emerges as an important tool to determine T_{ass} in the process of thermoassociation. A similar exercise has been performed on the graft copolymer, CMT-g-PEPO and the T_{ass} was found to be around 50-51 ˚C.

3.4.4. Fluorescence Spectroscopy

3.4.4.1. Fluorescence Spectroscopy for CMG-g-PNIPAm

Fluorescence spectroscopy has been extensively used to study the hydrophobic micro-environment of amphiphilic polymers in aqueous media with pyrene as an external probe. Two important properties of pyrene, a change in the intensity ratio of the first over third vibronic peak (I_1/I_3) in emission spectra and a (0, 0) band shift in excitation spectra upon the formation of hydrophobic micro-environment in aqueous media, are utilized to study the aggregation behavior of micelles. **Figure 3.5 (a)** shows the

change in the intensity ratio (I_1/I_3) of pyrene excitation spectra as a function of temperature for CMG, PNIPAM-NH_2 and two copolymers CMP10-5, CMP10-10. For the homopolymer PNIPAm-NH_2, there was no significant change in the intensity ratio at low temperature region (below LCST).

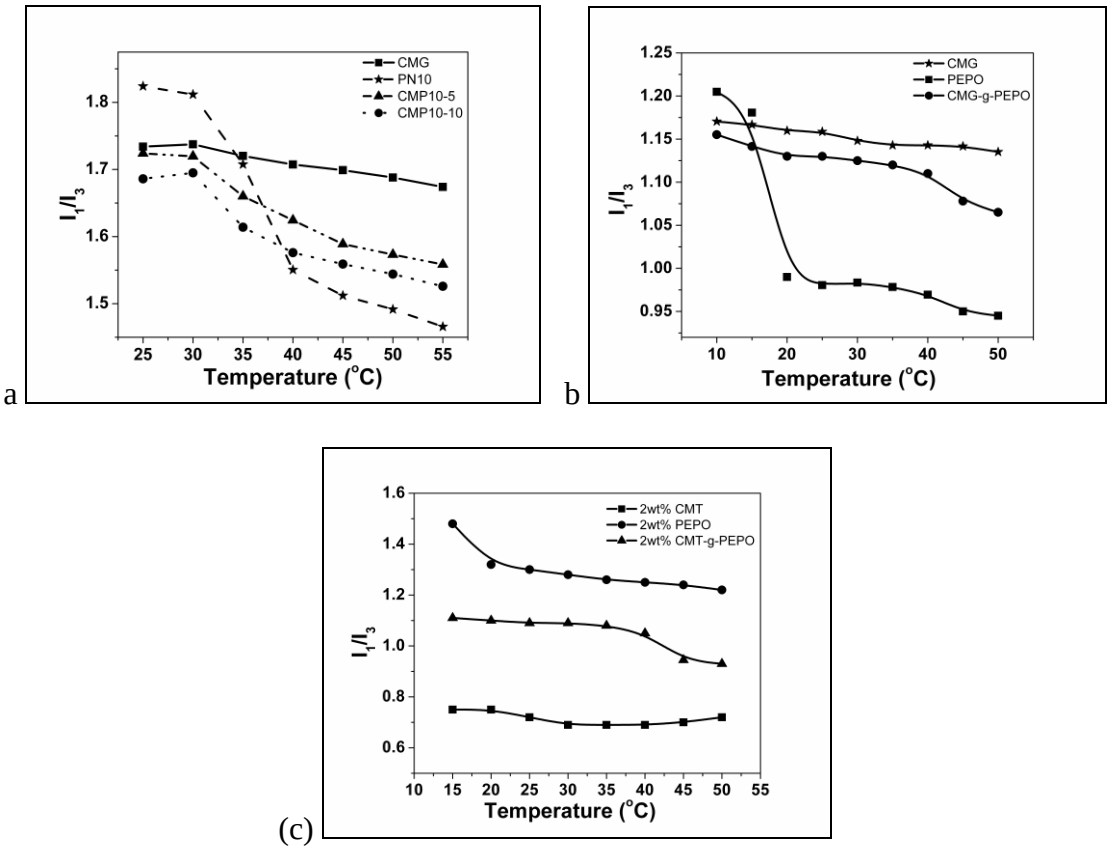

Figure 3.5*: (a) I_1/I_3 vs temperature for CMG, PNIPAm, CMP10-5 and CMP10-10 (C_p=2 mg/mL) (b) I_1/I_3 vs temperature for CMG, PEPO, CMG-g-PEPO 1:1 (C_p=1wt%) and (c) I_1/I_3 vs temperature for CMT, PEPO, CMT-g-PEPO 1:1 (C_p=2wt%)*

However, a sharp decrease in the intensity ratio was observed at temperature close to the LCST of the polymer (~32-33 ˚C), revealing the formation of hydrophobic micro-environment at this temperature. The high values of intensity ratio (I_1/I_3) indicate an aqueous polar environment whereas, lower values indicate the low polarity micro-environment where pyrene molecules are preferentially solubilized [24].

In the case of CMG homopolymer, there was no rapid decrease in the intensity ratio (I_1/I_3) at any temperature in the whole temperature range studied, indicating that there are no hydrophobic domains formed in the solution. Nevertheless, a small continuous decrease of the intensity ratio with temperature was observed which could be due to the behavior of pure pyrene solution. The graft copolymers, on the other hand showed a considerable decrease in the intensity ratio (I_1/I_3) above the LCST of the grafted PNIPAm side chains indicating the formation of hydrophobic microdomains. It can be attributed to the fact that, above the LCST of the grafted chains in the copolymer, a polymer-rich phase can form from the collapsed and precipitated PNIPAm chains, followed by a solubilization of pyrene in polymer-rich hydrophobic micro-environment. It is also seen that the hydrophobic microdomains obtained in graft copolymers was weaker as compared to the homopolymer, PNIPAm. A similar observation was also made in other thermo-associating graft copolymers that we have studied, namely, CMG-g-PEPO and CMT-g-PEPO. These results are shown in **figures 3.5 (b) and (c),** which clearly indicate the thermo-associating nature of the graft copolymers.

We also determined the critical aggregation concentration (cac) of CMG-g-PNIPAm (CMP10-5) by recording the ratio of intensity (I_1/I_3) against the polymer concentration 'C_p' (mg/mL). **Figure 3.6** shows the semi-log plot of I_1/I_3 versus C_p. From the **figure 3.6** the curve shows that at low polymer concentration, I_1/I_3 ~1.75, characteristic of pyrene in water (i.e. 1.8).

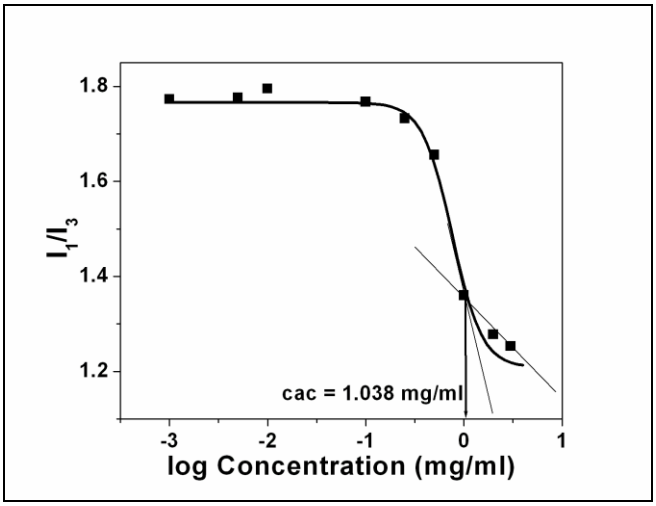

Figure 3.6: *Determination of critical aggregation concentration (cac) for CMP10-5 at 25 ˚C*

However, upon increasing the polymer concentration, I_1/I_3 starts to decrease indicating the onset of aggregation. The curve with 3 tangents and the cross over point obtained by using a lower horizontal tangent and a vertical tangent gave a cac of 1.38 mg/mL ~0.14 wt% of the polymer.

3.4.5. Viscometry

We show in **Figure 3.7 (a),** the concentrations dependence of viscosity for CMG, CMP10-5 and CMP10-10 at 25 ˚C. The viscosity of CMG increases gradually with increase in concentration. With the incorporation of PNIPAm into CMG there was a significant increase in viscosity as compared to the unmodified precursor, CMG. Especially, above C_p = 10 g/L there was a sharp increase in case of CMP10-5. The concentration, C_p = 10 g/L could be considered as the overlap concentration (C^*) above which the intermolecular hydrophobic associations play a major role in enhancing the viscosity.

a 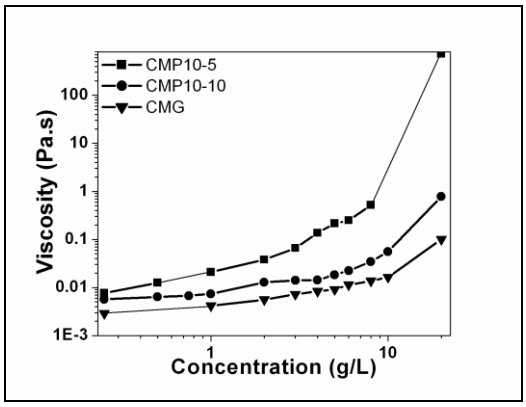

b 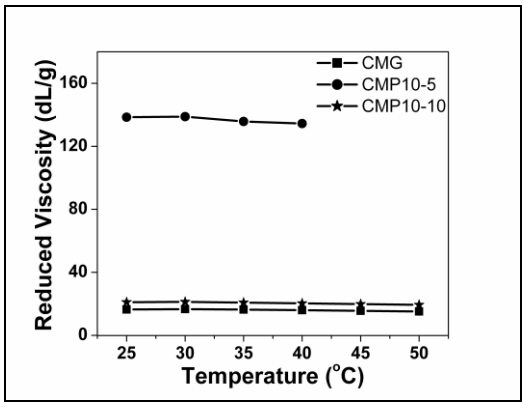

Figure 3.7: *(a) Concentration dependence of viscosity for CMG, CMP10-5 and CMP10- 10 at 25 ˚C. (b) Temperature dependence of reduced viscosity in water for CMG, CMP10-5 and CMP10-10*

However, with CMP10-10 we observe a lower viscosity compared to CMP10-5 which could be due to more hydrophobic nature of the sample. We show in **Figure 3.7 (b)** the temperature dependence of the reduced viscosity for CMG, CMP10-5 and CMP10-10. The reduced viscosity of CMG was not much affected by the temperature and there was only a slight decrease in viscosity with increasing temperature. However, with the incorporation of PNIPAm side chains into CMG (sample CMP10-5) the reduced viscosity increased significantly which would be attributed to the formation of hydrophobic associations from PNIPAm chains. With further increase in PNIPAm content (CMP10-10), the viscosity decreased due to increased hydrophobicity of PNIPAm.

3.4.6. Oscillatory Measurements

In most cases, the viscoelastic properties of associating polymer solutions have been described in terms of transient network theory [25-27]. The theory explains the real (G', storage modulus) and imaginary (G", loss modulus) parts of the complex viscoelastic

shear modulus in terms of Maxwell model, which is expressed by the following equations,

$$G' = Go \frac{\omega^2\tau^2}{1+\omega^2\tau^2} \quad (1)$$

$$G'' = Go \frac{\omega\tau}{1+\omega^2\tau^2} \quad (2)$$

where 'G_0', 'τ' and 'ω' are the plateau modulus, the relaxation time of the network and the angular frequency, respectively. The plateau modulus, G_0 is given by

$$G_0 = \upsilon kT \quad (3)$$

where υ gives the elastically active chains per unit volume and 'k' and 'T' are Boltzmann constant and absolute temperature respectively. In order to understand the viscoelastic nature of the CMG-g- PNIPAm copolymers, we performed oscillatory measurements on a typical sample of CMP10-5 at moderate concentrations.

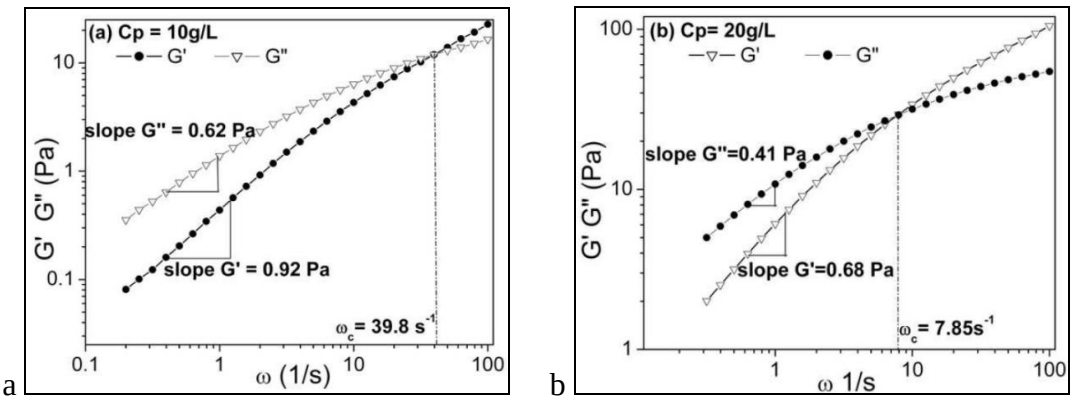

Figure 3.8*: The plots of storage modulus (G') and loss modulus (G") versus frequency for CMP10-5 at 25 ˚C for two concentrations (a) C_p = 10 g/L and (b) C_p = 20 g/L*

Figure 3.8 shows the typical frequency dependence of dynamic moduli (G' and G") obtained with an aqueous solution of CMP10-5 at C_p = 10 g/L and 20 g/L. At low frequency, G'<G" and the complex moduli did not follow the Maxwellian behavior since the slopes for G" and G' are far away from 1 and 2 respectively. This indicates that there could be multimode relaxation process in the system. At higher frequencies, G' and G" cross over at a characteristic frequency (ω_c = 39.8 rad/s for C_p = 10 g/L; ω_c

= 7.85 rad/s for C_p=20 g/L) which is related to the relaxation time of the network: $\tau = 1/\omega_c$. It can also be seen from the figure that, as the concentration increases, the 'ω_c' decreases and accordingly the relaxation time 'τ' increases. This is in line with the property that the thicker gels relax slower due to restricted molecular motion.

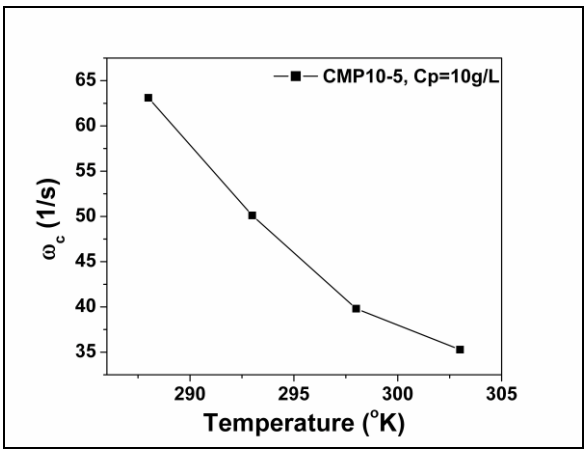

Figure 3.9: *The plot of cross over frequency (ω_c) as function of temperature for CMP10-5 (C_p = 10 g/L) from the oscillatory shear measurements*

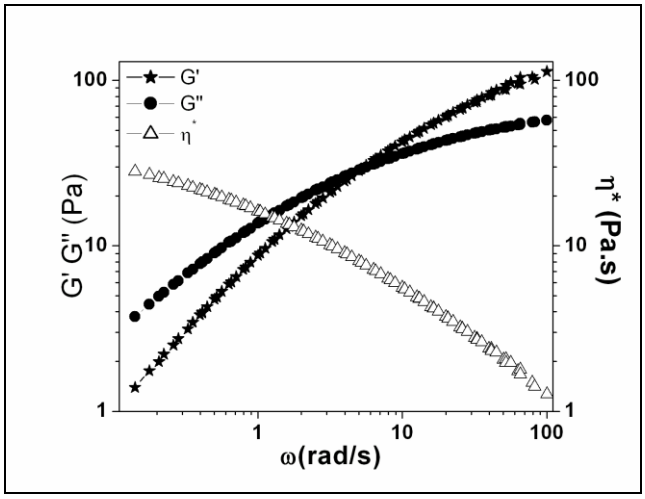

Figure 3.10: *TTS for CMP10-5 at T= 15, 20, 25 and 30 ˚C T_{ref} = 15 ˚C*

We also performed the oscillatory measurements on sample CMP10-5 with C_p = 10 g/L at various temperatures and the cross over frequency, ω_c was determined as a function of temperature. **Figure 3.9** shows the decrease in ω_c with increase in

temperature. This indicates that at higher temperature the thermo associations prevail which lead to slow relaxation of the gels. Estimation of 'E_a' from the Time-Temperature Superposition (TTS) gives the characteristic time scale for the associations in these polymers. The activation energy can be estimated from the relaxation time (τ) which is given as,

$$\tau = \tau_0 \exp\frac{E_a}{kT} \qquad (4)$$

where 'E_a' is the activation energy and τ_0 is the microscopic time corresponding to the diffusion of associating groups. The dynamic frequency sweep (DFS) measurements were performed on CMP10-5 (C_p=20 g/L) at different temperatures (T = 15, 20, 25 and 30 $^{\circ}$C) and a TTS was applied to the data. A master curve obtained is given in **figure 3.10** using a reference temperature, T_{ref} =15 $^{\circ}$C. It can be seen from **figure 3.10** that, the TTS procedure allows the superpositions of viscoelastic data by applying a frequency shift factor (a_T) and a modulus shift factor (b_T). The activation energy (E_a) determined experimentally in the temperature range of 15–30 $^{\circ}$C is of the order of 21.2 J/mol which is consistent with the values reported earlier for similar system [28, 29]. In the previous samples of CMP, although the molecular weight of the grafted PNIPAm was high enough (~10,000g/mol), we did not observe the thermo-thickening behavior in the aqueous solutions. We attribute this to the lower amount of grafting percentage which is about 20-25%. Therefore, in order to induce the thermothickening behavior, we synthesized CMG graft copolymers with higher grafting percentage and shorter PNIPAm chains MW (1190 and 2275 g/mol).

a 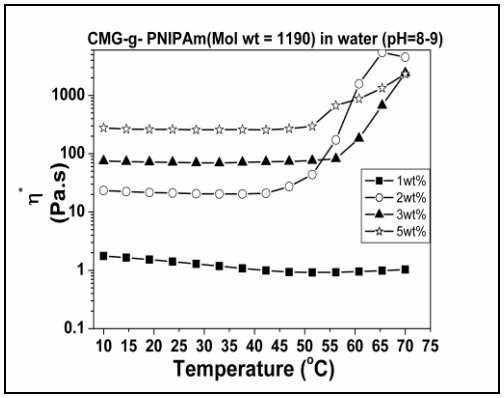

b 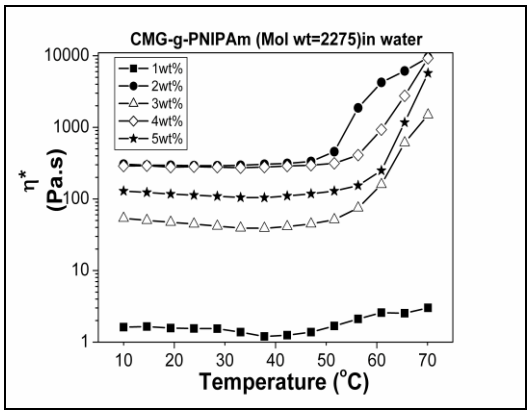

Figure 3.11: *Complex Viscosity as a function of temperature (pH=8-9) for (a) CMP01 and (b) CMP02*

Figure 3.11 shows the complex viscosity of CMP01 and CMP02 aqueous solutions as a function of temperature for different concentrations of polymers. It can be seen from figure that the solutions with C_p = 1% do not show significant change in the complex viscosity as a function of temperature and the temperature dependence viscosity remains rather flat. However, above C_p > 1 wt%, all the samples exhibit thermo-associating or thermothickening property with the T_{ass} in the range of 45-50 °C.

We also show in **figure 3.12 (a) and (b)** the frequency sweep experiments at 25 °C for C_p = 1wt% and 2wt% aqueous solutions of CMP01. For 1 wt% solution, the loss modulus G" is higher than storage modulus G' at all the frequency range studied and the sample behaves like a liquid. However, with an increase in polymer concentration (C_p= 2 wt%) G' becomes larger than G" and the gap between G' and G" becomes larger with the transition from a liquid-like behavior to a solid/gel like structure. Further, the complex moduli did not follow the Maxwellian behavior since the slopes for G" and G' are far away from 1 and 2 respectively. This clearly indicates the multimode relaxation process operating in the system.

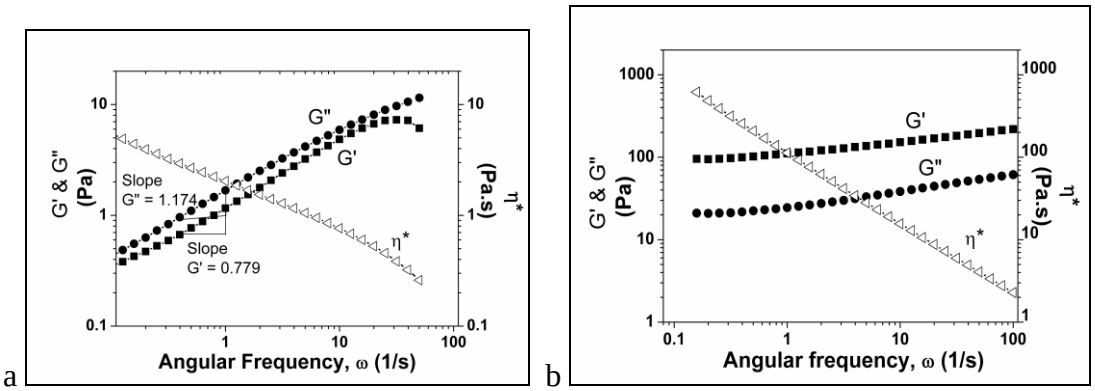

Figure 3.12: *The plots of storage modulus (G') and loss modulus (G") versus frequency for CMP01 at 25 ˚C (a) C_p = 10 g/L and (b) C_p = 20 g/L in water*

3.3.6.1. Visco-elastic Properties of CMG-g-PEPO and CMT-g-PEPO copolymers

We show in **figure 3.13** the complex viscosities of 1.0 wt% CMG-g-PEPO 1:1 aqueous solution with respect to temperature and compared with the homopolymers of CMG and PEPO. A slight decrease in viscosity with increasing temperature is observed for PEPO and CMG solutions. This is reasonable to expect since there is no formation of associations or aggregates in the homopolymer solutions alone. However, with the CMG-g-PEPO, the viscosities are much higher than PEPO and CMG homopolymers in the entire temperature range studied. This can be attributed to the presence of PEPO side chains which tend to associate and induce self-assembly.

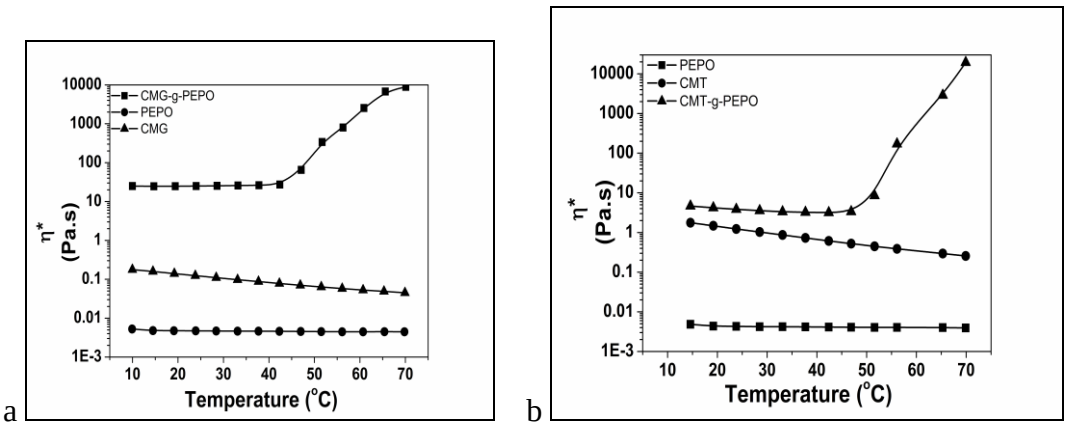

Figure 3.13: *Temperature dependence of complex viscosity of (a) 1wt% CMG, PEPO and CMG-g-PEPO and (b) 3wt% CMT, PEPO and CMT-g-PEPO*

Furthermore, it can be readily seen from the **figure 3.13(a)** that the influence of temperature is striking for CMG-g-PEPO wherein, there is a dramatic increase in complex viscosity at about 41-42 ˚C exhibiting strong thermo-thickening behavior induced by the local microphase separation of PEPO side chains at this temperature (T_{ass}) leading to the formation of transient network. The temperature at which these associations occur is further evidenced by the change in line width of PEPO chains in the NMR spectroscopy as discussed earlier.

Similarly, the complex viscosities of 3wt% CMT, PEPO and CMT-g-PEPO aqueous solutions are reported in **figure 3.13 (b).** The continuous drop in viscosity with increasing temperature is observed for PEPO and CMT solutions as expected since no associations or aggregate formations by them alone. At low temperatures, solutions of 3wt% CMT-g-PEPO showed an increase in viscosity compared to the CMT solutions itself. The polymer solution is characterized by an initial decrease of viscosity in the low temperature range followed by a strong thickening induced by the local microscopic phase separation of PEPO side chains at about 50 ˚C.

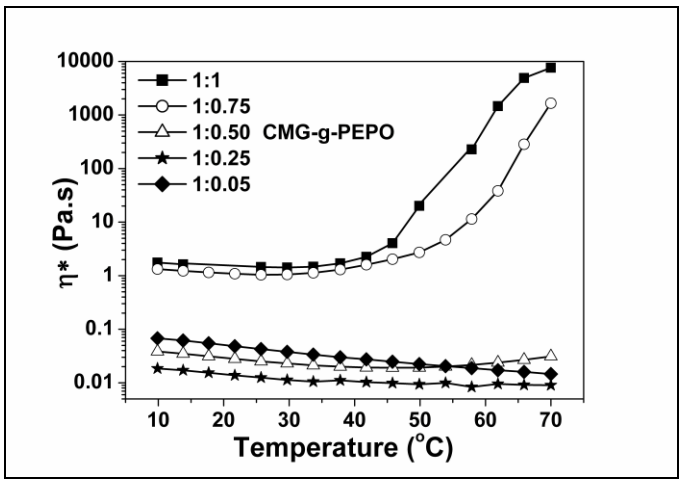

Figure 3.14: *Complex viscosity as function of temperature for 1wt% CMG-g-PEPO copolymers with varying PEPO content*

We also show in **figure 3.14**, the influence of PEPO content on the thermo-thickening behavior in the aqueous solutions. It can be seen that, the lower content of PEPO (CMG: PEPO ratio < 1:0.5) do not induce thermo-thickening behavior whereas, samples with CMG: PEPO ratio 1:0.75 and 1.0:1.0 exhibit very good thermo-thickening behavior at 41-42 ˚C.

The variation in dynamic moduli (*G′* and *G″*) with respect to temperature (in the range of 10-70 ˚C) for CMG, PEPO and CMG-g-PEPO is shown in **figure 3.15.** For the homopolymer PEPO, both the G'and G" are low and there is no significant change with respect to temperature.

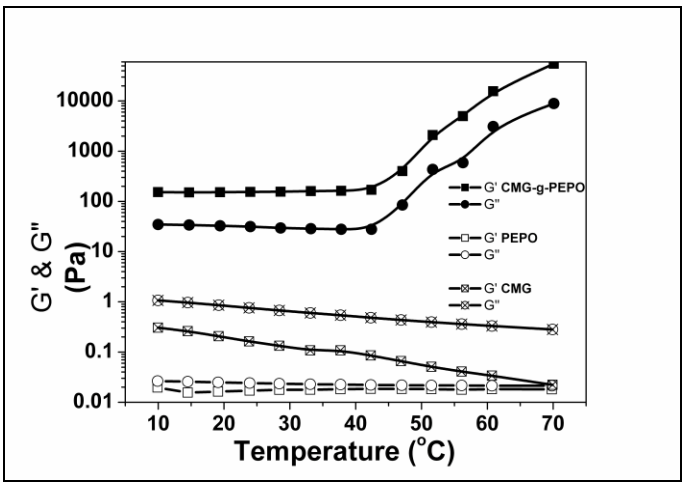

Figure 3.15*: Variation of dynamic moduli w.r.t. temperature for1wt% CMG, PEPO and CMG-g-PEPO (f =1 Hz)*

The homopolymer, CMG showed higher values of dynamic moduli (G' and G") compared to PEPO which is due to the higher MW of the CMG homopolymer. In both the homopolymers the G" > G' indicating the dominance of solution behavior in the temperature range studied. On the other hand, for the graft copolymer CMG-g-PEPO, the G' > G" in all the temperature range and shows a rapid increase in both the moduli at 40-41 ˚C exhibiting a thermo-thickening behavior. This temperature at

which the association takes place matches well with the earlier observation made with the complex viscosity (η^*) studies.

We show in **figure 3.16 (a)**, the frequency dependent viscoelastic properties (G', G" & η*) of CMG-g-PEPO and CMT-g-PEPO at 25 ºC with C_p = 2.0wt%. It can be readily seen that, CMG-g-PEPO shows more elastic behavior compared to CMT-g-PEPO at the same polymer concentration (C_p =2wt %). The G' > G" at all the frequencies studied (**figure 3.16 (a)**).

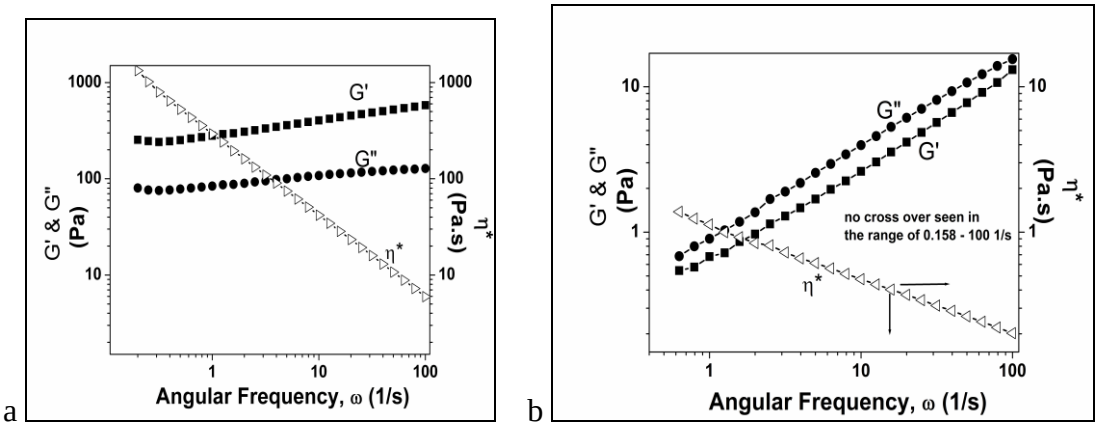

Figure 3.16: *Frequency dependence of viscoelastic parameters (G', G", η*) of (a) CMG-g-PEPO (b) CMT-g-PEPO in aqueous solution (C_p = 2wt %) at 25 ˚C*

On the other hand, in the case of CMT-g-PEPO, the G" > G' at all the frequencies studied indicating the dominance of a fuid-like behavior of the copolymer solution (**figure 3.16 (b)**).

In order to tune the thermoresponsive properties without changing the chemical nature of the synthetic side-chains grafted onto guar backbone, the influence of salt or surfactant was investigated on CMG-g-PEPO solutions.

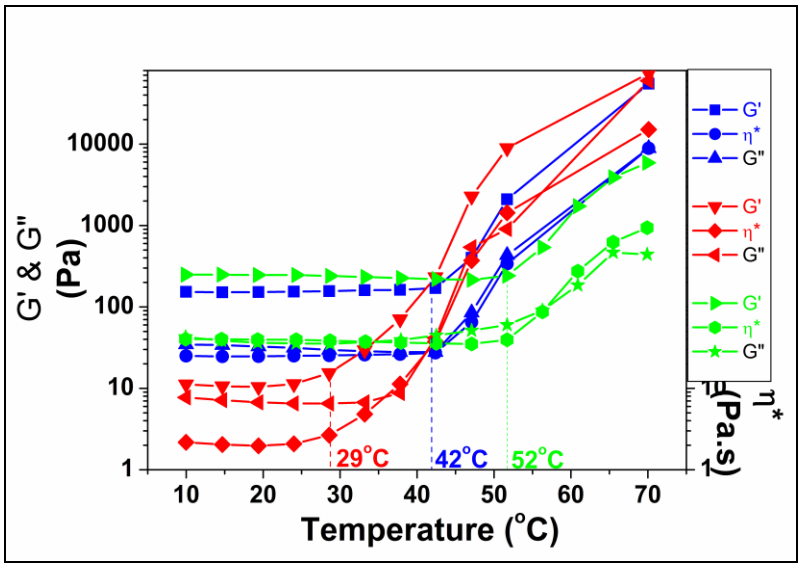

Figure 3.17: *Variation of moduli and complex viscosity with temperature for 1 wt% CMG-g-PEPO solutions in pure water, 0.6M KCl and 0.5wt% SDS*

It clearly appears that salt addition can be considered as an external trigger to easily tune the T_{ass} of the grafted copolymer since this critical temperature notably decreases with a KCl concentration (29 ˚C for KCl at 0.6 M). This phenomenon, well known as "salting-out" effect is ascribed to the decrease of PEPO solubility in salt conditions, which promotes the PEPO dehydration and thus, its hydrophobic self-association.

It further confirms that T_{ass} of grafted copolymers is governed by the thermodynamic properties of PEPO. Although, the thermo-induced association is retained, the salt addition leads to a slight lowering of the thermo thickening magnitude. Similarly a "salting-in" kind of effect is observed in the presence of surfactants (T_{ass}=52 ˚C for 0.5wt% SDS) wherein the PEPO solubility increases in surfactant and increases the T_{ass}.

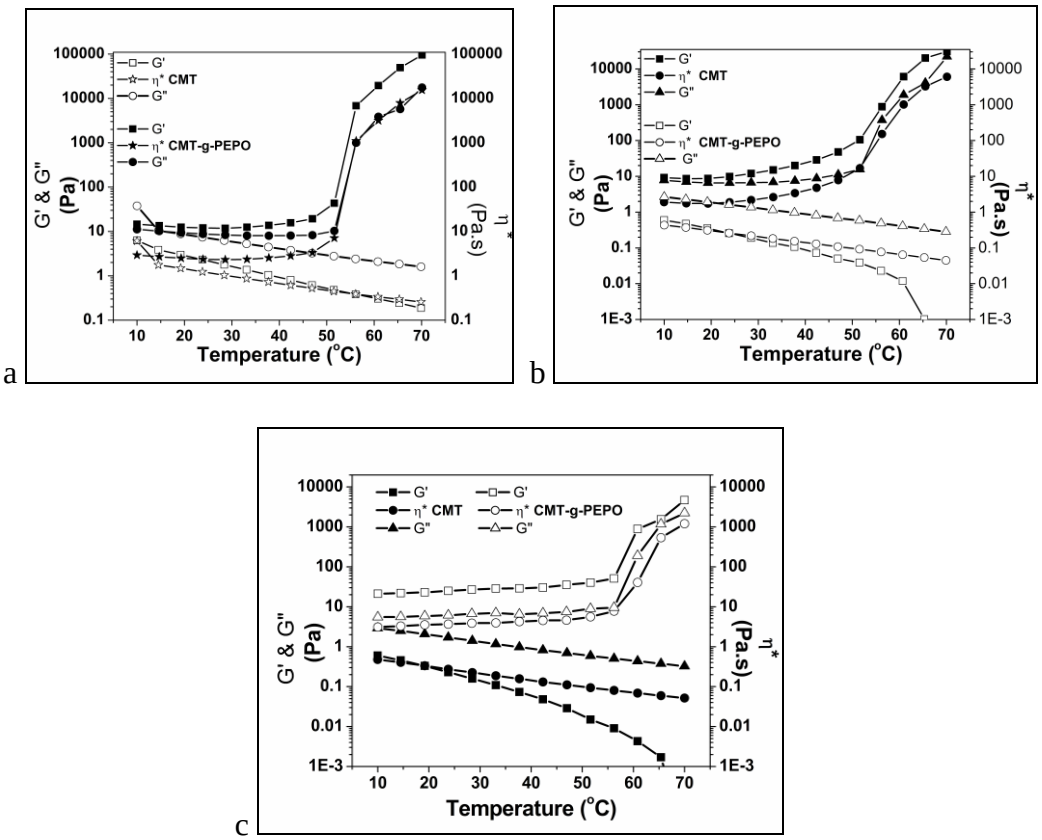

Figure 3.18: *Variation of moduli w.r.t. temperature for CMT-g-PEPO solutions in (a) pure water, (b) 0.6 M KCl and (c) 0.5wt% SDS*

The viscoelastic characteristics of CMT show a typical thermothinning behavior in the presence of surfactant. However, the graft copolymer CMT-g-PEPO at higher temperatures favor the formation of intermolecular hydrophobic association of PEPO chains and exhibit thermothickening properties at ~ 57 ˚C which is higher than that observed for aqueous solution at (~ 47 ˚C). It is can be attributed to greater solubility of CMT-g-PEPO in surfactant solution which increases the T_{ass} (**see figure 3.18**).

3.5. Conclusions

In this work, we have designed and synthesized thermo associating graft copolymers based on CarboxymethylGuar (CMG) and CarboxymethylTamarind (CMT) with LCST grafted chains of poly(*N*-isopropylacrylamide) (PNIPAm) and poly (ethylene oxide-co-propylene oxide) (PEPO) by coupling reaction between them using water-soluble coupling agent namely, 1-(3-(dimethylamino)propyl)-3-ethylcarbodiimide hydrochloride (EDC).

The graft copolymers, CMG-g-PNIPAm exhibited thermo-responsive behavior which was evidenced by the pyrene emission fluorescence measurements. Although the viscosity of CMG was increased upon the hydrophobic modification using PNIPAm, the thermo-thickening behavior was not observed due to the low content of PNIPAm side chain grafts. However, upon increasing the PNIPAm content. CMG-g-PNIPAm showed the thermo-associating behavior. At moderate concentrations (C_p=10-20g/L), the graft copolymer solutions showed soft gel-like nature and the viscoelastic properties (storage modulus, G' and loss modulus, G") were studied using oscillatory shear experiments. The activation energy, E_a of association was estimated from the TTS and was found to be ~21.0 J/mol.

The graft copolymers, CMG-g-PEPO and CMT-g-PEPO in aqueous solutions exhibited interesting thermo-thickening property which was investigated using rheology and fluorescence spectroscopy. The temperature of association (T_{ass}) was determined by microscopic line width measurements using NMR spectroscopy. The influence of salt and surfactants on the T_{ass} was also studied by rheology.

These thermo-associating polymers with the biodegradable nature of CMG and CMT can have potential applications as smart injectables in controlled release technology. They can also be used as thickeners in cosmetics and pharmaceutical formulations.

3.6. References

1. Liu, F.; Urban, M. W., Recent advances and challenges in designing stimuli-responsive polymers. *Progress in Polymer Science* **2010,** 35, (1), 3-23.

2. Meng, H.; Hu, J., A brief review of stimulus-active polymers responsive to thermal, light, magnetic, electric, and water/solvent stimuli. *Journal of Intelligent Material Systems and Structures* **2010,** 21, (9), 859-885.

3. Bokias, G.; Mylonas, Y.; Staikos, G.; Bumbu, G. G.; Vasile, C., Synthesis and Aqueous Solution Properties of Novel Thermoresponsive Graft Copolymers Based on a Carboxymethylcellulose Backbone. *Macromolecules* **2001,** 34, (14), 4958-4964.

4. Durand, A.; Hourdet, D., Synthesis and thermoassociative properties in aqueous solution of graft copolymers containing poly(N-isopropylacrylamide) side chains. *Polymer* **1999,** 40, (17), 4941-4951.

5. Kjoniksen, A. L.; Iversen, C.; Nystrom, B.; Nakken, T.; Palmgren, O., Light scattering study of semidilute aqueous systems of chitosan and hydrophobically modified chitosans. *Macromolecules* **1998,** 31, (23), 8142-8148.

6. Thatte, M. R. Synthesis and antibacterial assessment of water-soluble hydrophobic chitosan derivatives bearing quaternary ammonium functionality. Louisiana State University, Ph.D. Dissertation, **2004**.

7. Li, X.; Wu, W.; Liu, W., Synthesis and properties of thermo-responsive guar gum/poly (*N*-isopropylacrylamide) interpenetrating polymer network hydrogels. *Carbohydrate Polymers* **2008,** 71, (3), 394-402.

8. Zhang, H.; Zhong, H.; Zhang, L.; Chen, S.; Zhao, Y.; Zhu, Y., Synthesis and characterization of thermosensitive graft copolymer of *N*-isopropylacrylamide with biodegradable carboxymethylchitosan. *Carbohydrate Polymers* **2009,** 77, (4), 785-790.

9. Shi, H. Y.; Zhang, L. M., New grafted polysaccharides based on O-carboxymethyl- O-hydroxypropyl guar gum and N-isopropylacrylamide: Synthesis and phase transition behavior in aqueous media. *Carbohydrate Polymers* **2007,** 67, (3), 337-342.

10. Huh, K. M.; Hashi, J.; Ooya, T.; Yui, N., Synthesis and characterization of dextran grafted with poly (N-isopropylacrylamide-co-N, N-dimethylacrylamide). *Macromolecular Chemistry and Physics* **2000,** 201, (5), 613-619.

11. Chung, H. J.; Bae, J. W.; Park, H. D.; Lee, J. W.; Park, K. D. *Thermosensitive chitosans as novel injectable biomaterials* **2005,** Macromolecular Symposia, 224, (1), 275-286.

12. Kim, S. Y.; Cho, S. M.; Lee, Y. M.; Kim, S. J., Thermo and pH responsive behaviors of graft copolymer and blend based on chitosan and N-isopropylacrylamide. *Journal of applied polymer science* **2000,** 78, (7), 1381-1391.

13. Seetapan, N.; Mai-ngam, K.; Plucktaveesak, N.; Sirivat, A., Linear viscoelasticity of thermoassociative chitosan-g-poly (N-isopropylacrylamide) copolymer. *Rheologica acta* **2006,** 45, (6), 1011-1018.

14. Yang, Y.; Kataoka, K.; Winnik, F. o. M., Synthesis of Diblock Copolymers Consisting of Hyaluronan and Poly(2-ethyl-2-oxazoline). *Macromolecules* **2005,** 38, (6), 2043-2046.

15. Karakasyan, C.; Lack, S.; Brunel, F.; Maingault, P.; Hourdet, D., Synthesis and rheological properties of responsive thickeners based on polysaccharide architectures. *Biomacromolecules* **2008,** 9, (9), 2419-2429.

16. Karakasyan, C.; Legros, M.; Lack, S.; Brunel, F.; Maingault, P.; Ducouret, G.; Hourdet, D., Cold Gelation of Alginates Induced by Monovalent Cations. *Biomacromolecules* **2010,** 11, (11), 2966-2975.

17. Belbekhouche, S.; Ali, G.; Dulong, V.; Picton, L.; Le Cerf, D., Synthesis and characterization of thermosensitive and pH-sensitive block copolymers based on polyetheramine and pullulan with different length. *Carbohydrate Polymers* **2011,** 86, (1), 304-312.

18. Deguchi, S.; Akiyoshi, K.; Sunamoto, J., Solution property of hydrophobized pullulan conjugated with poly (ethylene oxide)-poly (propylene oxide)-poly (ethylene oxide) block copolymer. Formation of nanoparticles and their thermosensitivity. *Macromolecular rapid communications* **2003,** 15, (9), 705-711.

19. Dulong, V.; Mocanu, G.; Picton, L.; Le Cerf, D., Amphiphilic and thermosensitive copolymers based on pullulan and Jeffamine: Synthesis, characterization and physicochemical properties. *Carbohydrate Polymers* **2012,** 87, (2), 1522-1531.

20. Mocanu, G.; Mihai, D.; Dulong, V.; Picton, L.; Lecerf, D., New anionic amphiphilic thermosensitive pullulan derivatives. *Carbohydrate Polymers* **2011,** 84, (1), 276-281.

21. Kurisawa, M.; Yui, N., Modulated degradation of dextran hydrogels grafted with poly (N-isopropylacrylamide-co-N, N-dimethylacrylamide) in response to temperature. *Macromolecular Chemistry and Physics* **1998,** 199, (11), 2613-2618.

22. Staros, J. V. W., R. W.; Swingle, D. M., Enhancement by N-hydroxysulfosuccinimide of water-soluble carbodiimide-mediated coupling reactions. *Analytical biochemistry* **1986,** 156, (1), 220-222.

23. Nakajima, N. I., Y., , Mechanism of amide formation by carbodiimide for bioconjugation in aqueous media. Bioconjugate chemistry *Bioconjugate chemistry* **1995,** 6, (1), 123-130.

24. Shalaby, S. W.; McCormick, C. L.; Butler, G. B., Water-soluble polymers: synthesis, solution properties, and applications, Polymers for advanced technology **1991**, 3, (2), 95.

25. Macosko, C. W., & Larson, R. G., *Rheology: Principles, measurements, and applications*. Wiley-VCH: New York, **1994**.

26. Tanaka, F., & Edwards, S. F., Viscoelastic properties of physically crosslinked networks 1 . Transient network theory. *Macromolecules* **1992,** 25, 1516-1523.

27. Wang, S. Q., Transient network theory for shear-thickening fluids and physically

crosslinked networks. *Macromolecules* **1992,** 25, 7003–7010.

28. Durand, A., & Dellacherie, E., Aqueous solutions of native and hydrophobically

modified polysaccharides: Temperature effect. *Biomacromolecules* **2006,** 7, 958–964.

29. Tam, K. C., Farmer, M. L., Jenkins, R. D., & Bassett, D. R. , Rheological properties of hydrophobically modified alkali-soluble polymers-effects of ethylene-oxide chain length. *Journal of Polymer Science Part B: Polymer Physics* **1998,** 36, 2275-2290.

Synthesis of nanoparticles using Thermo-associating polymers

Chapter - IV

4.1. Introduction

Currently, nanometer sized materials are receiving increasing attention in biology and medicine. For example, metal nanoparticles are being widely explored for drug delivery and bio-sensing applications. Particularly, gold (Au) and silver (Ag) nanoparticles have become prominent because of their biocompatibility and non-toxicity. Further, they can be readily conjugated to a wide range of biomolecules such as amino acids, proteins, enzymes, DNA etc. without altering their biological activity. These nanoparticles exhibit interesting physical and chemical properties that arise from their smaller size and high surface/volume ratio, which differ appreciably, from those of bulk materials. A variety of techniques have been reported in the literature for the preparation of metallic nanoparticles and notable examples include salt reduction [1-3], reverse micelle process [4-7], thermal process [8, 9], irradiation [10, 11], laser ablation [12-15], and electrochemical synthesis [16-20].

In the commonly used salt reduction method, reducing agents such as sodium borohydride, sodium citrate and phosphines are used. However, the stability of nanoparticles obtained is not very good and there seems to be occurrence of aggregation of nanoparticles even with a small change in the pH and electrolyte environment. Furthermore, the use of toxic reducing agents like sodium borohydride and hydrazine can pose alot of environmental hazards. Therefore, alternative, environmentally friendly chemicals are being continuously under search for the synthesis of nanoparticles.

Polymers play an important role in controlling the formation and dispersion stability of nanoparticles, while avoiding their aggregation. Synthetic polymers like poly(vinyl alcohol) [PVA] [21-24], pol(acrylic acid) [PAA] [25-27] , poly(methacrylic acid) [PMAA] [28, 29], poly(vinylpyrrolidone) [PVP] [30-33], poly(allylamine hydrochloride) [PAH] [34, 35],

poly(ethyleneimine) [PEI] [36-38], PEGs [39, 40] and PVP [32, 33, 41] have been used for the synthesis of nanoparticles. Rita et al [41] reported the synthesis of silver nanoparticles using hydroquinone and sodium citrate as reducing agents with neutral polymers such as PVP and PVA as stabilizing agents. Besides in-situ reduction of silver ions in aqueous solution, a polymer matrix mediated reduction of silver ions has been found to be more suitable for the synthesis of polymer-silver nanocomposite particles for various biomedical applications [42-47]. Kim et al. [48] used various silver salts as starting materials and examined the effect of initial precursor content on the rate of nanoparticle formation. They found that in the presence of $AgBF_4$, $AgPF_6$ and $AgClO_4$ the initially fast rate was reduced after sometime, whereas in the case of silver nitrate ($AgNO_3$) the reaction rate was slower but constant. Park et al. [49] obtained gold nanoparticles by rapid addition of an aqueous solution of $HAuCl_4$ to an aqueous solution of ascorbic acid. At the same time, the use of natural polymers like starch, dextran, gum Arabic, heparin and hyaluronic acid has also been evaluated for the synthesis of nanoparticles [50-55]. Particularly, some of the polysaccharides have become prominent reducing agents in the preparation of metal nanoparticles. Because of their biocompatible and biodegradable nature, polysaccharides are becoming increasingly important in the preparation of metal nanoparticles for their applications in drug delivery. Further, since polysaccharides contain carbohydrate groups, the capping of Ag or Au NPs with polysaccharides makes the surface of nanoparticles carbohydrate rich which enable easy loading of drugs into nanoparticles.

In this chapter, we report on the synthesis and characterization of silver nanoparticles (AgNPs) using thermoassociating polymer namely, CMG-g-PEPO as reducing agent as well as capping agent. The advantage with CMG-g-PEPO is that, it plays a dual role of capping as well as reducing agent during the synthesis of AgNPs. Further, the

polymer layer on the nanoparticles can be made hydrophilic or hydrophobic with a small change in the temperature which will help in drug delivery applications. The AgNPs were prepared using two different concentrations of CMG-g-PEPO. The conformation of AgNPs formation was performed using UV/Vis spectroscopy. The optical and morphological properties of the AgNPs were studied using XRD, XPS, TEM and Raman spectroscopy. Finally, we demonstrated the use of these nanoparticles in controlled drug delivery applications. Doxorubicin hydrochloride (Dox), a well-known anticancer drug was loaded onto AgNPs and the release profiles of Dox from AgNPs were studied.

4.2. Experimental

4.2.1. Materials

Silver nitrate ($AgNO_3$) was purchased from S. D. Fine Chemicals Ltd, India and CMG-g-PEPO (M_n = 7.94x10^5 g/mol and M_w = 1.63x10^6 g/mol) was synthesized in the laboratory as described in Chapter III. Doxorubicin hydrochloride was received as a gift sample from RPG life sciences, Mumbai, India.

4.2.2. Methods

4.2.2.1. Preparation of AgNPs

A simple one step reaction of silver nitrate with CMG-g-PEPO was used to prepare AgNPs with the following procedure: First, aqueous solution of CMG-g-PEPO was prepared by dissolving 4 mg CMG-g-PEPO (0.02wt%) in 20 mL deionized water with continuous stirring and heating at 70 °C. After complete dissolution, pH of the solution adjusted to ~12 using dil. NaOH and the reaction vessel was wrapped with aluminum foil. Then, 1.0 mL of 0.1N $AgNO_3$ (0.0169 g) was added dropwise and the reaction mixture was kept under continuous stirring for 80 min. In a short time after addition of $AgNO_3$, the solution turned into a clear yellow color indicating the

formation of AgNPs (i.e. reduction from Ag^{+} to Ag°). Eventually, the color became light brown in the presence of CMG-g-PEPO. The progress of the reaction was monitored by recording UV-Vis absorption intermittently. Aliquots of reaction bulk were withdrawn at given time intervals (5µl to 0.5mL after every 30 min of the reaction) and the UV-Vis spectra were recorded.

Two different concentrations of CMG-g-PEPO, (i) 4 mg of CMG-g-PEPO in 20mL of deionized water (0.02wt%) and (ii) 60 mg of CMG-g-PEPO in 20mL of deionized water (0.3wt%) were used to prepare AgNPs and the samples were coded as 0.02wt% and 0.3wt% polymer treated AgNPs respectively. The flow diagram for the synthesis of AgNPs is shown in **Scheme 4.1**.

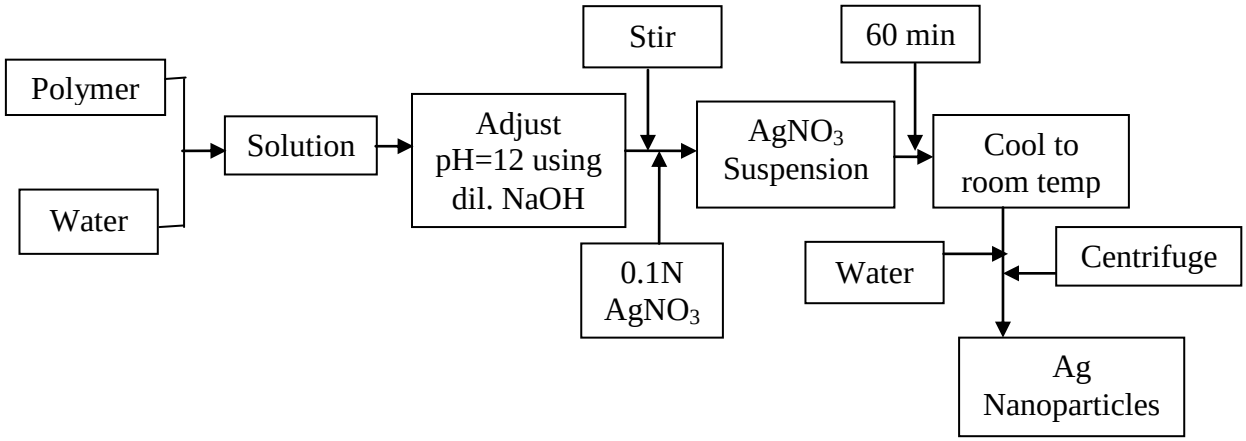

Scheme 4.1: *Flow diagram for the synthesis of Silver Nanoparticles*

4.3. Characterization

4.3.1. UV-Vis Spectroscopy

UV-visible adsorption spectra of silver nanoparticles were recorded on a SHIMADZU 1610 PC UV-2450 UV-vis spectrophotometer, Japan in the range 1000 – 200 nm. Aliquots of solutions were taken out at different time intervals during the synthesis. The change in surface Plasmon resonance of AgNPs, before and after loading of Dox was also monitored by UV-Vis spectroscopy.

4.3.2. IR spectroscopy

All the polymers were analyzed by FTIR using a Perkin Elmer, Spectrum One (Transmittance mode). 3 mg of sample was thoroughly mulled with potassium bromide (97 mg) and placed in the sample holder. The samples were scanned in the range of 4000 to 450 cm^{-1}.

4.3.3. Fluorescence spectroscopy

Fluorescence spectroscopy measurements were carried out to study the stability of Dox after binding with CMG-g-PEPO reduced AgNPs. Fluorescence spectra of free Dox solution and Dox-loaded AgNPs were recorded on Cary Eclipse Fluorescence Spectrophotometer, Varian, USA.

4.3.4. Static Light Scattering (SLS)

The SLS measurements were performed using a Brookhaven Instruments corporation UK 90 Plus particle size analyzer. The scattering intensity was measured at 90˚ angle. All AgNPs solutions were prepared in double distilled water at 2 mg/mL concentration. Prior to the measurements, the scattering cell was rinsed thrice with the filtered solution. All the experiments were performed at room temperature in triplicate.

4.3.5. Zeta potential measurements

The surface charge of AgNPs before and after loading of Dox was determined by measuring zeta potential. The electrode probe was dipped in a dilute AgNPs solution. Electric field of 7.0 V/cm was applied across two electrodes. Zeta potential was determined with input of pH. For each measurement, 5 runs were averaged with each run employing 10 cycles for 3 minutes. The data was analyzed using zeta pals software of Brookhaven instruments.

4.3.6. Transmission electron microscopy (TEM)

The morphology of nanoparticles was investigated using a high-resolution transmission electron microscope (HR-TEM) at 300 kV (Cs = 0.6 mm, resolution 1.7Å), Technai-FEI 3010. A drop of dilute AgNPs solution (2 mg/mL) was placed on a polymer coated copper grid. Grid was then allowed to dry in air and stored in desiccator before taking for microscopy.

4.3.7. X-ray diffraction (XRD)

The samples were characterized by X-ray diffraction with Philips PW1030 equipment running with CoKα radiation and a Fe filter at 40 kV and 30 mA.

4.3.8. X-ray photon Spectroscopy (XPS)

XPS spectra were recorded on a VG Microtech Multilab ESCA3000 spectrometer equipped with non-monochromatised Mg-Kα X-ray source (h_n = 1253.6 eV).

4.3.9. Raman Spectroscopy

Raman spectra were recorded on a Horiba JY LabRAM HR 800 Raman spectrometer coupled with microscope in reflectance mode with 514 nm excitation laser source and a spectral resolution of 0.3 cm^{-1}.

4.3.10. Drug loading and Drug release studies in polymeric nanoparticles

A known amount of Dox was added to a dispersion of AgNPs, prepared earlier. The solution was then incubated for 24 h at room temperature followed by centrifugation at 15000 rpm for 1h. The material thus obtained after centrifugation was separated from the supernatant liquid and redispersed in milli Q water. The supernatant liquid in PBS was assayed by UV-Vis spectroscopy at 478 nm.

The percentage loading of Dox on AgNPs was estimated by the following formula:

$$\%Loading = \frac{Total\ amount\ of\ Dox\ added - Amount\ of\ Dox\ in\ Supernatant}{Total\ amount\ of\ Dox\ added} X\ 100$$

The release of Dox from Dox-loaded AgNPs was studied using the following procedure: Dox loaded AgNPs were placed in sealed dialysis bag (MWCO 3.5 KDa) immersed in 25 mL of release buffer in a capped centrifuge tube.

The centrifuge tubes were placed in an incubator shaker with gentle shaking at 25 ˚C and 37 ˚C, respectively. At predetermined time intervals of every 1 h for the Day 1 and continued for every 12 h for 14 days, 2 mL aliquots of release medium was withdrawn from the tube and replaced with the same amount of fresh buffer. The amount of doxorubicin present in the collected buffer samples was determined by ultraviolet-visible spectrophotometric analysis. The release experiments were conducted in duplicate and were taken for calculations.

The percentage of Dox released was calculated using the equation below,

$$\%\ Cumulative\ Dox\ Released = \frac{W_t}{W_c} \text{ x } 100$$

Where W_c is the total Dox content in the dialysis bag and W_t is the Dox content in the PBS medium at time ‘t’.

4.4. Results and Discussion

4.4.1. Synthesis of AgNPs

In this study, we have used a thermo-associating polymer namely, CMG-g-PEPO for its reduction and stabilization efficacy towards the synthesis of AgNPs. CMG-g-PEPO is an interesting water-soluble polymer and undergoes a Lower Critical Solution Temperature (LCST) phenomenon at 42 ˚C. The hypothesis in our work is that the capping of CMG-g-PEPO onto AgNPs makes the surface of AgNPs rich in

carbohydrate with the –OH functional groups which will help in the subsequent attachment of large number of biomolecules for drug delivery applications. The schematics of CMG-g-PEPO capped AgNPs loaded with doxorubicin HCl is shown in **figure 4.1**.

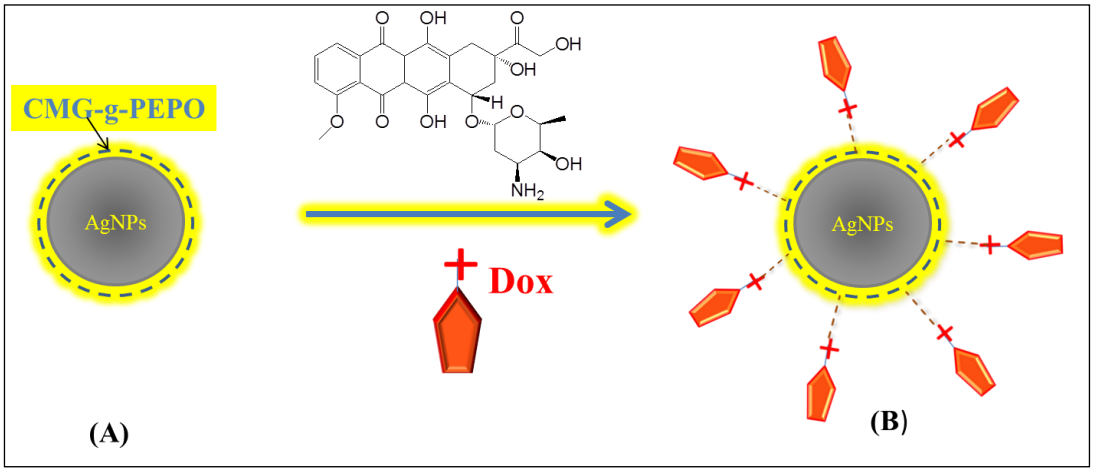

Figure 4.1: *Schematic representation of CMG-g-PEPO capping onto AgNP and loading of Dox*

The formation and evaluation of AgNPs (A) was performed by following up the UV-Vis spectra of silver nanoparticles. AgNPs exhibit an intense absorption peak at 410nm, due to the surface plasmon excitation, which represents the collective excitation of conduction electrons in the metal.

The evolution of UV-Vis spetra of AgNPs using two different concentrations of CMG-g-PEPO solutions is shown in **figure 4.2 (a) & (b)**

(a) 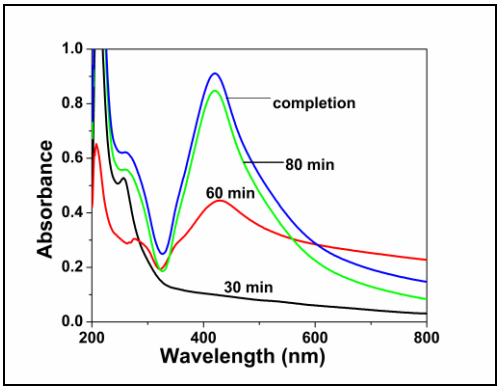

(b) 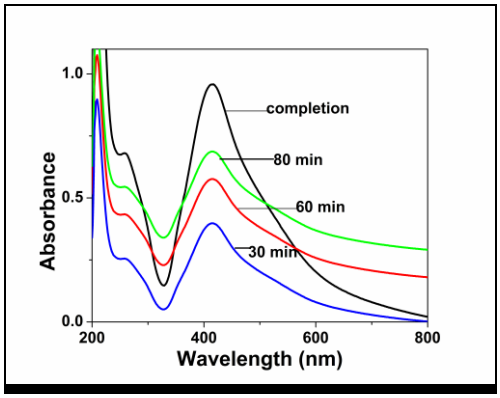

Figure 4.2: *The surface-plasmon absorbance spectrum of colloidal Ag NPs formed from CMG-g-PEPO solution (410-420 nm) with polymer concentrations of (a) 0.02wt% (b) 0.3wt%*

The observation of yellow color in the reaction mixture clearly indicates the formation of AgNPs. In the UV-Vis spectra show strong peaks with maxima around 410-420 nm corresponding to the typical surface plasmon resonance (SPR) of conducting electrons from the surface of silver nanoparticles. It can be readily seen from **figure 4.2** that, the intensity of absorption increased with time with no significant difference in the peak position or shift in SPR (at 410-420 nm), signifying a continuous reduction of the silver ions. It is also observed that increasing polymer concentration enhanced the synthesis of nanoparticles especially at short times (~30 min). The in-situ reduction of silver salts to AgNPs can be expressed as:

$$>R{-}OH + Ag^{+} \rightarrow >R{-}O{-}Ag + H^{+}$$
$$>R{-}O{-}Ag \rightarrow {-}R{=}O + Ag^{0}$$
$$>R{-}OH + Ag^{+} \rightarrow {-}R{=}O + Ag^{0} + H^{+}$$

4.4.2. Fluorescence Spectroscopy

The stability of Dox molecule after loading onto AgNPs was studied using fluorescence spectroscopy. The emission spectra of Dox and Dox-loaded AgNPs in solution were recorded from 490 to 800 nm at a fixed excitation of 480 nm; the spectra recorded are shown in **Figure 4.3**.

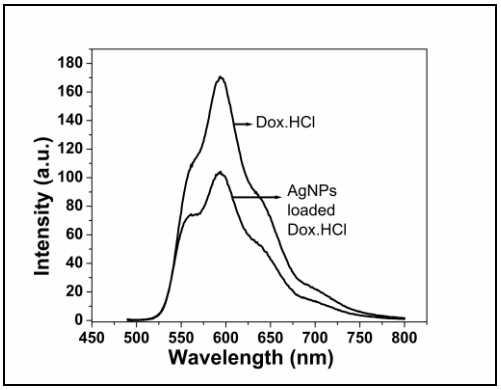

Figure 4.3: *Fluorescence spectra of Dox and Dox Loaded AgNPs solution*

There was no major change in the spectral profile of Dox-loaded AgNPs, and the peaks at 592 and 634 nm, observed for pure Dox, were retained. The decrease in peak intensities after capping with CMG-g-PEPO can be explained by slight quenching of Dox emission that is known to occur when fluorophores are close to metal nanoparticle surface. However, the preservation of fluorescence marks indicates the stability of Dox after loading onto AgNPs.

4.4.3. Transmission Electron Spectroscopy

Figure 4.4 shows the TEM images of as synthesized AgNPs with two different concentrations of CMG-g-PEPO (a) 0.02wt%; (b) 0.3wt% and (c) Dox loaded AgNP of (a). It can be revealed from **figure 4.4** that the nanoparticles are more or less spherical in shape and nearly monodisperse in nature. The size of the particles ranged from 10-25 nm.

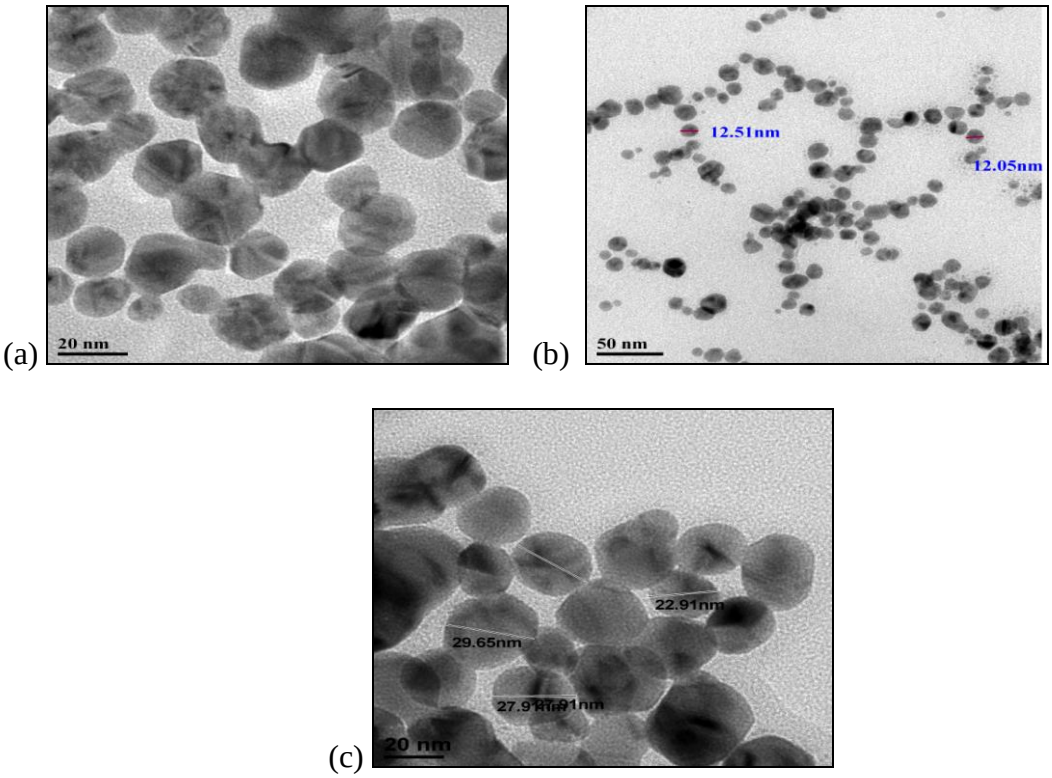

Figure 4.4: *TEM of AgNPs capped by functionalized CMG-g-PEPO (a) 0.02wt%, (b) 0.3wt% and (c) Dox loaded 0.02wt%*

We also show in **figure 4.5** the Selected Area Electron Diffraction (SAED) pattern of AgNPs (a) obtained with 0.02wt% CMG-g-PEPO and (b) the same with incorporation of Dox.

The SAED pattern shown in **figure 4.5** exhibit concentric rings with intermittent bright dots which indicate the crystalline nature of AgNPs obtained. These rings arise due to the diffraction from the (111), (200), (220) and (311) planes of face-centered cubic (fcc) silver.

(a) 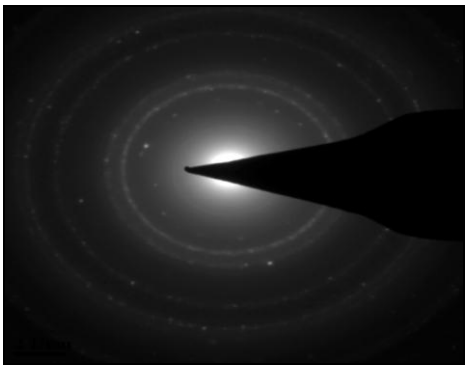 (b) 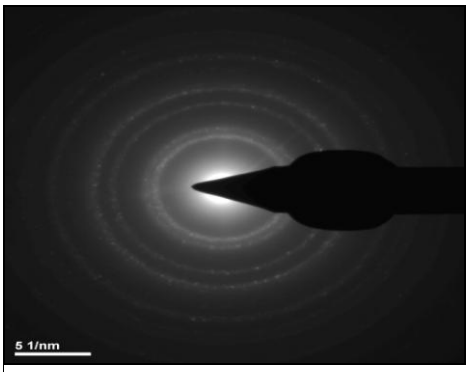

Figure 4.5: *SAED patterns of AgNPs without (a) and with (b) Dox loading*

The crystalline nature of the obtained AgNPs was further supported from X-Ray Diffraction studies.

4.4.4. X-Ray Diffraction

The XRD technique was used to determine and confirm the crystal structure of silver nanoparticles. **Figure 4.6** shows the x-ray diffraction pattern of AgNPs obtained using 0.02wt% CMG-g-PEPO.

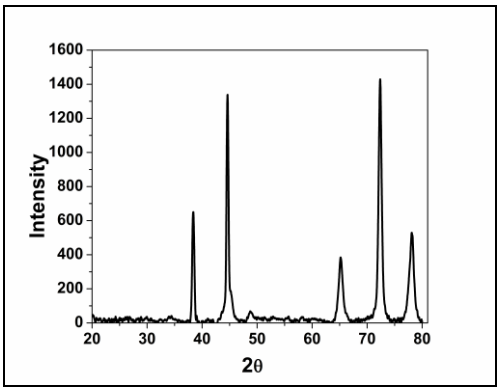

Figure 4.6: *X-ray diffraction pattern of silver nanoparticles, indicating face-centered cubic (fcc) crystal structure*

It can be seen from the figure that there are five well defined characteristic diffraction peaks at 38.3°, 44.4°, 65.1°, 72.3°, and 78.1° respectively, corresponding to (111),

(200), (220), (311), and (222) planes of face-centered cubic (fcc) crystal structure of metallic silver (**Figure 4.6**)

The interplanar spacing (d_{hkl}) values (2.34, 2.02, 1.42, 1.31, and 1.22 Å) calculated from the XRD spectrum of silver nanoparticles is in agreement with the standard silver values. Thus, the XRD pattern, further corroborates the highly crystalline nature of nanoparticles observed from SAED pattern and high-resolution TEM image (**Figure 4.4**). The lattice constant calculated from this pattern was 4.082 Å, a value which is in agreement with the value reported in the literature for silver standard values of JCPDS PDF04-0783. These observations clearly confirm the crystalline nature of AgNPs obtained in our work.

4.4.5. Static Light Scattering (SLS) and Zeta Potential of AgNPs

It is well established that SLS measurements of colloidal systems provide information on the particle size, hydrodynamic diameter and zeta potential of nanoparticles. Particularly, the zeta potential is directly proportional to the stability of colloidal systems and is an index of the magnitude of the interaction between colloidal particles which gives insight into the stability of particles. The large +ve or –ve zeta potential tends to repel the particles and prevents the agglomerations.

The zeta potential of AgNPs obtained treating with 0.02wt% and 0.3wt% of CMG-g-PEPO were found to be -18.34 mV and -24.34 mV, respectively. This clearly indicates that the AgNPs are surrounded with CMG-g-PEPO, which is an anionic polymer and helps nanoparticles to attain stability by means of electrostatic stability. Higher the polymer content on the nanoparticles, higher is the zeta potential which is evident from the above results of zeta potentials. Upon loading of cationic drug molecule, Dox onto nanoparticles, the zeta potential decreased to -13.32 mV and -11.98 mV, respectively for AgNPs treated with 0.02wt% and 0.3wt% CMG-g-PEPO.

This decrease is attributed to the presence of positively charged Dox onto the AgNPs. In order to study the influence of drug loading and temperature on the size of nanoparticles, we undertook SLS studies of the AgNPs as a function of (a) polymer content (b) temperature and (c) with and without drug loading (**See figure 4.7**).

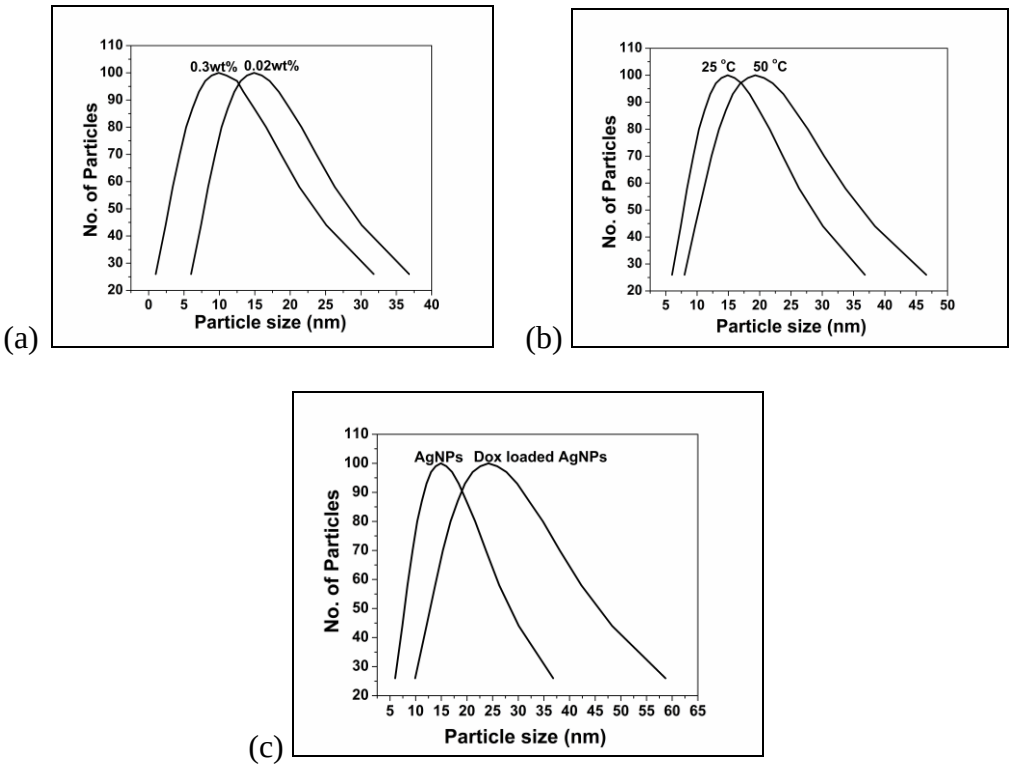

Figure 4.7: *Particle size determination as function (a) polymer concentration (b) temperature (c) AgNPs with and without Dox loading*

It can be seen from **figure 4.7(a)** that the particle size decreases from 15 nm to 9.8 nm with increase in polymer content surrounding the AgNPs. It is interesting to see from **figure 4.7(b)** that, the AgNPs wrapped with CMG-g-PEPO exhibit thermo associating behavior when the temperature was raised from 25 ˚C to 50 ˚C. The particle size increased from 10-15 nm to 20-25 nm upon increasing temperature above the LCST of polymer. This could be attributed to the swelling of polymer coils and increase in iscosity as a result of the association of PEPO chains in the polymer above the LCST.

We observe a slight increase in the size of nanoparticles upon loading of the drug, Dox onto AgNPs. We show in **figure 4.7(c)** the size of AgNPs with and without Dox at 25 °C. It can be seen that, the size of AgNPs increased from 12-15 nm to 23-25 nm upon incorporation of Dox.

4.4.6. Drug Release behavior of Dox loaded AgNPs

The drug release behavior of Dox loaded AgNPs was investigated using a dialysis membrane (MWCO ~3500) containing Dox-loaded AgNPs. The membrane was immersed in a PBS at pH 7.4 and the release of Dox in the PBS was studied as a function of time over a period of 14 days. We show in **figure 4.8** the release profiles of Dox from AgNPs at two temperatures, 25 ˚C and 37 ˚C (below and at physiological temperature which is close to LCST of the polymer ~ 42 ˚C).

The release of Dox from AgNPs was plotted in terms of cumulative drug released versus time. It can be seen from figure 9 that a burst release of Dox (~ 5-10% of the total loaded Dox) occurred in the first 2-3 hr which is attributed to the quick release of loosely bound / unbound Dox molecules onto the AgNPs. After the burst release in the initial period, the release was slow and almost at constant rate at 25 ˚C.

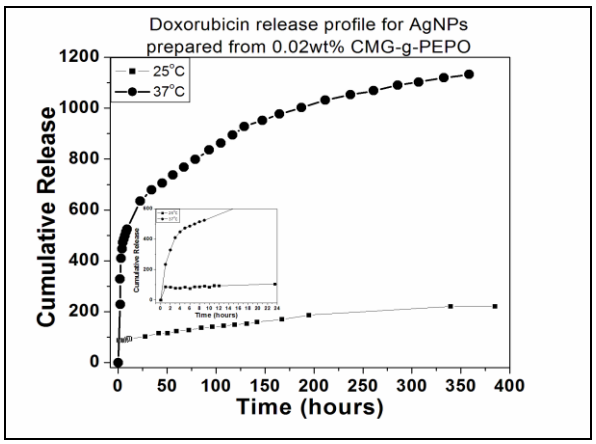

Figure 4.8: *Release profiles for Doxorubicin loaded onto AgNPs at two temperatures 25 ˚C and 37 ˚C for 0.02wt% (inset is a release profile for the first 24 hours)*

However, at 37 ˚C the release of Dox was much faster and more amount of drug was released w.r.t. time. This could be due to the expansion of polymer coils and loosening of the polymer structure on the AgNPs above LCST as a result of the thermoassociating behavior of the polymer. This can enhance the diffusion of higher amount of Dox molecules with faster rate. This is indeed, observed in the release profiles of Dox at 37 ˚C. The above results clearly indicate that the release of drug, Dox is influenced by the thermoassociating nature of the polymer surrounding the AgNPs. Therefore, by controlling the LCST of the polymer, there is a good scope to device drug incorporated nanoparticles with tailored drug release profiles.

4.4.7. X-ray Photoelctron Spectroscopy (XPS)

To provide further information on the structure and chemical state, an analysis of AgNPs with and without dox was performed using XPS. The Ag 3d, O1s and C1s core level spectra of AgNPs obtained with low (0.02wt %) (left) and high (0.3wt %) (right) concentrations of polymer (CMG-g-PEPO) are shown in **figure 4.9.** The positions, intensities and change in oxidation state of Ag 3d are compared for AgNPs with and without dox loading. From **figure 4.9 (a) and (b)** it is clear that, Ag $3d_{5/2}$ and Ag $3d_{3/2}$ peaks are present. The $3d_{5/2}$ peak at 368.5 ± 0.2eV corresponds to Ag^0 whereas that occurring at 367.5 ± 0.1eV is due to Ag^+. This clearly indicates that the dox molecule is held by AgNPs through charge transfer from silver metal to dox. The detected Ag^+ could be attributed to the formation of oxidized surfaces of AgNPs[56] .

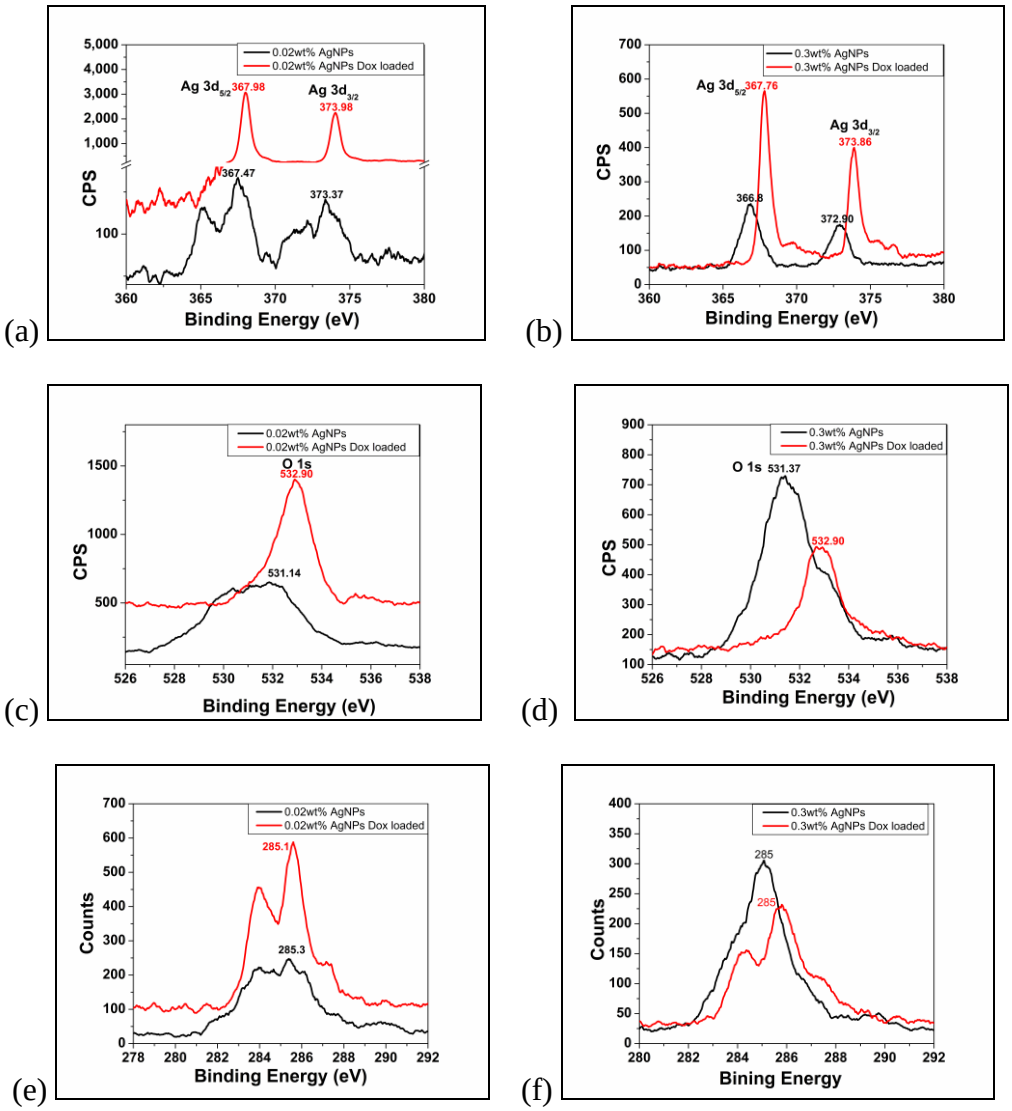

Figure 4.9: *The Ag 3d (a,b), O1s (c,d) and C1s (e,f) core level XPS spectra of AgNPs with and without loading dox molecule obtained with low (0.02wt%) (left) and high (0.3wt%) (right) concentration of polymer (CMG-g-PEPO)*

From the O1s core level spectra of AgNPs with and without dox loading and with low and high concentration polymer, it can be seen that, O 1s peaks appears at binding energies of 531.5 ± 0.4eV and 532.9 eV (from **figure 4.9 (c) and (d)),** possibly implying two or more oxygen atoms from different groups are involved in the polymer-dox interactions. Finally, from the C 1s core level spectra, the strong peak appearing at the binding energy of 285 eV indicates that the –COOH and >C=O are

the likely binding sites coming from dox and the polymer. These studies clearly indicate the presence of dox onto AgNPs upon loading with drug molecule.

4.4.8. Raman Spectroscopy

In order to find out the possible functional groups of the capping agent (CMG-g-PEPO) associated in the capping and stabilization of AgNPs and to further confirm the incorporation of dox onto the AgNPs, Raman spectra were recorded with and without loading of the dox drug molecule. For comparison, the Raman spectrum of neat dox molecule was also recorded and given in the inset of **figure 4.10.**

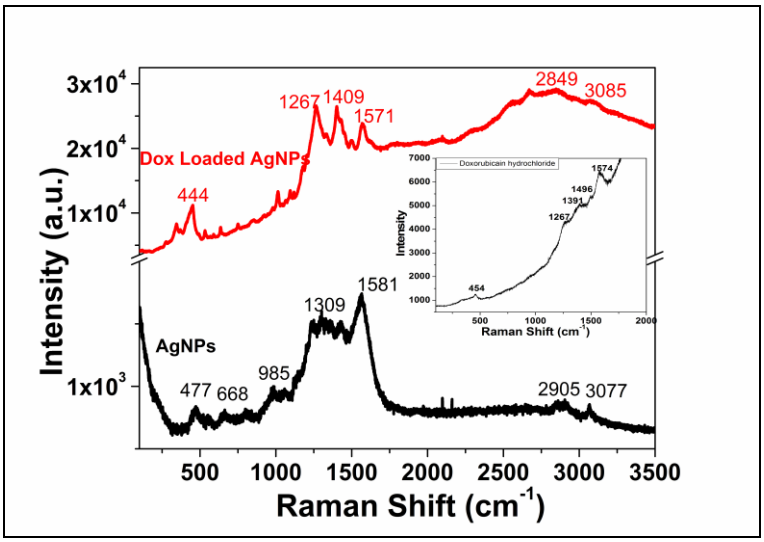

Figure 4.10*: Raman spectra of 0.02wt% AgNPs with and without dox*

In the spectrum of AgNPs (without loading of dox), the peaks at 1309 cm^{-1} and 1581 cm^{-1} can correspond to the symmetric and asymmetric -C=O stretching vibrations of carboxylate group. Thus, it can be concluded that carboxylate groups of the polymer are involved in capping of the AgNPs. However, some –OH groups of the polymer may also take part in stabilizing the AgNPs.

Upon incorporating Dox molecule onto AgNPs, one can see the characteristic peaks of the dox molecule which appear at 444 cm^{-1} and 1571 cm^{-1}. These peaks can be seen from the Raman spectra of neat dox molecule given in the inset of **figure 4.10.**

These studies clearly confirm the capping and stabilization of AgNPs by the polymer, CMG-g-PEPO and further the incorporation of dox onto AgNPs.

4.5. Conclusions

In summary, we have reported on the synthesis and characterization of AgNPs using a thermo-associating polymer namely, CMG-g-PEPO. The polymer acts as both reducing agent as well as stabilizing/capping agent. The confirmation of formation of AgNPs was done using UV/Vis spectroscopy which gave a surface Plasmon resonance in the range of 400-420 nm. The TEM images indicated the size of nanoparticles in the range of 10-20 nm. We also demonstrated the use of these nanoparticles in the controlled release of Doxorubicin hydrochloride (Dox), an anticancer drug. The binding of Dox onto the polymer and AgNPs was investigated by XPS and Raman Spectroscopy.

4.6. References

1. Kumar, A.; Vemula, P. K.; Ajayan, P. M.; John, G., Silver-nanoparticle-embedded antimicrobial paints based on vegetable oil. *Nature Materials* **2008,** 7, (3), 236-241.

2. Sileikaite, A.; Prosycevas, I.; Puiso, J.; Juraitis, A.; Guobiene, A., Analysis of silver nanoparticles produced by chemical reduction of silver salt solution. *Mater. Sci.-Medzg* **2006,** 12, 287-291.

3. Tolaymat, T. M.; El Badawy, A. M.; Genaidy, A.; Scheckel, K. G.; Luxton, T. P.; Suidan, M., An evidence-based environmental perspective of manufactured silver nanoparticle in syntheses and applications: A systematic review and critical appraisal of peer-reviewed scientific papers. *Science of the Total Environment* **2010,** 408, (5), 999-1006.

4. Bae, D.-S.; Kim, E.-J.; Bang, J.-H.; Kim, S.-W.; Han, K.-S.; Lee, J.-K.; Kim, B.-I.; Adair, J. H., Synthesis and characterization of silver nanoparticles by a reverse micelle process. *Metals and Materials International* **2005,** 11, (4), 291-294.

5. Lopez-Miranda, A.; Lopez-Valdivieso, A.; Viramontes-Gamboa, G., Silver nanoparticles synthesis in aqueous solutions using sulfite as reducing agent and sodium dodecyl sulfate as stabilizer. *Journal of Nanoparticle Research* **2012,** 14, (9), 1-11.

6. Eastoe, J.; Hollamby, M. J.; Hudson, L., Recent advances in nanoparticle synthesis with reversed micelles. *Advances in colloid and interface science* **2006,** 128, 5-15.

7. Dung, T. T. N.; Buu, N. Q.; Quang, D. V.; Ha, H. T.; Chau, N. H.; Ly, N. T.; Trung, N. V. In *Synthesis of nanosilver particles by reverse micelle method and study*

of their bactericidal properties, Journal of Physics: Conference Series, 2009; IOP Publishing: **2009**; p 012054.

8. Li, R.; Kobayashi, H.; Tong, J.; Yan, X.; Tang, Y.; Zou, S.; Jin, J.; Yi, W.; Fan, J., Radical-Involved Photosynthesis of AuCN Oligomers from Au Nanoparticles and Acetonitrile. *Journal of the American Chemical Society* **2012,** 134, (44), 18286-18294.

9. Salavati-Niasari, M.; Khansari, A.; Davar, F., Synthesis and characterization of cobalt oxide nanoparticles by thermal treatment process. *Inorganica Chimica Acta* **2009,** 362, (14), 4937-4942.

10. Chen, P.; Song, L.; Liu, Y.; Fang, Y.-e., Synthesis of silver nanoparticles by gamma-ray irradiation in acetic water solution containing chitosan. *Radiation Physics and Chemistry* **2007,** 76, (7), 1165-1168.

11. A.Arunshirwaikar; , N. P. A. S.; , K. B.; , P. L. R., Drug utilisation and evaluation of adjuvant therapy in mild to severe asthma patients *Asian Journal of Pharmaceutical and Clinical Research* **2012,** 5, (2), 151-154.

12. Amendola, V.; Meneghetti, M., Laser ablation synthesis in solution and size manipulation of noble metal nanoparticles. *Phys. Chem. Chem. Phys.* **2009,** 11, (20), 3805-3821.

13. Compagnini, G.; Scalisi, A. A.; Puglisi, O., Ablation of noble metals in liquids: a method to obtain nanoparticles in a thin polymeric film. *Phys. Chem. Chem. Phys.* **2002,** 4, (12), 2787-2791.

14. Murray, P. T.; Shin, E., Synthesis of Ag Nanoparticles by Through Thin Film Ablation. *Silver nanoparticles,* **2010,** edited by David Pozo Perez, chap 7.

15. Murray, P. T.; Shin, E., Formation of silver nanoparticles by through thin film ablation. *Materials Letters* **2008,** 62, (28), 4336-4338.

16. Khaydarov, R. A.; Khaydarov, R. R.; Gapurova, O.; Estrin, Y.; Scheper, T., Electrochemical method for the synthesis of silver nanoparticles. *Journal of Nanoparticle Research* **2009,** 11, (5), 1193-1200.

17. Rodriguez-Sanchez, L.; Blanco, M. C.; Lopez-Quintela, M. A., Electrochemical synthesis of silver nanoparticles. *The Journal of Physical Chemistry B* **2000,** 104, (41), 9683-9688.

18. Ma, H.; Yin, B.; Wang, S.; Jiao, Y.; Pan, W.; Huang, S.; Chen, S.; Meng, F., Synthesis of silver and gold nanoparticles by a novel electrochemical method. *ChemPhysChem* **2004,** 5, (1), 68-75.

19. Starowicz, M.; StypuÅ‚a, B.; BanaÅ›, J., Electrochemical synthesis of silver nanoparticles. *Electrochemistry communications* **2006,** 8, (2), 227-230.

20. Yin, B.; Ma, H.; Wang, S.; Chen, S., Electrochemical synthesis of silver nanoparticles under protection of poly (N-vinylpyrrolidone). *The Journal of Physical Chemistry B* **2003,** 107, (34), 8898-8904.

21. Black, J. R.; Cammaratta, V.; Gaddy, G. A.; Slaten, B. L.; Mills, G., Reversible Formation of Silver Nanoparticles in Poly (vinyl alcohol)-Based Thin Films via Electrochemical Switching, *Nanotech* **2007**, 4, 355-358.

22. Filippo, E.; Serra, A.; Manno, D., Poly (vinyl alcohol) capped silver nanoparticles as localized surface plasmon resonance-based hydrogen peroxide sensor. *Sensors and Actuators B: Chemical* **2009,** 138, (2), 625-630.

23. Sharma, V. K.; Yngard, R. A.; Lin, Y., Silver nanoparticles: green synthesis and their antimicrobial activities. *Advances in colloid and interface science* **2009,** 145, (1-2), 83-96.

24. Temgire, M. K.; Joshi, S. S., Optical and structural studies of silver nanoparticles. *Radiation Physics and Chemistry* **2004,** 71, (5), 1039-1044.

25. Bajpai, S. K.; Bajpai, M.; Gautam, D., In situ Formation of Silver Nanoparticles in Regenerated Cellulose-Polyacrylic Acid (RC-PAAc) Hydrogels for Antibacterial Application. *Journal of Macromolecular Science, Part A* **2013,** 50, (1), 46-54.

26. Gui, R.; Wan, A.; Jin, H.; Li, H.; Zhou, C., Rijun Gui, Ajun Wan, Hui Jin, Huili Li, Chixing Zhou. Amphiphilic polymer-template synthesis and pH-triggered phase transfer of luminescent silver nanocrystals. *Materials Letters* **2013**, 96, 20-23.

27. Liu, X.; Zhang, C.; Yang, J.; Lin, D.; Zhang, L.; Chen, X.; Zha, L., Silver nanoparticles loading pH responsive hybrid microgels: pH tunable plasmonic coupling demonstrated by surface enhanced Raman scattering. *RSC Advances* **2013**, 3, 3384-3390.

28. Duran, N.; Marcato, P. D., Nanobiotechnology perspectives. Role of nanotechnology in the food industry: a review. *International Journal of Food Science & Technology* **2012**.

29. Stuart, M. A. C.; Huck, W. T. S.; Genzer, J.; MÃ¼ller, M.; Ober, C.; Stamm, M.; Sukhorukov, G. B.; Szleifer, I.; Tsukruk, V. V.; Urban, M., Emerging applications of stimuli-responsive polymer materials. *Nature Materials* **2010,** 9, (2), 101-113.

30. Elizondo, N., Green Synthesis and Characterizations of Silver and Gold Nanoparticles. In *Green Chemistry - Environmentally Benign Approaches*, Kidwai, D. M., Ed. 2012; p 156.

31. Jin, W. J.; Lee, H. K.; Jeong, E. H.; Park, W. H.; Youk, J. H., Preparation of Polymer Nanofibers Containing Silver Nanoparticles by Using Poly (N-vinylpyrrolidone). *Macromolecular rapid communications* **2005,** 26, (24), 1903-1907.

32. Pastoriza-Santos, I.; Liz-MarzÃ¡n, L. M., Formation of PVP-protected metal nanoparticles in DMF. *Langmuir* **2002,** 18, (7), 2888-2894.

33. Shin, H. S.; Yang, H. J.; Kim, S. B.; Lee, M. S., Mechanism of growth of colloidal silver nanoparticles stabilized by polyvinyl pyrrolidone in-irradiated silver nitrate solution. *Journal of colloid and interface science* **2004,** 274, (1), 89-94.

34. Ocwieja, M.; Adamczyk, Z., Controlled release of silver nanoparticles from monolayers deposited on PAH covered mica. *Langmuir* **2013,** 29, (11), 3546-3555.

35. Yang, Z. H.; Yang, L. L.; Bai, S.; Zhang, Z. F.; Cao, W. X., Stable luminescent films and hollow spheres comprising CdTe nanoparticles. *Nanotechnology* **2006,** 17, (8), 1895.

36. Goon, I. Y. Synthesis and Modification of Magnetic Nanoparticles for Highly Sensitive Sensing. The University of New South Wales, Ph.D. Dissetation, **2010**.

37. Pulit, J.; Banach, M.; Kowalski, Z., Chemical Reduction as the Main Method for Obtaining Nanosilver. *Journal of Computational and Theoretical Nanoscience* **2013,** 10, (2), 276-284.

38. Sharma, A. K.; Shankhwar, S.; Gaur, M. S., PEI-conjugated AuNPs as a sensing platform for arsenic (AS-III). *Journal of Experimental Nanoscience* **2013**, (ahead-of-print), 1-14.

39. Merza, K. S.; Al-Attabi, H. D.; Abbas, Z. M.; Yusr, H. A., Comparative Study on Methods for Preparation of Gold Nanoparticles. *Green and Sustainable Chemistry* **2012,** 2, (1), 26-28.

40. Otsuka, H.; Nagasaki, Y.; Kataoka, K., PEGylated nanoparticles for biological and pharmaceutical applications. *Advanced drug delivery reviews* **2012,** 64, 246-255.

41. Patakfalvi, R.; Viranyi, Z.; Dekany, I., Kinetics of silver nanoparticle growth in aqueous polymer solutions. *Colloid & Polymer Science* **2004,** 283, (3), 299-305.

42. Jayakumar, R.; Menon, D.; Manzoor, K.; Nair, S. V.; Tamura, H., Biomedical applications of chitin and chitosan based nanomaterials:A short review. *Carbohydrate Polymers* **2010,** 82, (2), 227-232.

43. Liao, H.; Nehl, C. L.; Hafner, J. H., Biomedical applications of plasmon resonant metal nanoparticles. *Nanomedicine* **2006,** 1, (2), 201-208.

44. Nair, L. S.; Laurencin, C. T., Silver nanoparticles: synthesis and therapeutic applications. *Journal of biomedical nanotechnology* **2007,** 3, (4), 301-316.

45. Vigneshwaran, N.; Nachane, R. P.; Balasubramanya, R. H.; Varadarajan, P. V., A novel one-pot green synthesis of stable silver nanoparticles using soluble starch. *Carbohydrate research* **2006,** 341, (12), 2012-2018.

46. Wu, Q.; Cao, H.; Luan, Q.; Zhang, J.; Wang, Z.; Warner, J. H.; Ar Watt, A., Biomolecule-assisted synthesis of water-soluble silver nanoparticles and their biomedical applications. *Inorganic chemistry* **2008,** 47, (13), 5882-5888.

47. Yen, H. J.; Hsu, S. h.; Tsai, C. L., Cytotoxicity and immunological response of gold and silver nanoparticles of different sizes. *Small* **2009,** 5, (13), 1553-1561.

48. Kim, H. S.; Ryu, J. H.; Jose, B.; Lee, B. G.; Ahn, B. S.; Kang, Y. S., Formation of silver nanoparticles induced by poly (2, 6-dimethyl-1, 4-phenylene oxide). *Langmuir* **2001,** 17, (19), 5817-5820.

49. Park, H. K.; Lim, Y. T.; Kim, J. K.; Park, H. G.; Chung, B. H., Nanoscopic observation of a gold nanoparticle-conjugated protein using near-field scanning optical microscopy. *Ultramicroscopy* **2008,** 108, (10), 1115-1119.

50. Gardea-Torresdey, J. L.; Gomez, E.; Peralta-Videa, J. R.; Parsons, J. G.; Troiani, H.; Jose-Yacaman, M., Alfalfa sprouts: a natural source for the synthesis of silver nanoparticles. *Langmuir* **2003,** 19, (4), 1357-1361.

51. Liu, Y.; Chen, S.; Zhong, L.; Wu, G., Preparation of high-stable silver nanoparticle dispersion by using sodium alginate as a stabilizer under gamma radiation. *Radiation Physics and Chemistry* **2009,** 78, (4), 251-255.

52. Mohan, Y. M.; Raju, K. M.; Sambasivudu, K.; Singh, S.; Sreedhar, B., Preparation of acacia stabilized silver nanoparticles: A green approach. *Journal of Applied Polymer Science* **2007,** 106, (5), 3375-3381.

53. PanÃ¡cÌŒek, A.; Kvitek, L.; Prucek, R.; Kolar, M.; Vecerova, R.; Pizurova, N.; Sharma, V. K.; Tat'jana NevecÌŒnÃ¡, a.; Zboril, R., Silver colloid nanoparticles: synthesis, characterization, and their antibacterial activity. *The Journal of Physical Chemistry B* **2006,** 110, (33), 16248-16253.

54. Park, Y.; Hong, Y. N.; Weyers, A.; Kim, Y. S.; Linhardt, R. J., Polysaccharides and phytochemicals: a natural reservoir for the green synthesis of gold and silver nanoparticles. *Nanobiotechnology, IET* **2011,** 5, (3), 69-78.

55. Shan, J.; Tenhu, H., Recent advances in polymer protected gold nanoparticles: synthesis, properties and applications. *Chemical Communications* **2007**, (44), 4580-4598.

56. Farah, A. A.; Alvarez-Puebla, R. A.; Fenniri, H., Chemically stable silver nanoparticle-crosslinked polymer microspheres. *Journal of colloid and interface science* **2008,** 319, (2), 572-576.

Synthesis and Characterization of Superabsorbent Polymers [SAPs] based on Polysaccharides

Chapter - V

5.1. Introduction

Recently, there is a growing interest in the development of superabsorbent polymers [SAPs] all over the world because of their potential applications in various areas [1-2]. SAPs are hydrophilic crosslinked macromolecular network, which can absorb and hold large amount of water (100-1000 g of water per g of polymer) [2-3] and biological fluids. Because of their high swelling and absorption property, they find applications in diverse fields such as, personal hygiene products, medical, agriculture, textile and paper industries. Nearly, 900,000 tonnes of superabsorbent polymers are now produced annually [4]. Of this, 90 % of the total production goes in the manufacture of personal care products such as disposable baby diapers and feminine sanitary pads [5] since these polymers are found to absorb body fluids (blood, urine, saliva and perspiration) [6] in many personal care products.

5.1.1. Chronology of SAP development

The research on SAPs started in the United States Department of Agriculture (USDA), with a focus on application development for Corn starch which was available in abundance at very low cost. In 1969, Guggleimelli et al. of USDA accidentally discovered and issued a patent for synthesizing a superabsorbent polymer based on hydrolysed starch-g-poly(acrylonitrile) [HSPAN] [7] . Many companies in USA, realizing the potential for such highly absorbent products, obtained license under the USDA patent. Subsequently, new superabsorbent polymers based on crosslinked sodium polyacrylates were successfully developed in USA and Japan.

Japanese used SAPs extensively in personal care products and the commercial production of SAPs started in Japan in 1978. In the USA these products were reintroduced in 1985, when Proctor and Gamble's "ULTRA PAMPERS" disposable

baby diapers containing SAP came into market [4]. At the same time low-fluff diapers (containing 4-5 g of SAPs per diaper) were marketed in Japan. This was followed by the introduction of thinner diapers in other Asian countries, Europe and USA. More and more improved varieties of SAPs are being developed and have started replacing cellulose fluff in large quantities. The major producers of SAPs in the world are BASF, Germany; Nippon Shokubai, Japan; Degussa, Germany; Dow Chemicals, USA; Sumitomo Seika Chemicals, Japan; Sanyo Chemicals, Japan; San-Dia Polymers, China; Kolon Chemicals, South Korea, Formosa Plastics, Taiwan; Stockhausen, Germany; Nalco, USA [5,9].

5.1.2. Types of superabsorbent polymers

There are two major types of superabsorbent polymers available in the market today. They are (a) semi-synthetic and (b) fully synthetic.

Hydrolyzed starch-g-copolymers [HSPAN] and carboxymethyl cellulose graft copolymers fall under the category of semi-synthetic SAPs whereas, fully synthetic SAPs are based on the following:

(i) Poly(acrylic acid) alkali metal salts

(ii) Poly(alkoxy hydroxy propyl) acrylates

(iii) Poly(acrylic acid copolymers)

(iv) Poly(acrylic acid) grafted polyamide fibers

(v) Hydrolyzed poly(acrylonitrile)

(vi) Poly(maleic anhydride) vinyl-polymers

Basically, all the superabsorbent polymers are water-soluble polyelectrolytes, which are made insoluble by formation of three-dimensional network structure in the polymer using di or tri functional crosslinking agents. The crosslink density is an

important property which affects both the extent and rate of fluid absorption. Generally, higher the degree of crosslinking, higher is the modulus of gel and lower is the extent of absorption [5] of fluid.

5.1.3. Polysaccharide based SAPs

Most of the commercially available SAPs are crosslinked, partially neutralized sodium polyacrylates with very high molecular weights and have no biodegradability [6]. Therefore, SAPs producers all over the world are now concerned about the environmental problem caused by the non-biodegradability of acrylic based SAPs in disposable diapers and/ sanitary pads. Further, the toxicity and carcinogenity of residual monomers in polyacrylate based SAPs might pose problems with their use in drug delivery and personal care products.

In this context, SAPs based on renewable resource materials will be of interest due to their biocompatibility, biodegradability and non-toxicity [7]. Therefore, SAPs based on polysaccharides are attracting increasing attention lately and a few reports on the synthesis and characterization of SAPs, based on carrageenan's and sodium alginate are made in the literature [8, 9]. SAPs based on combination of Na-alginate and CMCNa have been reported since CMCNa alone gives SAP with lower gel strength. Yoshimura et al [10, 11] have synthesized and characterized SAPs based on cotton cellulose, chitin and starch using succinic anhydride as a crosslinking agent and 4-dimethylaminopyridine (DMAP) as an esterification catalyst since it is effective especially, for the esterification of secondary and tertiary –OH groups. The mechanism of crosslinking proposed is based on the partial formation of a diester between the polysaccharide –OH groups and succinic anhydride.

The SAPs obtained using cotton cellulose and succinic anhydride in the presence of DMAP showed the absorbency of water in the range of 350-400 g/g. Further, they

showed higher absorbency in NaCl solutions as compared to sodium polyacrylate based SAPs. Similar observations were also made on SAPs based on chitin and succinic anhydride.

Demitri et al. [12] have reported on the SAPs based on the crosslinking of cellulose derivatives (sodium carboxymethyl cellulose; CMCNa and hydroxyethyl cellulose; HEC) with citric acid. In these SAPs combinations of CMCNa and HEC were taken in the weight ratio of 3:1 and it was shown that the presence of HEC promotes intermolecular crosslinking rather than intramolecular crosslinking. Similarly, the combination of carboxymethyl cellulose (CMC) and sodium alginate (Na-Alg) was used for the synthesis of SAPs. It is important to note that a good mechanical strength at very large uptake of fluid is a desirable feature of SAPs. In this context, Anbergen and Oppermann [18] have reported on the elasticity and swelling behavior of CMCNa and HEC hydrogels prepared using DVS as a crosslinking agent.

5.1.3.1. Synthetic methodologies for the preparation of polysaccharide based SAPs

In general, polysaccharide based SAPs can be prepared in two ways:

1. Graft copolymerization of suitable monomer onto polysaccharides in the presence of a cross-linker
2. Direct crosslinking of polysaccharides using certain crosslinking agents

In the graft copolymerization, the initiator generates a free radical on the anhydroglucose unit (AGU) of the polysaccharide and subsequently, these free radicals initiate the graft polymerization of the vinyl monomers and crosslinking on the polysaccharide back bone chain. More commonly used initiators are ceric ammonium nitrate (CAN), [Ce^{4+} salts], manganese salts, persulfates, $FeSO_4/H_2O_2$ etc.

In the direct crosslinking of polysaccharides various crosslinking agents such as glutraldehyde, epichlorohydrin, citric acid (CA), succinic anhydride (SA), divinyl sulphone (DVS) have been employed. In the present work, we have used the direct crosslinking technique.

Although there are a few reports on the synthesis of SAPs based on polysaccharides, the polysaccharides namely, CMG and HPG have not been fully explored. Therefore, in the present work we have synthesized superabsorbent hydrogels based on cross linked CMG and HPG and studied their properties. Commercial CMG and HPG were obtained from the market and purified using standard procedure which involved: acetone extraction, drying, aqueous solution preparation, centrifugation, dialysis and freeze drying. The structural characterization of CMG and HPG were performed using IR and NMR spectroscopy. Two different crosslinking agents namely, citric acid (CA) and divinyl sulfone (DVS) were used with varying amounts to synthesise SAPs. The structure, swelling properties and the mechanical strengths of the obtained hydrogels were investigated.

5.2. Experimental

5.2.1. Materials

Carboxymethyl Guar (CMG) and Hydroxypropyl Guar (HPG) were commercial products and were kindly provided by Hindustan Gums, Haryana, India. CMG and HPG were purified [13] before use. The crosslinker, divinyl sulphone (DVS) was obtained from Aldrich, USA and Citric acid (CA) along with other reagents was of analytical grade and obtained from Merck, India. The analytical grade chemicals were used as received. Water was purified using a Millipore laboratory unit (Q- Millipore, 18.2MΩ).

5.2.2 Method

5.2.2.1. Synthesis of SAPs based on CMG-HPG-CA

The polysaccharides, CMG and HPG were purified using a method previously mentioned. A typical procedure for the synthesis of CMG-HPG-CA is given in the following: A 2-wt% solution of CMG and HPG (3:1) was prepared by adding 0.75g of CMG and 0.25g of HPG to 50ml DI water and stirred for 5-6 hrs. After complete dissolution of both the polymers, samples were stored in refrigerator overnight. The reaction mixture was then taken out and bought to room temperature followed by addition of known quantity of citric acid. Stirring was continued for 2 hrs and the solutions were poured into petri dish and kept in oven at 80 ˚C for 24 hrs under vacuum. The dried sample was soaked in DI water for 24 hrs. After complete swelling, the sample was filtered to remove any soluble moieties and the product was then isolated either by (i) acetone precipitation and drying or (ii) by lyophilization.

5.2.2.2. Synthesis of SAPs based on CMG-HPG-DVS

In a typical procedure for the synthesis of CMG-HPG-DVS, 2-wt% solution of CMG and HPG (3:1) was prepared by adding 0.75g of CMG and 0.25g of HPG to 50ml DI water and stirred for 5-6 hrs. After complete dissolution of both the polymers, samples were stored in refrigerator overnight. The reaction mixture was then taken out and bought to the room temperature and 1 ml 1M KOH (0.001mole) was added to the polymer solution and cooled to 0 ºC. After cooling, 0.846ml of 0.1N DVS solution (~1wt-% crosslinking) was added and stirred for half an hour for complete mixing of crosslinker and kept at 25 ºC for 24 hrs. During this time, the gelation took place and the swollen gel was washed with DI water, filtered and precipitated in acetone and vacuum dried.

5.2.3. Characterization

5.2.3.1. FT-IR spectroscopy

The FT-IR spectra of CMG, HPG, CMG-HPG-CA and CMG-HPG-DVS samples were recorded in a Perkin Elmer Spectrum-1-spectrometer with diffuse reflectance accessory using a KBr disc.

5.2.3.2. Equilibrium Swelling Measurements

The equilibrium swelling (grams of liquid absorbed per gram of dry polymer) of the samples was measured by immersing a known weight of a dry sample in a liquid and allowing it to reach equilibrium swelling (~15-20 hrs, depending on the particle size). In a typical procedure, a dry sample of the polymer (ca. 0.250 g) was immersed in excess of liquid at 25 ^{o}C and allowed to swell and reach equilibrium. The swollen gel was then separated from unabsorbed water by filtration and then weight was measured.

The equilibrium swelling (Q) was calculated according to the following equation:

$$\mathbf{Q = (W_2 - W_1) / W_1} \qquad (1)$$

Where, W_1 and W_2 are the weights of the dry and the swollen gel samples respectively.

Further, the Q values in aqueous NaCl solutions (concentration 0.9 and 3.5%) were investigated similarly. These concentrations correspond to those of physiological saline and seawater, respectively. All swelling data reported are the average values of three measurements.

5.2.3.3. Mechanical measurements

5.2.3.3.1. In-situ gelation by Rheometer

The in-situ gelation was studied in terms of viscoelastic properties (storage modulus, G'and the loss modulus G") of aqueous solutions of CMG, HPG and DVS at 25 °C and 35 °C. Experiments were performed on an Anton Paar MCR-301, controlled stress rheometer by using a cone-and-plate geometry (diameter = 50mm, angle = 1◦). The parameters, G' and G" were measured as a function of time at two different temperatures, 25 °C and 35 ^{o} C. The percentage strain was 1.0 % and the frequency was 0.1 Hz throughout the experiment. The time at which the cross over between G' and G" occurs is considered as the time of gelation.

5.2.3.3.2. In-situ gelation using Dynamic Mechanical Analysis

We also studied the in-situ gelation in a RSA –III Dynamic Mechanical Analyzer using locally fabricated cup-and-bob type of geometry with the dimensions of 25 mm dia and height 10mm of cup in which the bob rests. The solution which undergoes the gelation was introduced in the cup. The sinusoidal oscillation was performed uniaxially as a function of time keeping the frequency at 0.1 Hz and the strain of 1.0%. The storage modulus (E') was measured as a function of time at two different temperatures, 25 °C and 35 ^{o}C. The time at which the modulus remained constant was taken as the time for completion of gelation.

5.2.3.3.3. Mechanical strength of hydrogels by Uniaxial Compression

The mechanical strength of the hydrogels was determined by uniaxial compression of hydrogel samples between two parallel plates in RSA III (TA Instruments) at 25 °C. In a typical protocol for the compression test, 15mm dia cylindrical swollen gel was punched out and accurately positioned between two parallel plates. A preloaded force

of 0.03N was imposed to the upper plate at the beginning of measurement to ensure complete contact to the gel surface. The force versus % strain was measured for samples with different degrees of crosslinking. The yield strength was measured at the fracture of the hydrogel.

5.2.3.3.4. Mechanical strength of hydrogels by Uniaxial Tension

In dynamic mechanical test of films in tension, it is necessary to maintain a static force that is greater than the peak force level reached in the dynamic oscillation. If this condition is not met, then sample buckling will occur (because films cannot support a compressive stress) which shortens the part of the stress signal. Films with fixed dimensions length of 35mm (length) x 7 mm (width) x 0.15-0.2 mm (thickness) were cut and swollen to equilibrium and then taken for measurements. A preloaded force of 0.01N was then imposed onto the film.

5.2.3.4. Morphological Analysis

Scanning electron microscopy (SEM) and environmental SEM (ESEM) measurements (Quanta 3D FEG 400, FEI, USA) were performed to characterize the morphology of hydrogel in the dry and wet states respectively. The hydrogel disks were fractured in liquid nitrogen (- 196 °C). For SEM characterization, swollen hydrogels were freeze-dried and the hydrogel cross-section was observed under standard SEM conditions. For ESEM measurement, the fractured swollen hydrogels were characterized without further preparation. The ESEM chamber was pre-set at 5 °C with a pressure 180 Pa.

5.2.3.5. Cell viability

NIH3T3 (Mouse Embryonic fibroblast cell line) cells were grown in Dulbecco's Modified Eagle's medium (DMEM, Gibco, Carlsbad, CA, USA) supplemented with

bovine calf serum to a final concentration of 10% and penicillin / streptomycin under 5% CO_2 atmosphere at 37º C.

Cytotoxicity assay:

The cytotoxicity of gel solution on NIH3T3 was assessed by MTT (3-(4,5-dimethylthiazol-2-yl)-2,5-diphenyltetrazolium bromide) assay. For MTT assay, cells were seeded at the density of 104 cells/ well in 96 well plates and incubated for 12-16 hrs at 37º C before starting the treatment. Cells were treated with increasing concentration of gel solution (in the range of 0.1µg/ ml to 5µg/ ml) and incubated for 48 hrs. At the end of incubation period, MTT solution was added to a final concentration of 0.05 mg/ ml to each well and incubated in dark at 37 ˚C for 4 hrs. Formazan crystals were dissolved by adding 100 µl DMSO to each well and the optical absorbance was measured at 540 nm on a plate reader. The readings in untreated cells were considered to be 100 % viable.

5.2.3.6. Biodegradability

The biodegradability of the SAPs (CMG:HPG-CA and CMG:HPG-DVS) was measured by mixing the sample (0.1% each) separately in the activated sludge water sample collected from the sewage treatment plant and was kept at 27 ˚C for 30 days without any aeration and agitation. The biodegradability was evaluated by monitoring the biological oxygen demand (BOD) by titration method IS: 3025 as a standard protocol, which detected the consumption of the oxygen during the evaluation.

5.2.3.7. Sample Preparation

2wt% CMG: HPG (3:1) and different amounts of crosslinker (CA/DVS) samples were used for swelling studies and to have self standing hydrogels, 4wt% CMG: HPG (3:1) with crosslinker were used for all the mechanical measurements.

5.3. Results and discussion

5.3.1. Synthesis of CMG-HPG-CA and CMG-HPG-DVS Superabsorbent Polymers

The superabsorbent polymers CMG-HPG-CA and CMG-HPG-DVS were synthesized using two different crosslinking agents namely, citric acid and divinyl sulphone. The combination of CMG and HPG was taken in the ratio of (CMG: HPG) 3:1 on the weight basis. It is interesting to note that the presence of HPG is necessary to promote intermolecular crosslinking rather than intramolecular, which results in stable gel formation. Infact, the use of only CMG alone for the reaction gives rise to a very poor intermolecular crosslinking leading to the formation of water-soluble polymer. Therefore, the idea of good crosslinking property of HPG and better swelling property of CMG encouraged us to use blends of CMG and HPG for the synthesis of SAPs. The mechanisms of crosslinking of CMG: HPG blends with CA and DVS are shown in **Scheme 5.1 (a) & (b)**

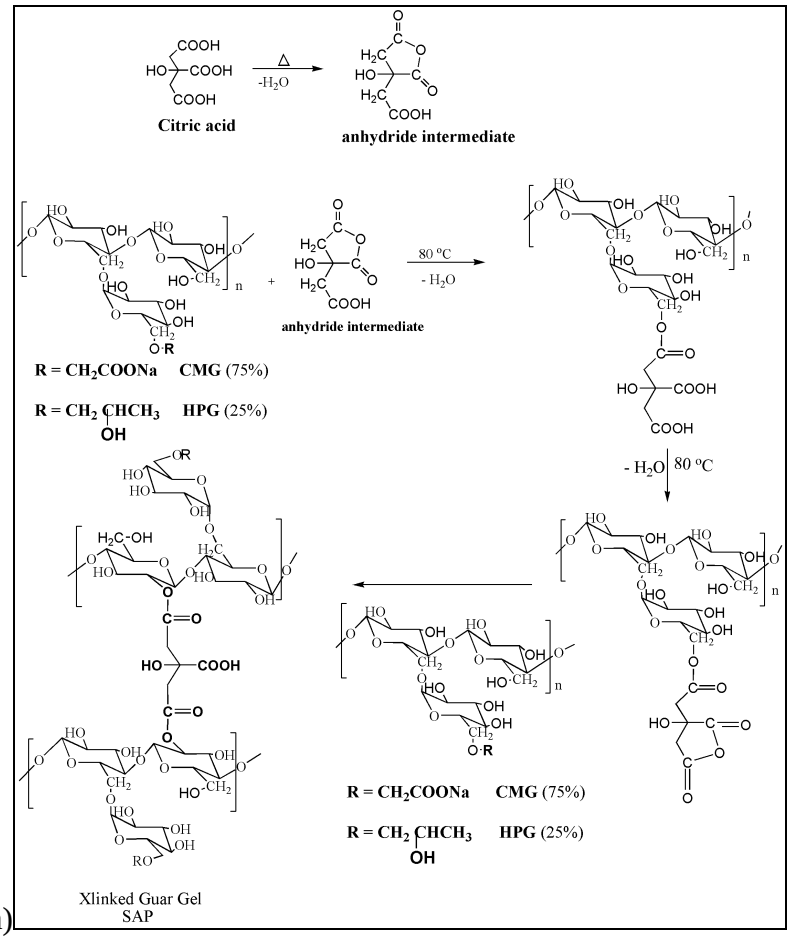

(a)

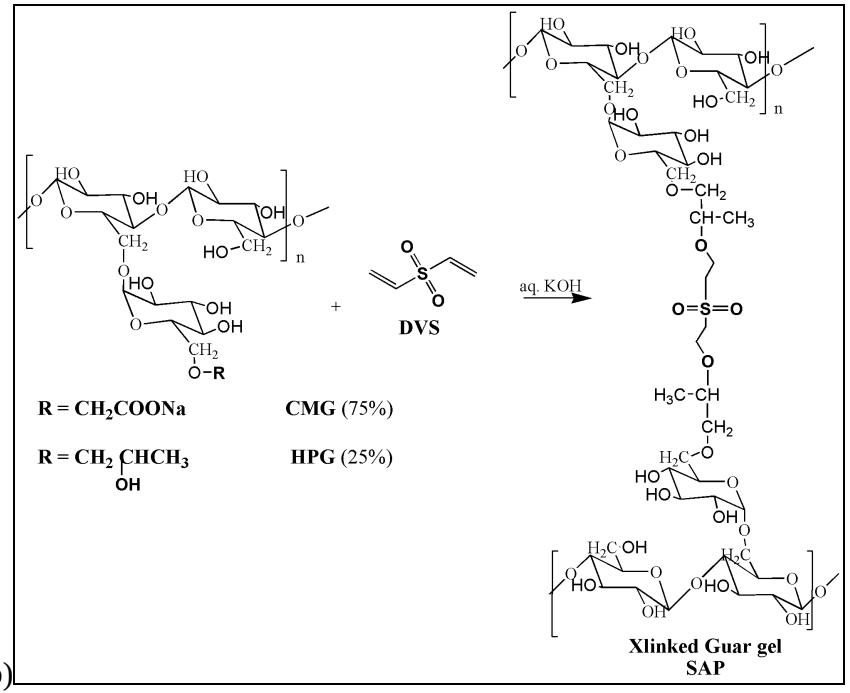

(b)

Scheme 5.1: *Crosslinking of CMG: HPG using (a) citric acid and (b) divinyl sulphone*

It can be seen from **Scheme 5.1(a)** that, CA undergoes dehydration to yield cyclic anhydride which reacts with the –OH of HPG / CMG. Subsequently, another cyclic anhydride can be achieved into the CA structure through the other two unreacted carboxylic groups allowing the reaction with other –OH group of HPG/ CMG effecting the crosslinking reactions. Therefore, an esterification mechanism is proposed to explain the crosslinking reaction in CMG/ HPG blends. In the case of crosslinking of CMG / HPG with DVS, the crosslinking reaction occurs via the hydroxyl groups of polysaccharide forming an ether bond as shown in **Scheme 5.1(b)**

In the combination of CMG with HPG, the CMG being a polyelectrolyte is hydrophilic in nature and majority of the –OH groups at the C_6 position are substituted by carboxymethyl groups. Therefore, for the crosslinking reaction only a few –OH groups at C6 position along with most of the other less reactive –OH groups at C_2 and C_3 positions are available. This could be one of the reasons for poor crosslinking efficiency of CMG.

Further, the presence of charges on CMG induces electrostatic repulsion which can impede the intermolecular contacts leading to poor crosslinking. HPG, on the other hand is non-ionic and the –OH groups are more reactive because of less steric hindrance which promote the formation of intermolecular chemical bridges, thus allowing the macromolecules to stabilize into a 3-D polymer network.

The final crosslinked polymers, CMG-HPG-CA and CMG-HPG-DVS with different degrees of crosslinking were obtained by precipitation in acetone and vacuum drying. The structural characterization of polymers was done by FT-IR Spectroscopy.

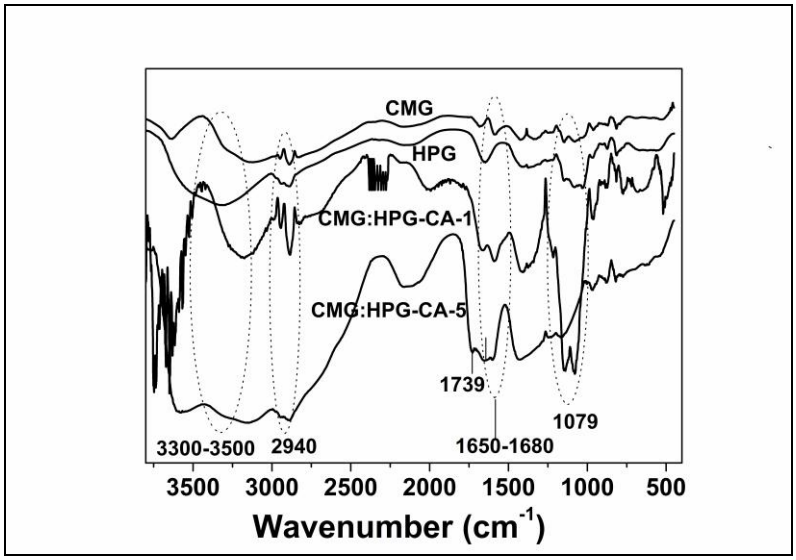

Figure 5.1*: IR spectra of CMG, HPG and CMG-HPG-CA-1 and CMG-HPG-CA-5*

The presence of broad absorption band at 3300cm^{-1}-3500 cm^{-1} is assigned to -OH stretching and the sharp peak at 2940 cm^{-1} is due to –CH stretching in all the four polymers. The absorption band appearing at 1650 cm^{-1} is due to the carboxylate salt [14] present in CMG, CMG-HPG-CA 1wt% and CMG-HPG-CA 5wt% but also appears in HPG that could be assigned to presence of stretching of water molecule which tend to overlap. The –C-O-C- glycidic bridges bending appear at 1140 cm^{-1}.The presence of sharp peak at 1739 cm^{-1} is more prominent in CMG-HPG-CA 5wt% due to formation of ester linkage in the crosslinked system (**from figure 5.1**).

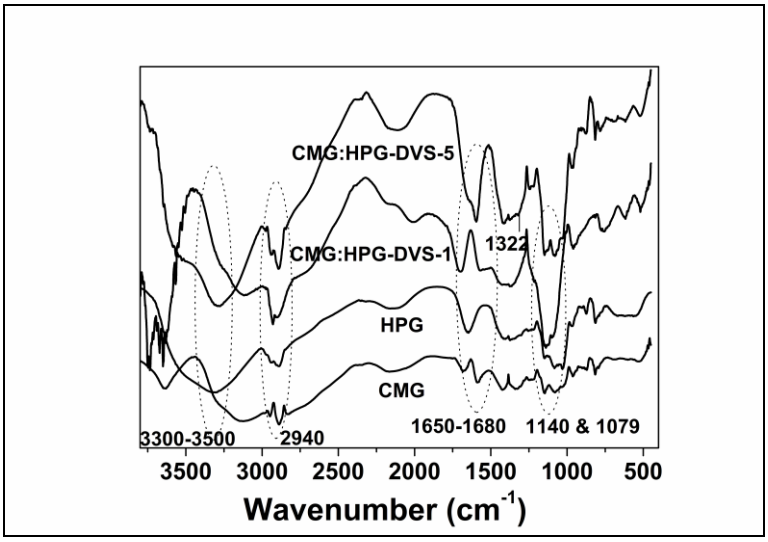

Figure 5.2: *IR Spectra of CMG, HPG, CMG-HPG-DVS-1 and CMG-HPG-DVS-5*

In **figure 5.2,** the IR spectra of CMG, HPG, CMG:HPG-DVS1 & CMG:HPG-DVS5 are shown. The characteristic peaks at 1148cm^{-1} and 1322 cm^{-1} arise due to to SO_2 linkages of -HPG-DVS-1 and CMG-HPG-DVS-5. The presence of broad absorption band in the range of 3300-3500cm^{-1} is assrigned to –OH stretching of the polysaccharide part. The peak at 2940cm^{-1} belongs to –CH stretching in all the polymers investigated. The absorption band appearing at 1650 cm^{-1} is due carboxylate salt [14] present in CMG, CMG-HPG-DVS-1 and CMG-HPG-DVS-5 but also appears in HPG that could be assigned to the presence of stretching of water molecule whereas the –C-O-C- glycosidic bridges bending appears at 1140 cm^{-1}.

5.3.2. Equilibrium swelling in SAPs

The equilibrium swelling capacity of SAPs depend upon the degree of crosslinking, degree of ionization in the polymer, interactions between the polymer- solvent and the presence of salts in the external solution (i.e. ionic strength of external solution).

We show in **figure 5.3**, the equilibrium swelling capacity of CMG-HPG-CA and CMG-HPG-DVS samples as a function of degree of crosslinking.

(a) 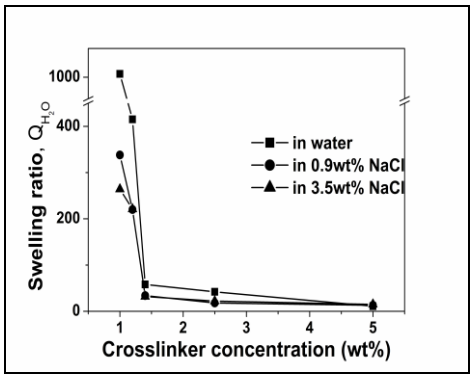

(b) 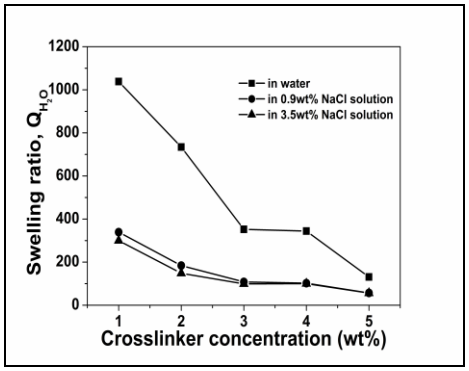

Figure 5.3: *Effect of (a) Citric Acid and (b) Divinyl sulphone concentration on absorbency in water, 0.9wt% NaCl and 3.5wt% NaCl*

It is interesting to note that, when an attempt was made to crosslink homopolymers CMG and HPG individually with crosslinking agents CA and DVS (with 1%), the gelation did not take place and on the contrary water soluble polymers are obtained. This can be attributed to the fact that, in these reactions the crosslinking takes place intramolecularly leading to the formation of soluble polymers. Only in the presence of HPG, the gelation is more significant due to intermolecular crosslinking of HPG in combination with CMG. As shown in **figure 5.3(a) and (b)**, the equilibrium swelling capacity of both CMG-HPG-CA and CMG-HPG-DVS polymer decrease with increase in CA and DVS contents. This is of course well established fact that, the swelling capacity decreases with increase in crosslinking of the network. The equilibrium swelling capacity of both the polymers in water almost reaches ~ 1.0 litre/g at 1.0wt% crosslinking.

It can be readily seen from the figure that the swelling capacity of polymers crosslinked with CA decreases rapidly with increase in degree of crosslinking. Whereas, for the polymers crosslinked with DVS, the decrease in swelling capacity is rather gradual. Further, the swelling capacity of CMG-HPG-DVS samples is higher

even at high content of DVS. This must be due to more number of oxygen atoms in the crosslinked structure which can induce H-bonding interaction between polymer and water.

Although increasing the ionic strength always reduces the equilibrium swelling capacity of polyelectrolyte gels, a higher sensitivity to ionic strength is displayed by CMG-HPG-CA samples. This can be seen from **figure 5.4**, where we show the comparative results of equilibrium swelling capacities of CMG-HPG-CA and CMG-HPG-DVS with 5% crosslinking agent. The effect of ionic strength of the external solution (0.9% and 3.5% NaCl) on the equilibrium swelling capacity is also shown in **figure 5.4**.

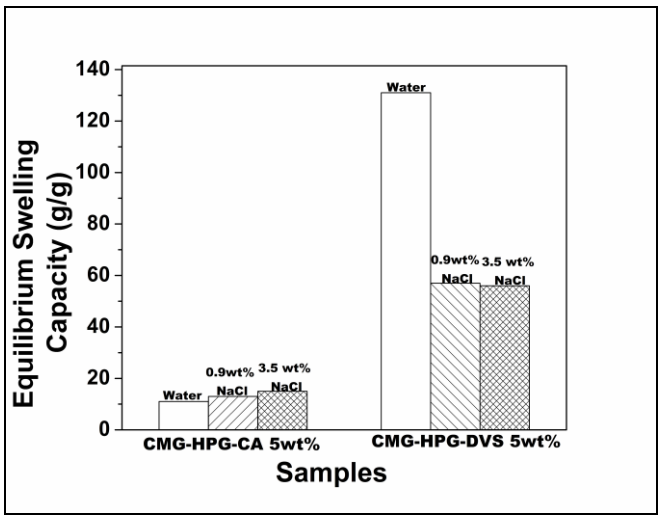

Figure 5.4: *Swelling ratios of CMG-HPG with 5wt% Citric acid and Divinyl sulphone crosslinked respectively in DI water, 0.9wt% NaCl and 3.5wt% NaCl*

The decrease in swelling capacity in salt solutions is commonly observed in ionic hydrogels which is often attributed to a charge screening effect by additional cations which leads to a decreased osmotic pressure (ionic pressure) difference between the hydrogel network and the external solution.

5.3.3. Incipient Gelation by in-situ modulus measurements

The gelation time in the crosslinking reaction between CMG: HPG and DVS was studied by in-situ measurement of storage modulus (G') and loss modulus (G") of aqueous solution of the reaction mixture as a function of time at two different temperatures. The measurements were performed in an Anton Paar rheometer and the details are given in an experimental section.

(a) 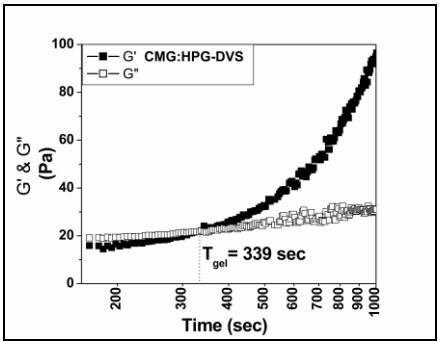

(b) 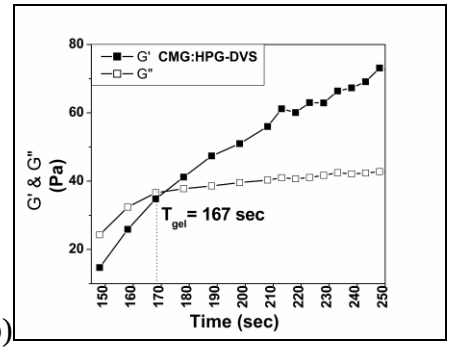

Figure 5.5: *Influence of temperature on the time of gelation for 4wt% CMGHPG DVS sample by oscillatory measurements at (a) 25 °C, (b) 35 °C*

We show in **figure 5.5** the plots of G' and G" of CMG:HPG and DVS solution mixture with 4.0 wt% DVS content with respect to time at 25 °C and 35 °C. In the initial period, when the reation mixture is still in the liquid state, G" > G', indicating the dominance of viscous behavior. However, with increase in time, G' > G" and the solution transforms into a gel due to the crosslinking reaction between CMG-HPG and DVS. In the first approximation, the time corresponding to the crossover of G' and G" (G'=G") can be considered as an indication for the incipient gelation.

From the figure 5.6, it can be readily seen that for the crosslinking reaction with 4.0 wt% DVS, the crossover occurs at ~ 340 seconds and ~ 170 seconds respectively, for the reactions at 25 °C and 35 °C. It can be seen that by increasing the reaction temperature by 10 °C, the sol-gel transition time reduces by 50%. It can also be seen

from the same figure that, the values of G' increase sharply after the incipient gelation and probably reach a plateau value after the complete gelation exhibiting high value of modulus (G').

In order to examine the complete gelation process, we performed gelation experiments in a Dynamic Mechanical Analyser (DMA) using RSA-III DMA Spectrometer. The storage modulus (E') was monitored as a function of time for the reaction between CMG: HPG and DVS (4.0 wt %) at temperatures 25 °C and 35 °C. The experimental protocol is discussed in the previous sections.

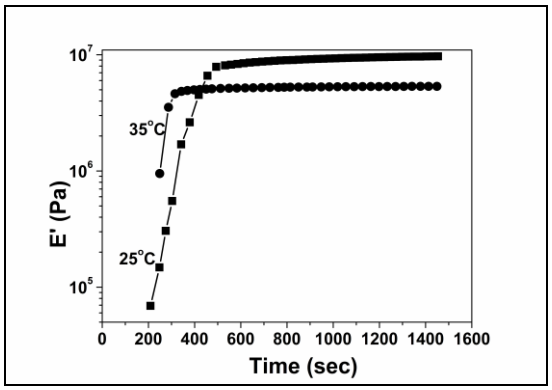

Figure 5.6: *Influence of temperature on the time of complete gelation at for 4wt% CMGHPG DVS crosslinker by dynamic mechanical analysis test at 25 °C and 35 °C*

We show in **figure 5.6** the plots of E' versus time for CMG: HPG and DVS (4.0 wt %) at 25 °C and 35 °C. It is observed from the **figure 5.6** that, E' increases with time sharply and attains a plateau value after complete gelation. The obtained gels after complete gelation were found to have very high modulus with good mechanical strength.

5.3.4. Uniaxial Compression of Swollen Gels

The mechanical strength of hydrogel can be studied by modulus measurements. Particularly, the uniaxial compression tests are easier to perform and give reproducible results. The mechanical strength of CMG: HPG hydrogels crosslinked

with 8.0 wt% CA and DVS were determined by uniaxial compression of hydrogels (of dimensions 15.0 mm dia X 10.8 mm height) between two parallel plates of RSA-III (TA instruments, USA) using Dynamic Mechanical Analyzer at 25 °C. The crosshead speed was maintained at 1mm/min. the detailed measurements protocol is discussed in the experimental section. The appearance of swollen hydrogels and mounting of sample in DMA is shown in **figure 5.7**.

(a)  (b) 

Figure 5.7*: (a) swollen hydrogels sample punched from discs (b) Punched disc mounted between two parallel plates of DMA*

The plots of Force versus strain for the swollen hydrogels of CMG: HPG-CA and CMG: HPG-DVS with 8.0 wt% crosslinking are shown in **figure 5.8**.

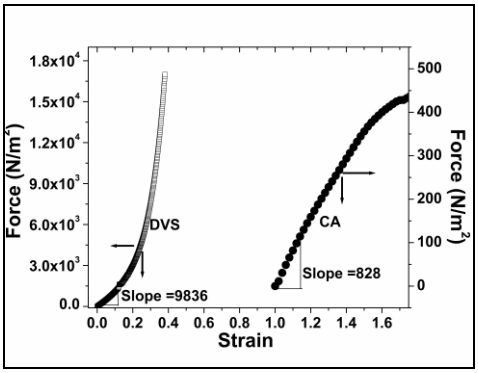

Figure 5.8: *Comparison of Modulus for equilibrium swollen CMG: HPG-CA and CMG: HPG-DVA (8wt% crosslinked gels) CA and DVS gels*

It can be seen from the **figure 5.8** that, the DVS crosslinked hydrogels show higher modulus compared to the CA crosslinked hydrogels. Further, the DVS crosslinked

hydrogels exhibit strain hardening behavior with exponential increase in Force at low strains whereas, CA crosslinked hydrogels show more elastic behavior with soft nature. From these results it can be concluded that DVS crosslinked hydrogels are more homogenous in nature with well crosslinked structure.

5.3.5. Scanning Electron microscopy

The microstructures of the polymers after treatments with solvents/freeze drying were examined by SEM **figure 5. 9.** The SEM micrographs showed that the microstructures of the polymers changed from small pores to loose macro-pores upon treatments with solvents/freeze drying. With the increase of the mean pore size, the specific surface area of the polymer is increased greatly, leading to increase in the water absorption rate.

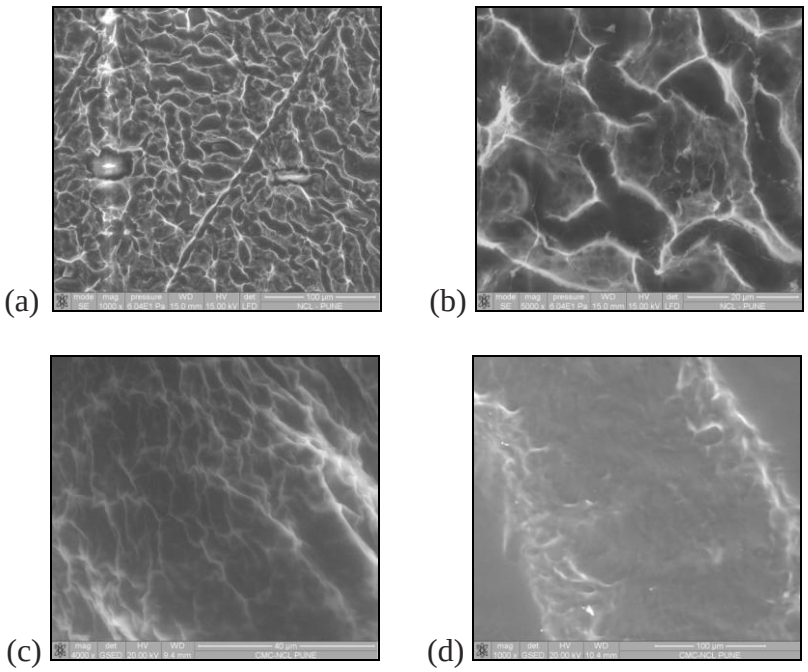

Figure 5.9: *SEM micrographs of swollen hydrogels in freeze-dried state: (a) CMG:HPG -CA 4wt% (b) CMG:HPG -CA 8wt%, ESEM micrograph of swollen hydrogel (c) CMG:HPG-CA 1wt% (d) CMG:HPG-CA 5wt%*

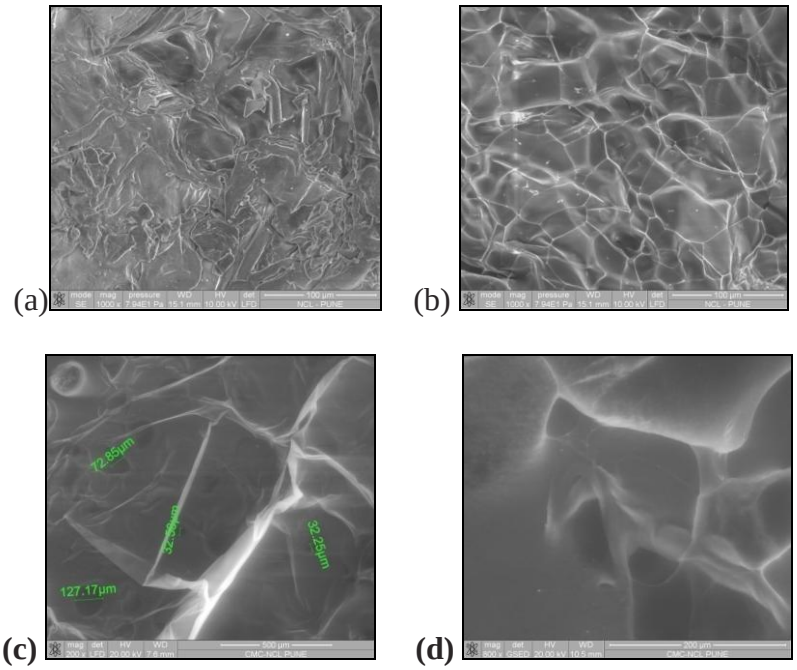

Figure 5.10: *SEM micrographs of swollen hydrogels in freeze-dried state: (a) CMGHPG -DVS 4wt% (b) CMGHPG -DVS 8wt%, ESEM micrograph of swollen hydrogel (c) CMGHPG-DVS 1wt% (d) CMGHPG-DVS 5wt%*

To confirm the presence of a microporous structure within the newly synthesized CMGHPG DVS hydrogel treated with extraction in acetone, SEM and ESEM micrographs were taken. In both cases, it can be observed that the xerogel structure is quite similar to that reported in the literature for microporous hydrogels desiccated through the same procedure [1, 15]. The numerous foldings on the gel surfaces suggest that a connected microporosity is likely to be present. In fact, the structures characterized by a higher microvoids show remarkably higher sorption uptakes. However a detailed investigation is necessary to draw conclusions from morphology.

5.3.6. Cell viability

Biocompatibility is the property of material of not having toxic or injurious effects on biological systems. Cell culture assays are used to assess the biocompatibility of a material or extract through the use of isolated cells *in vitro*. These techniques are useful in evaluating the toxicity or irritancy potential of materials and chemicals. They provide an excellent way to screen materials prior to *in vivo* tests.

Cytotoxicity is the property of material of being toxic to cells. Therefore, cell viability is a technique of determination of living or dead cells, based on a total cell sample. Viability measurements may be used to evaluate the death or life of cancerous cells and the rejection of implanted organs. The MTT cytotoxicity assay is a method by which one can accurately measure the toxicity on as few as 950 cells. MTT is a colorimetric method that measures the reduction of yellow 3-(4, 5-dimethylthiazol-2-yl)-2,5-diphenyl tetrazolium bromide by mitochondial succinate dehydrogenase. Because the cellular reduction is only catalyzed by living cells, it is possible to quantify the percentage of living cells in a solution.

The MTT assay can be used to evaluate the cytotoxicity of extractable materials of medical devices, Toxic compounds, Toxins and environmental pollutants, Potential anti-cancer drugs and antibodies to examine growth inhibiting potential. The major advantages of the MTT assay are the quantitative ability and can be done on either extracts or by direct contact with the material.

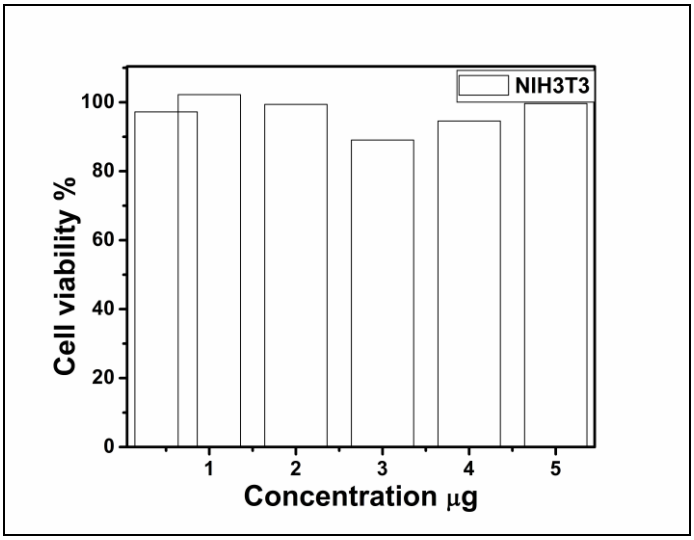

Figure 5.11: *Cell Viability for CMG: HPG-DVS SAP*

Figure 5.11 shows cell viability versus incubation time with different concentrations of SAPs. The results in figure show a very high survival rate for CMG:HPG-DVS gel leading to significantly higher viabilities, measured nearly 90%. These studies indicate that CMG:HPG-DVS SAPs don not show any cytotoxicity even at higher concentrations and exhibit very good biocompatibility.

Further study concerning the biocompatibility of the CMG: HPG DVS SAPs with respect to fibroblast cell line was performed with the aim of acquiring more information concerning its biocompatibility. 3T3 fibroblasts was used to perform biocompatibility studies in terms of cell viability and proliferation after contact with media conditioned by the material

5.3.7. Biodegradability

Biodegradability of various materials can be measured by continuous Biological Oxygen Demand (BOD) test which is one of the most common measures of pollutant organic material in water. BOD indicates the amount of decable organic matter present in water. Therefore, a low BOD is an indicator of good quality water, while a high BOD indicates polluted water. Dissolved oxygen (DO) is consumed by bacteria

when large amounts of organic matter from sewage or other discharges are present in the water.

In order to make the test quantitative, the samples must be placed in an airtight container and kept in a controlled environment for a preselected period of time. In the standard test, a 300-mL BOD bottle is used and the sample is incubated at 20°C for five days[16]. The BOD is then calculated from the initial and final dissolved oxygen (DO) concentration.

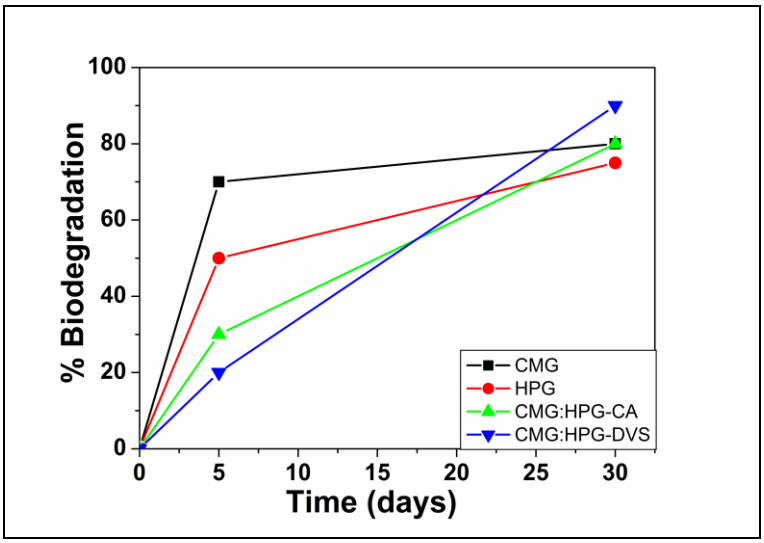

Figure 5.12: *Biodegradability of CMG, HPG, CMG:HPG-CA and CMG:HPG-DVS at 27 ˚C*

We show in **figure 5.12,** the biodegradation of CMG, HPG, CMG:HPG-CA and CMGHPG-DVS was measured by continous BOD test monitored on 5th and 30th day. The biodegradation of unmodified CMG and HPG was fast and the degradation was 50-70% in the first 5 days and reached amost 80% in 30days. Whereas, the SAPs showed slower degradation initially (upto 20-30%) in 5 days but exhibited nearly 80-90% degradation in 30 days. These studies clearly confirmed the biodegradable nature of the SAPs that we have synthesized. This is a desirable feature of the present days SAPs.

5.4. Conclusions

In this chapter, we have reported on the synthesis and characterization of new SAPs based on crosslinked polysaccharides namely, Carboxymethyl Guar (CMG) and Hydroxypropyl Guar (HPG). These polysaccharides are cheap, abundantly available and not fully explored for the synthesis of SAPs. The crosslinking of CMG and HPG in combination was effected using two different crosslinking agents, namely citric acid (CA) and Divinyl sulphone (DVS). The characterization of SAPs in terms of swelling and mechanical strength was performed by equilibrium swelling capacity and dynamic mechanical measurements. The SAPs exhibited good swelling characteristics and particularly, SAPs with DVS crosslinking showed better mechanical strength in the swollen state. The biodegradability and Cytotoxicity/Cell viability studies were performed on the SAPs and found to be biodegradable (~ 90% in 30 days), non-toxic with good cell proliferation. These materials have potential applications as biodegradable SAPs.

5.5. References:

1. Sannino, A., Application of Superabsorbent Hydrogels for The Optimization of Water Resources in Agriculture. **2008**.

2. Zohuriaan-Mehr, M. J.; Kabiri, K., Superabsorbent polymer materials: a review. *Iranian Polymer Journal* **2008,** 17, (6), 451.

3. Buchholz, F. L.; Peppas, N. A., *Superabsorbent polymers: science and technology*. American Chemical Society: 1994.

4. Parry, M., Pampers: The Disposable Diaper War **2009**.

5. Kiatkamjornwong, S.; Mongkolsawat, K.; Sonsuk, M., Synthesis and property characterization of cassava starch grafted poly [acrylamide- co-(maleic acid)] superabsorbent via γ-irradiation. *Polymer* **2002,** 43, (14), 3915-3924.

6. Buchanan, K. J.; Hird, B.; Letcher, T. M., Crosslinked poly (sodium acrylate) hydrogels. *Polymer Bulletin* **1986,** 15, (4), 325-332.

7. Zamani, A., *Superabsorbent polymers from the cell wall of zygomycetes fungi*. Chalmers University of Technology, Ph.D Dissertation, **2010**.

8. Pourjavadi, A.; Barzegar, S.; Mahdavinia, G., MBA-crosslinked Na-Alg/CMC as a smart full-polysaccharide superabsorbent hydrogels. *Carbohydrate polymers* **2006,** 66, (3), 386-395.

9. Wang, Y.; Liu, M.; Ni, B.; Xie, L., κ-Carrageenan–Sodium Alginate Beads and Superabsorbent Coated Nitrogen Fertilizer with Slow-Release, Water-Retention, and Anticompaction Properties. *Industrial & Engineering Chemistry Research* **2012,** 51, (3), 1413-1422.

10. Yoshimura, T.; Matsuo, K.; Fujioka, R., Novel biodegradable superabsorbent hydrogels derived from cotton cellulose and succinic anhydride: Synthesis and characterization. *Journal of Applied Polymer Science* **2006,** 99, (6), 3251-3256.

11. Yoshimura, T.; Yoshimura, R.; Seki, C.; Fujioka, R., Synthesis and characterization of biodegradable hydrogels based on starch and succinic anhydride. *Carbohydrate polymers* **2006,** 64, (2), 345-349.

12. Demitri, C.; Del Sole, R.; Scalera, F.; Sannino, A.; Vasapollo, G.; Maffezzoli, A.; Ambrosio, L.; Nicolais, L., Novel superabsorbent cellulose based hydrogels crosslinked with citric acid. *Journal of Applied Polymer Science* **2008,** 110, (4), 2453-2460.

13. Gupta, N. R.; Ghute, P. P.; Badiger, M. V., Synthesis and characterization of thermo-sensitive graft copolymer of carboxymethyl guar and poly (*N*-isopropylacrylamide). *Carbohydrate polymers* **2011,** 83, (1), 74-80.

14. Dodi, G.; Hritcu, D.; Popa, M. I., Carboxymethylation of guar gum: Synthesis and characterization. *Cellulose Chemistry and Technology* **2011,** 45, (3), 171.

15. Marcì, G.; Mele, G.; Palmisano, L.; Pulito, P.; Sannino, A., Environmentally sustainable production of cellulose-based superabsorbent hydrogels. *Green Chem.* **2006,** 8, (5), 439-444.

16. Fujioka, R.; Tanaka, Y.; Yoshimura, T., Synthesis and properties of superabsorbent hydrogels based on guar gum and succinic anhydride. *Journal of Applied Polymer Science* **2009,** 114, (1), 612-616.

“Click Chemistry” approach for the synthesis of APs and Hydrogels

Chapter - VI

6.1. **Introduction**

Since the discovery of the Cu(I)- catalyzed version of the 1,3-dipolar cycloaddition between azides and alkynes (CuAAC), referred to as "Click Chemistry", this reaction has received a great deal of interest in diverse fields such as, biconjugation in-vitro and in-vivo, dendrimer synthesis, polymer ligation, combinatorial organic synthesis and surface science [1]. Recently, click chemistry has also shown great success in synthesizing various functional materials including hydrogels because of its high efficiency, reliability and selectivity [2, 3]. Typically, 1, 3-dipolar cycloaddition can be accomplished with a fast rection speed, no byproducts and good stability under physiological conditions. Therefore, it has become increasingly attractive in the fields of tissue engineering and drug delivery, particularly for hydrogel synthesis. For example, Malkoch et *al*.[4] synthesized diacetylene and tetrazide –functionalized poly(ethylene glycol) (PEG) derivatives, which reacted with each other to form a PEG based hydrogel having well defined network structure with improved mechanical properties (**Scheme 6.1**)

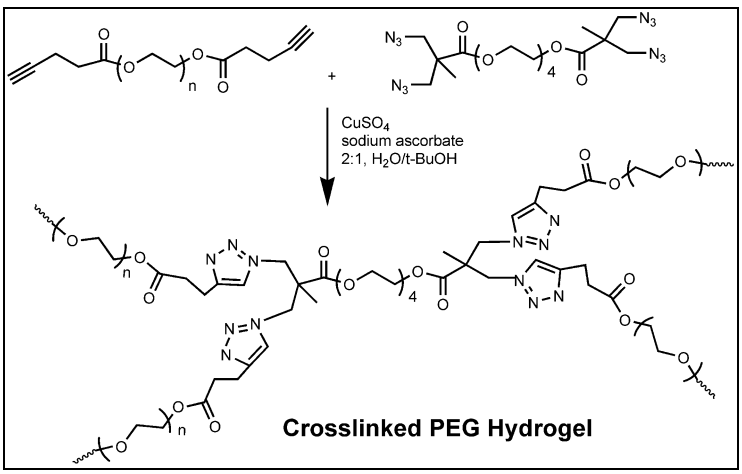

Scheme 6.1: *Modular approach for hydrogel construction based on Click chemistry and PEG-based building blocks*

Some macromolecular derivatives such as poly(vinyl alcohol) (PVA) and hyaluronic acid (HA) form hydrogels by the 1,3-dipolar cycloaddition reaction cataylsed by Cu (I)[5].

Xiaohong Hu et *al*.[6] synthesized biological hydrogels from hyaluronic acid (HA), gelatin (G) and chondroitin sulphate (CS) by "Click Chemistry" approach (**see scheme 6.2**).

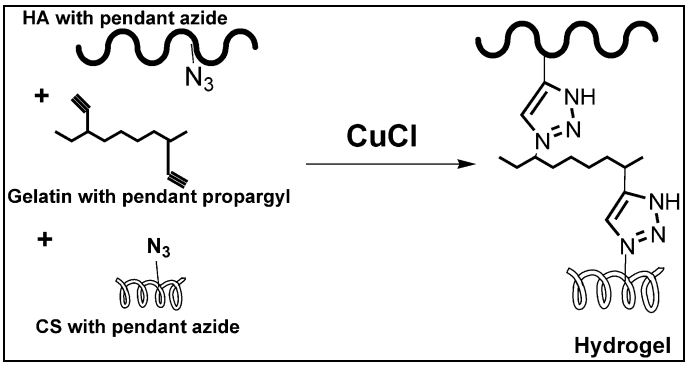

Scheme 6.2: *Schematic illustration to show formation of the hydrogel through click chemistry using HA, G and CS*

Gloria Huerta-Angeles et *al*. [7] reported on the synthesis of highly substituted amide hyaluronan derivatives with tailored degree of substitution and their crosslinking via click chemistry approach. The crosslinking reaction of azido- and alkynyl-amide derivates of HA led to the formation of highly organized and porous networks, which due to their high stability against degradation are potential candidates for application as drug delivery systems, or scaffolds in tissue engineering (**see scheme 6.3**).

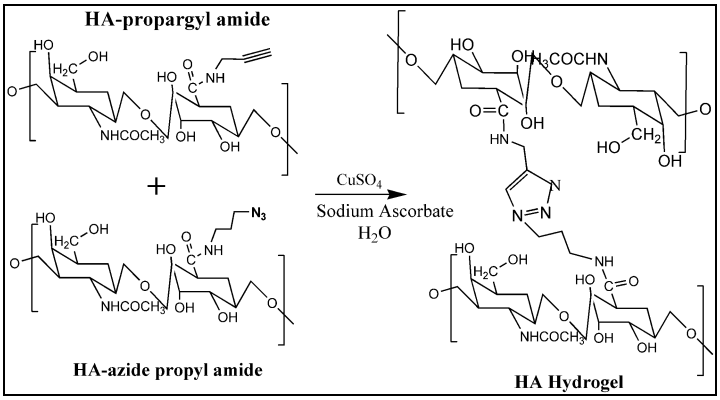

Scheme 6.3: *Crosslinking reaction between HA-propargyl amide (HA-Pr) and HA-azide propyl amide (HA-APA) leading to gel formation*

The synthesis of novel thermo-responsive biohybrid grafted copolymers by exploiting the efficient, versatile and robust copper-catalysed azide-alkyne Huisgen cycloaddition (CuAAC) to graft PEO-co-PPO onto guar backbone was reported by Tizzotti et *al*.[8] (**see scheme 6.4**).

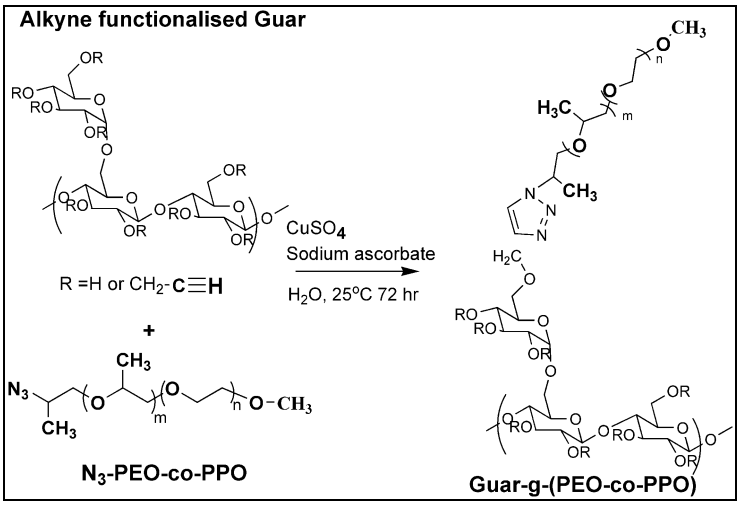

Scheme 6.4: *Synthesis of Guar-g-(PEO-co-PPO)*

In a recent report, the rheological and degradative studies have demonstrated that, the Diel-Alder click reaction is a suitable crosslinking method for Hyaluronic acid [9-11].

We present here an approach for the synthesis of biodegradable polymeric hydrogels based on the use of hydrolysable and cleavable linkages such as carbonate esters and

disulphides. We have used Hyaluronic acid (HA) as a starting material to synthesize hydrogels using click-chemistry approach.

The tetrabutylammonium salt of hyaluronic acid (HA-TBA) was modified respectively with alkyne and azide groups which are connected to the HA-TBA backbone through (biodegradable) hydrolysable carbonate esters and subsequently, were cross-linked via 'click' chemistry in the presence of copper catalyst.

It is known that such carbonate esters hydrolyse under physiological conditions and gives rise to degraded product along with CO_2 [12]. On the other hand, HA hydrogels with cleavable disulphide linkages are biodegradable due to the reduction of disulfide bonds by dithiothreitol (DTT) [13]. The hydrogels obtained were characterized for presence of functional groups in their structure using FT-IR and NMR spectroscopy.

The preparation of HA-TBA hydrogel with hydrolysable carbonate esters involves the following steps: (i) synthesis of tetrabutyl ammonium salt of hyaluronic acid (HA-TBA) (ii) synthesis of prop-2-ynyl 1H –imidazole-1-carboxylate and 3-azidopropyl-1H-carboxylate from the reaction between di(1H-imidazol-1-yl)methanone and prop-2-yn-1-ol and 3-azidopropan-1-ol, respectively. (3-azidopropan-1-ol was prepared from 1, 3-Chloropropanol and activated sodium azide) (iii) Synthesis of alkyne pendant HA-TBA (iv) Synthesis of azide pendant HA-TBA then, (v) Click reaction between products of steps (iii) & (iv).

In the preparation of HA-Na hydrogel with the disulphide cleavable linkage, the following steps are involved: (i) preparation of prop-2-ynyl2-(2-(2-aminoethyl) disulfanyl) ethylcarbamate from the reaction between prop-2-ynyl 1H –imidazole-1-carboxylate and cystamine (ii) reaction between prop-2-ynyl2-(2-(2-aminoethyl) disulfanyl) ethylcarbamate and HA-Na to obtain alkyne pendant of HA-Na with

cleavable disulphide linkages (iii) synthesis of an azide pendant HA-Na (iv) click reaction between products of steps (ii) & (iii).

6.2. Experimental

6.2.1. Materials

Propargyl alcohol (PA-OH), di(1H-imidazol-1-yl)methanone, 3-chloropropanol, sodium azide, Cystamine dihydrochloride, hyaluronic acid sodium salt (HA-Na)(Mw~$3.1X10^5$ Da), Dowex 50WX-8-40 ion exchange resin and 1-ethyl-3-3-dimethylaminopropyl carbodiimide (EDC) were purchased from Sigma-Aldrich, USA. Sodium ascorbate and tetra butyl ammonium hydroxide (TBA-OH) were purchased from S.D. Fine Chemicals, India. Polyethylene glycol (20 kDa), dichloromethane, ether, ethyl acetate, dimethyl sulfoxide (DMSO), copper sulfate ($CuSO_4$), magnesium sulfate and sodium sulfate, sodium hydroxide, isopropanol, chloroacetic acid, tetrabutylammonium hydrogen sulfate, methanol, hydrochloric acid and triethylamine (TEA), were purchased from Merck, India.

6.2.2. Methods

6.2.2.1. HA-TBA hydrogels with carbonate esters linkages

6.2.2.1.1. Synthesis of tetra butyl ammonium salt of HA (HA-TBA)

In a 500 mL beaker, ion-exchange resin, Dowex 50WX-8-400 (12.5 g) was first washed with water (3 x 250 mL). Then, TBA-OH (24.5 mL) was added to the Dowex resin and stirred for 30 min. The resulting Dowex-TBA resin was separated by filtration and stored. Sodium salt of HA-Na (5 g) was dissolved in water (100 mL), and added to the Dowex-TBA resin (10 g). After stirring for 3 h, the supernatant was filtered through 0.45 µm filter to remove the Dowex resin and the clear solution of HA-TBA was then lyophilized.

6.2.2.1.2. Synthesis of prop-2-ynyl 1H –imidazole-1-carboxylate

A dry 500 mL three necked round bottom flask was charged with di(1H-imidazol-1-yl)methanone (29.19 g, 180 mmol) and dichloromethane (200 mL) yielding a turbid suspension. Prop-2-yn-1-ol (5.82 mL, 100 mmol) was added under vigorous stirring yielding a clear solution upon dissolution of the propargyl alcohol. After 1 h reaction at room temperature the reaction mixture was extracted with water (3 x 35 mL). The organic layer was dried over sodium sulfate. After filtering off the sodium sulfate the liquid was evaporated by rotary evaporation and prop-2-ynyl 1H –imidazole-1-carboxylate was obtained as a dry powder (11.86 g; 79 % yield). ^{1}H-NMR in $CDCl_3$: δ (ppm) 2.6 (t, 1H, HC≡C-), 5.0 (d, 2H, CH_2-O), 7.0 (s, 1H, C=CH-N), 7.4 (s, 1H, N-CH=C), 8.1 (s, 1H, N-CH=N).

6.2.2.1.3. Synthesis of an alkyne modified HA-TBA

In a 100 mL dry round bottom three necked flask, *HA-TBA* (1.0 g, 0.0026 mol) was dissolved in anhydrous DMSO (20 mL). To the reaction mixture prop-2-ynyl 1H –imidazole-1-carboxylate (0.12 g 7.96 X 10^{-4} mol) was added and the reaction mixture was stirred overnight at 50 °C under the nitrogen atmosphere.

Subsequently, the reaction mixture was put in dialysis bags (Mw cut off ~ 3.5 kDa; Spectra Por) and dialyzed against pure water for 5 days. After lyophilization, the alkyne modified of HA-TBA was obtained as white fluffy powder.

6.2.2.1.4. Synthesis of 3-azidopropan-1-ol

3-Chloropropanol (15 mL; 17 g; 0.18 mol), activated sodium azide (23.37 g; 0.359 mol) and tetrabutylammonium hydrogen sulfate (0.5 g) were dissolved in 40 mL water and stirred at 80°C for 24 h followed by overnight stirring at room temperature. The solution was extracted with 100 mL ether three times and dried over sodium

sulfate. The ether was removed by rotary evaporation and 3-azidopropanol was obtained as a liquid and was purified by vacuum distillation (boiling point 62°C at 3-4 mbar). Yield was 71 %. ^{1}H-NMR in $CDCl_3$: δ (ppm) 1.84 (m, 2H, C-CH_2-C), 3.46 (t, 2H, CH_2-N_3), 3.76 (t,2H, CH_2-O).

6.2.2.1.5. Synthesis of 3-azidopropyl 1H-imidazole-1-carboxylate

A 250 mL three necked round bottom flask was charged with di(1H-imidazol-1-yl)methanone (9.12 g, 0.056 mol) and ethyl acetate (100 mL) which formed a turbid suspension. 3-Azidopropan-1-ol (0.037 mol, 3.48 mL, 3.79 g) was added dropwise under vigorous stirring upon which the reaction mixture turned into a clear solution. After 2 h reaction at room temperature, the solution was extracted with water (3 x 100 mL). The organic layer was dried over sodium sulfate. After filtering off the sodium sulfate, the solvent was evaporated by rotary evaporation and 3- azidopropyl 1H-imidazole-1-carboxylate was obtained as a liquid.

6.2.2.1.6. Synthesis of an azide modified HA-TBA

In a dry 100 mL round bottom flask, *HA-TBA* (1.0 g, *2.6* X 10^{-3} mol) was dissolved in anhydrous DMSO (20 mL). To this mixture, 3- azidopropyl 1H-imidazole-1-carboxylate (0.128 g, 6.5 X 10^{-4} mol) was added and the reaction was stirred overnight at 50 °C under the nitrogen atmosphere. Subsequently, the reaction mixture was put in dialysis bags (Mw cut off 3.5 kDa; Spectra Por) and dialysed against pure water for 5 days. After lyophilisation azide derivative of HA-TBA was obtained as a white fluffy powder.

6.2.2.1.7. Click reaction between alkyne modified and azide modified HA-TBA

Alkyne modified HA-TBA (12.5 mg) and azide modified HA-TBA (12.5 mg) were swollen in pure water (420 µl). This solution was added to 536 µl of a 50 % (w/w in

pure water) polyethylene glycol solution (which helps in making hydrogel in microenvironment) and vortexed for 60 sec. $CuSO_4$ (17 µl of a 50 mg/mL stock solution) and sodium ascorbate (17 µl of a 50 mg/mL) were added followed by briefly vortexing. The reaction was allowed to proceed for 30 min followed by the addition of water (10 mL) and 3 centriufation (1000 g / 3 min)/washing steps with 10 mL water.

6.2.2.2. HA hydrogel containing disulphide linkages

6.2.2.2.1. Synthesis of prop-2-ynyl 2-(2-(2-aminoethyl)disulfanyl)ethylcarbamate

A dry round bottomed flask was charged with cystamine dihydrochloride (13.0 g, 57.75 mmol), sodium hydroxide (4.62 g, 115.5 mmol) and water (20 mL). After 1 h stirring at room temperature, the mixture was evaporated to remove the water. Then the residue was redissolved in dichloromethane (40 mL), filtered (to remove undissolved particles) and dried over sodium sulfate. By filtering the sodium sulfate and evaporating by rotary evaporation, cystamine (8.74 g; 67% yield) was obtained as yellow oil after drying in vacuum. Then, Cystamine (4.4 g, 28.52 mmol) was dissolved in dichloromethane (30 mL) and prop-2-ynyl-1H–imidazole-1-carboxylate (3.47 g) dissolved in dichloromethane (20 mL), was added dropwise to the reaction mixture. The reaction was carried out under stirring at room temperature for 24 h. Then, the solvent was evaporated and the residue was treated with NaH_2PO_4 (100 mL, pH 4.2) and subsequently, extracted with ether (3 x 30 mL) to remove the diprop-2-ynyl 2,2'-disulfanediylbis(ethane-2,1-diyl)dicarbamate. The pH of the aqueous solution was adjusted to pH 9.0 with 1 M NaOH and extracted with ethyl acetate (3 x 40 mL). The organic phase was combined and dried over anhydrous sodium sulfate, filtered, and evaporated to yield a yellow liquid with a yield of 44.2%.

6.2.2.2.2. Synthesis of alkyne modified HA-Na

In a 100 mL round bottom flask, HA-Na (0.667 g, 4.13 mmol) was dissolved in DMSO/H_2O (50 mL) (v/v=1:1) mixture. To this mixture prop-2-ynyl 2-(2-(2-aminoethyl)disulfanyl)ethylcarbamate (0.963 g, 4.13 mmol), NHS (0.947 g, 8.26 mmol) and EDC (1.577 g, 8.26 mmol) were added. The reaction mixture was stirred overnight at 50 ^oC for 24 h. Subsequently, the reaction mixture was purified by dialysis in dialysis tube (MWCO ~3500 Da) and lyophilized to obtain alkyne modified HA-Na as white fluffy powder.

6.2.2.2.3. Synthesis of azide modified HA-Na

In a 100 mL dry round bottom flask, HA-Na (0.667 g, 4.13 mmol) was dissolved in DMSO/H_2O (50 mL) (v/v=1:1) mixture. To this mixture, 2-azidoethanamine (0.963 g), NHS (0.947 g, 8.26 mmol) and EDC (1.577 g, 8.26 mmol) were added. The reaction was stirred overnight at 50 ^oC for 24 h. Subsequently the reaction mixture was purified by dialysis in dialysis tube (MWCO ~3500 Da) and lyophilized to obtain azide modified HA-Na as white fluffy powder.

6.2.2.2.4. Click reaction between alkyne modified and azide modified HA-Na

Alkyne modified HA-Na (8.875 mg) and azide modified HA-Na (8.875 mg) was swollen in 400 µl DI water. This swollen mass was added to 635 µl of 24 % (w/w in pure water) polyethylene glycol solution which helps in making hydrogel in microenvironment. The mixture was vortexed for 60 s and then kept at rest for 15 min. $CuSO_4$ (17 µl of a 50 mg/mL) and sodium ascorbate (17 µl of a 50 mg/mL) were added to initiate click reaction. The reaction was allowed to proceed for 3 h followed by the addition of water (2 mL) and 3 centrifugation (6000 r/min × 2 min)/washing steps with 1 mL water. Finally the obtained hydrogel was stored in 1 mL water.

6.2.3. Characterization

6.2.3.1. FT-IR spectroscopy

FT-IR spectra of samples were recorded on a FT-IR spectrum-1 Perkin Elmer Spectrometer, UK in a diffused reflectance mode. The samples were mulled with KBr and the frequency range used was from 4000 to 400 cm^{-1}.

6.2.3.2. ^{1}H-NMR Spectroscopy

^{1}H and ^{13}C-NMR spectra were recorded using a Bruker DRX-500 spectrometer operating at a proton frequency of 500.13 MHz and ^{13}C frequency of 68 MHz. A 5 mm QNP probe was used at room temperature. Samples were made in 5 mm NMR tube using D_2O or $CDCl_3$ and TMS as a reference for chemical shifts.

6.2.4. Results and Discussion

In our work, we have used HA as a starting material for synthesizing hydrolysable and cleavable hydrogels through click chemistry approach. HA is a linear polysaccharide consisting of alternating β-1,4-linked units of β-1,3-linkedglucoronic acid (GlcA) and N-acetylglucosamine (GlcNAc). HA is a main component of the extracellular matrix in connective, epithelial and neural tissues and is known to play an important role in organ development, cell proliferation and migration. **Figure 6.1** shows the chemical structure of HA-Na (in the inset) along with ^{1}H-NMR and ^{13}C-NMR spectra. The assignment of peaks in ^{1}H and ^{13}C-NMR spectra confirms the structure of HA.

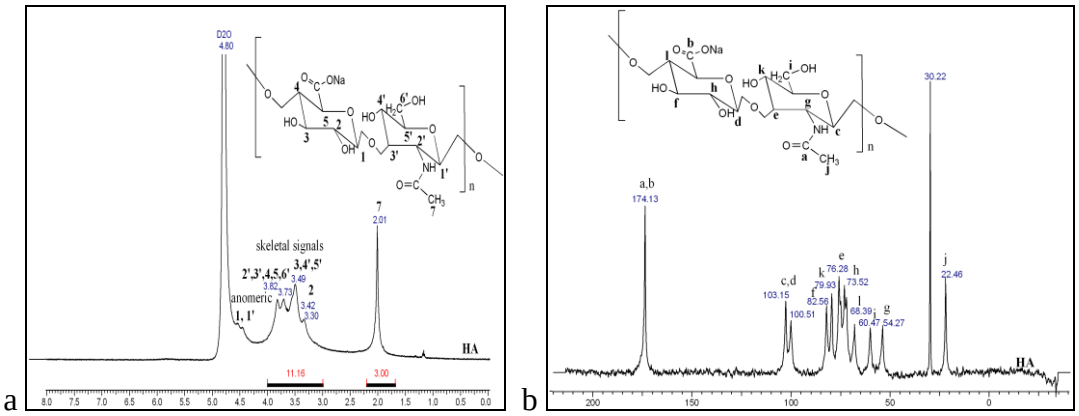

Figure 6.1: *(a) ^{1}H-NMR and (b) ^{13}C-NMR spectra of Hyaluronic Acid (sodium salt)*

6.2.4.1. Synthesis of HA-TBA hydrogels containing carbonate esters

6.2.4.1.1. Synthesis of HA-TBA

Physico-chemically modified HA may significantly differ from native HA, and most modified HA derivatives retain the biocompatibility and other biological properties of HA. The chemical modification of HA generally involves the modification of the carboxyl groups and hydroxyl groups [14-16]. In this work, we have made an attempt to modify HA by introducing an alkyne and azide pendant functional groups. To accomplish this, the H^{+} ion of the HA carboxyl group was exchanged with the TBA-OH using a previously reported method [17].

HA-TBA was prepared by simple ion exchange method, lyophilized and then dissolved in anhydrous DMSO for further modifications. The reaction pathway is shown in **scheme 6.5**. The formation of the HA-TBA was confirmed by IR and ^{1}H-NMR. The HA-TBA shows a signal at 3.2 ppm for -CH_2 of the tetrabutyl unit in the ^{1}H-NMR spectrum and signals from 0.95-1.55 ppm for the -CH_3. The FT-IR spectrum shows two broad absorbance peaks at 2800~3000 cm^{-1} and around 1500 cm^{-1} .

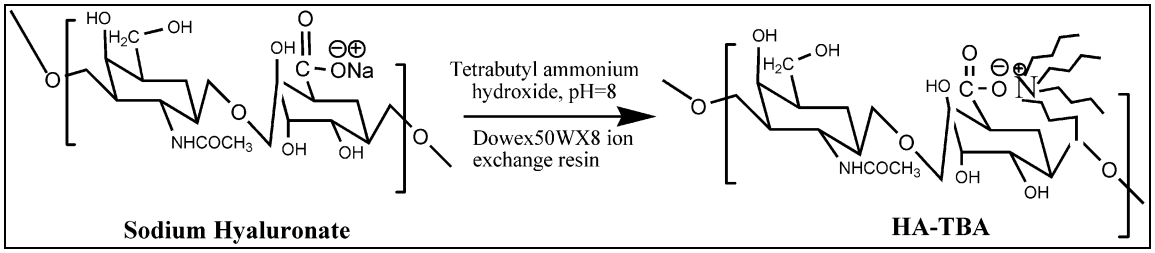

Scheme 6.5: *Synthesis of HA-TBA*

6.2.4.1.2. Synthesis of prop-2-ynyl 1H –imidazole-1-carboxylate

Prop-2-ynyl 1H –imidazole-1-carboxylate was synthesized by the reaction between di(1H-imidazol-1-yl)methanone and prop-2-yn-1-ol. The reaction pathway is shown in **scheme 6.6**.

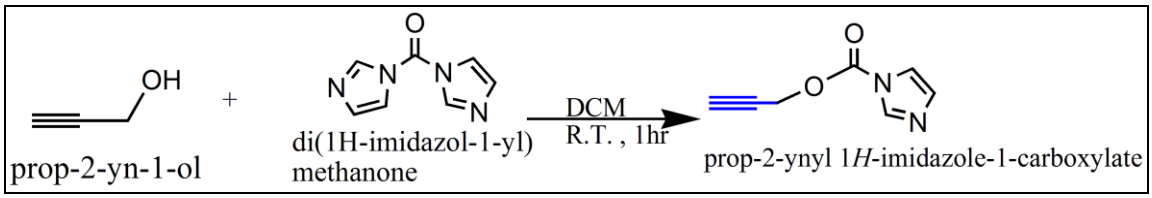

Scheme 6.6: *Synthesis of prop-2-ynyl 1H –imidazole-1-carboxylate*

The mechanism of di(1H-imidazol-1-yl)methanone mediated coupling is well understood. The first step involves partial protonation of the basic imidazole nitrogen, protonated N-acetylimidazole has a pKa of ~ 3.6, leading to an activated species which is then attacked by prop-2-yn-1-ol to give Prop-2-ynyl 1H –imidazole-1-carboxylate.

^{1}H-NMR spectrum of prop-2-ynyl 1H-imidazole-1-carboxylate is shown in **figure 6.2**.

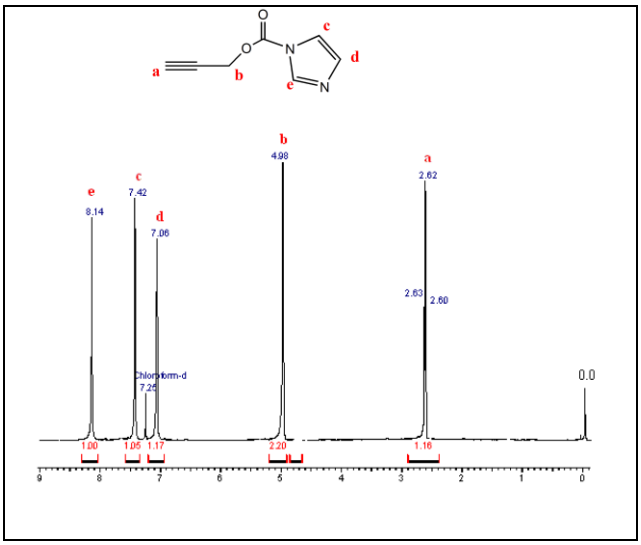

Figure 6.2: *^{1}H- NMR spectrum of prop-2-ynyl 1H –imidazole-1-carboxylate*

^{1}H-NMR in $CDCl_3$ δ (ppm): 2.6 (t, 1H, HC≡C-), 4.9 (d, 2H, CH_2-O), 7.0 (s, 1H, C=CH-N), 7.4 (s, 1H, N-CH=C), 8.1 (s, 1H, N-CH=N). These NMR peak assignments confirm the structure of prop-2-ynyl 1H –imidazole-1-carboxylate.

6.2.4.1.3. Synthesis of an alkyne modified HA-TBA

Alkyne functionalized HA-TBA was synthesized by coupling the above mentioned compound, prop-2-ynyl 1H –imidazole-1-carboxylate to HA-TBA (**Scheme 6.7**). It is the –OH of the HA-TBA that reacts with the –C=O of prop-2-ynyl 1H –imidazole-1-carboxylate and leaving imidazole as a side product.

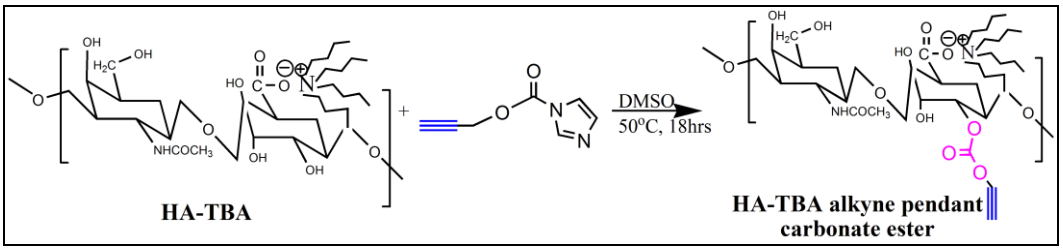

Scheme 6.7: *Synthesis of an alkyne modified HA-TBA*

The alkyne modified HA-TBA product swells in DMSO and Water. The ^{1}H-NMR and FT-IR spectra confirms the structure of the compound. ^{1}H-NMR in D_2O δ (ppm): 5.01 HA, O-C(CH)-O, 4.88, C≡C-CH_2, 3.5-4.3 HA, 0.9-1.5 -CH_3 and -CH_2 of the tetrabutyl unit, IR: 2128 cm-1 alkyne triple bond, 3290cm-1 alkyne –C-H and 1380cm^{-1} carbonate linkage stretching.

6.2.4.1.4. Synthesis of 3-azidopropan-1-ol and 3-azidopropyl 1H-imidazole-1-carboxylate

The reaction pathway for the preparation of 3-azidopropan-1-ol and 3- azidopropyl 1H-imidazole-1-carboxylate is shown in **Scheme 6.8**. The azide ion (N_3^-) can be obtained from sodium azide (NaN_3) which is a very effective nucleophile. It reacts with 3-chloropropanol in a SN_2 reaction to form 3-azidopropanol, thereby forming a C-N bond required for triazole ring. Subsequently, the 3-azidopropanol was reacted with di(1H-imidazol-1-yl)methanone to form and 3-azidopropyl 1H-imidazole-1-carboxylate.

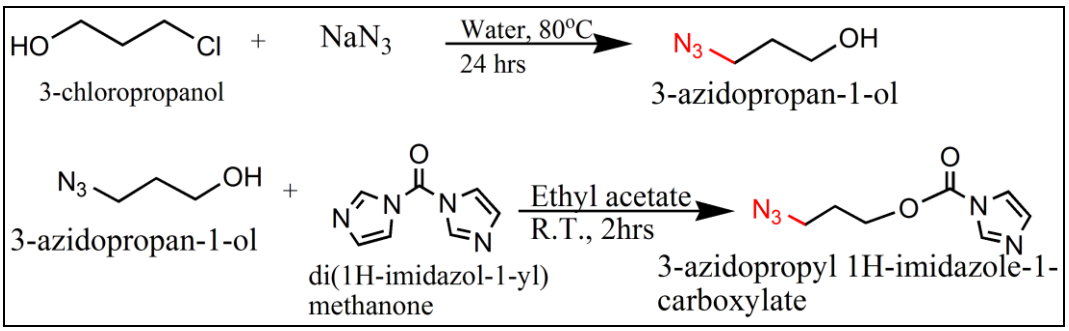

Scheme 6.8: *Synthesis of* 3-azidopropan-1-ol and *3-azidopropyl 1H-imidazole-1-carboxylate*

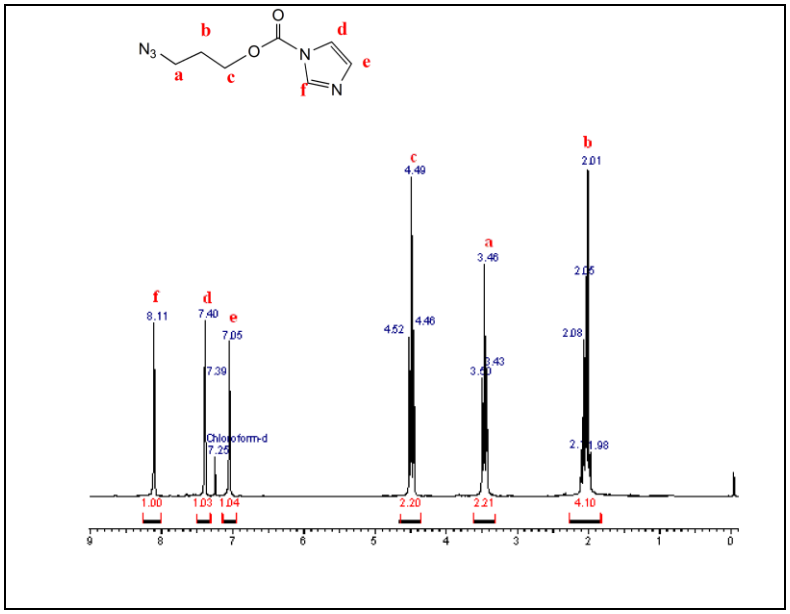

Figure 6.3: *^{1}H-NMR Spectra of 3-azidopropyl 1H-imidazole-1-carboxylate*

The ^{1}H spectrum of 3-azidopropyl 1H-imidazole-1-carboxylate is shown in figure 6.3. The details are as follows, ^{1}H-NMR in $CDCl_3$ δ (ppm): 2.03 (m, 2H, CH_2-CH_2-CH_2), 3.45 (t, 2H, N_3-CH_2), 4.47 (t, 2H, CH_2-O), 7.0 (s, 1H, C=CH-N), 7.4 (s, 1H, N-CH=C), 8.1 (s, 1H, N-CH=N).

6.2.4.1.5. Synthesis of an azide modified HA-TBA

Azide functionalized HA-TBA was synthesized by coupling of 3-azidopropyl 1H-imidazole-1-carboxylate to HA-TBA (**Scheme 6.8**). It is the –OH of the HA-TBA that reacts with the –C=O of 3-azidopropyl 1H-imidazole-1-carboxylate and imidazole is a side product.

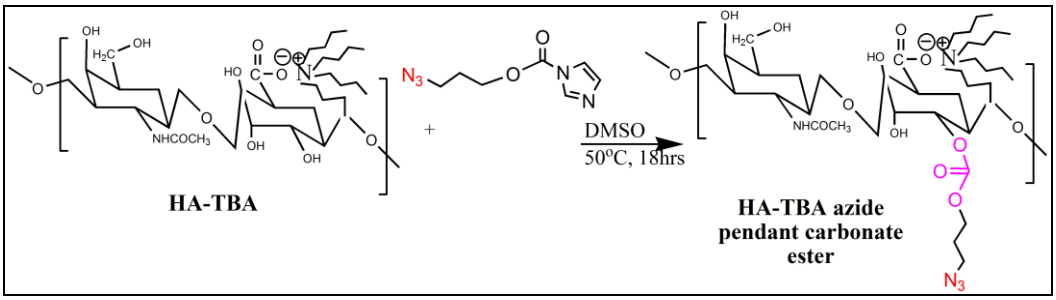

Scheme 6.9: *Synthesis of an azide modified HA-TBA*

The azide modified HA-TBA product swells in DMSO and Water. The NMR details are shown below (NMR spectra is not given), ^{1}H-NMR in D_2O δ (ppm): 2.02, C≡C-CH_2, 3.5-4.3 HA, 4.36 CH_2-CH_2-O, 5.02 HA, O-C(CH)-O, IR: 2100 cm^{-1} N_3, 1380cm^{-1} carbonate linkage stretching. The assignment of peaks in the ^{1}H-NMR and IR spectra confirms the structures of both prop-2-ynyl 1H–imidazole-1-carboxylate, 3-azidopropyl 1H-imidazole-1-carboxylate compounds.

6.2.4.1.6. Click reaction between alkyne modified and azide modified HA-TBA

The covalent cross-linking of the HA chains, through the formation of a triazole ring by ‘clicking’ alkyne modified HA-TBA and azide modified HA-TBA, was performed in aqueous medium (**Scheme 6.10**). An aqueous solution containing both was emulsified using PEG. The ‘click’ reaction was performed under standard conditions by addition of $CuSO_4$ and sodium ascorbate. The obtained hydrogel was washed with water and centrifuged to remove unreacted reactant. The conversion of the azide and alkyne moieties to a triazole ring was confirmed by FT-IR spectroscopy.

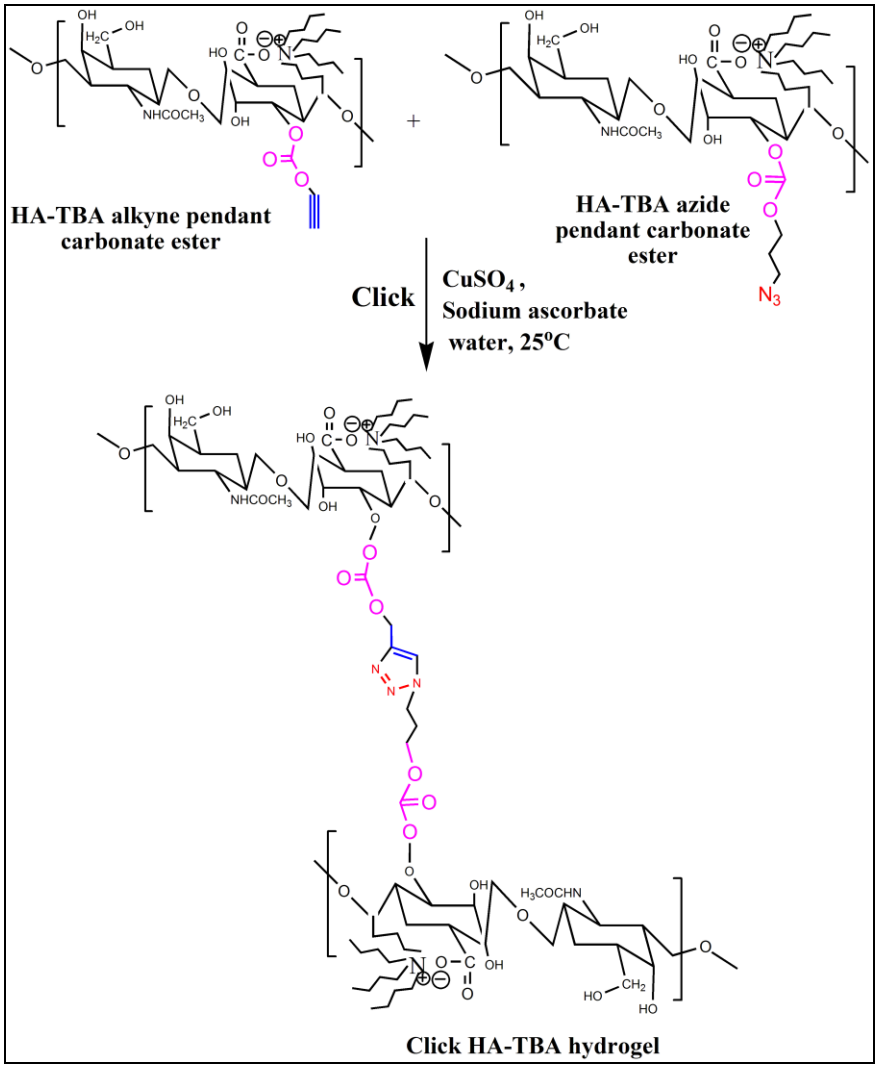

Scheme 6.10: *Click reaction between alkyne modified and azide modified HA-TBA*

The product obtained after the click reaction was insoluble in any solvent and further characterization was difficult. The formation of hydrogel via click reaction was confirmed by FT-IR spectroscopy, where in the decrease in intensity of the azide stretching peak at about 2100 cm^{-1} is observed and the presence of triazole ring formation was confirmed by the peak at 842 cm^{-1} for o-substituted aromatic ring. The C=N and C=C stretching at 1607 cm^{-1} in the FT-IR spectra of the gel confirms the click reaction (**figure 6.4 (b)**)

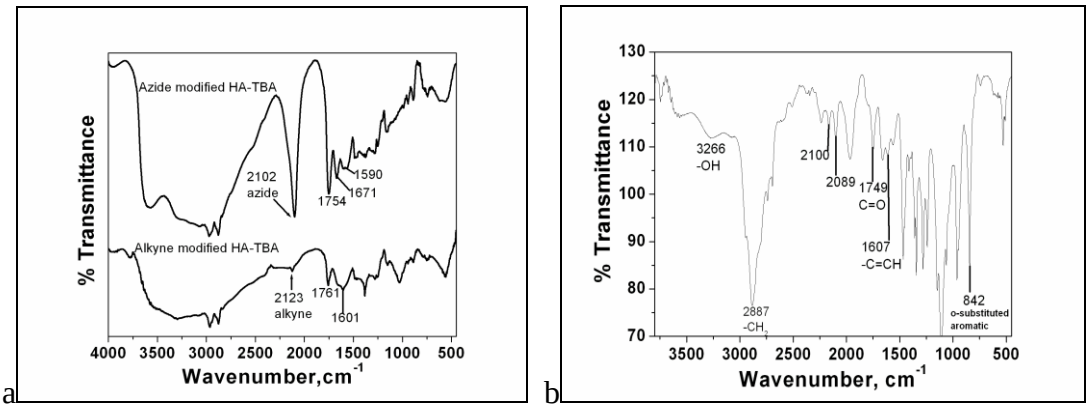

Figure 6.4: *IR spectra (a) Alkyne and azide modified HA-TBA (b) Gel after click reaction*

6.2.4.1.7. Synthesis of prop-2-ynyl 2-(2-(2-aminoethyl)disulfanyl)ethylcarbamate

The prop-2-ynyl 1H –imidazole-1-carboxylate is reacted with cystamine to give prop-2-ynyl 2-(2-(2-aminoethyl)disulfanyl)ethylcarbamate (**Scheme 6.11**)

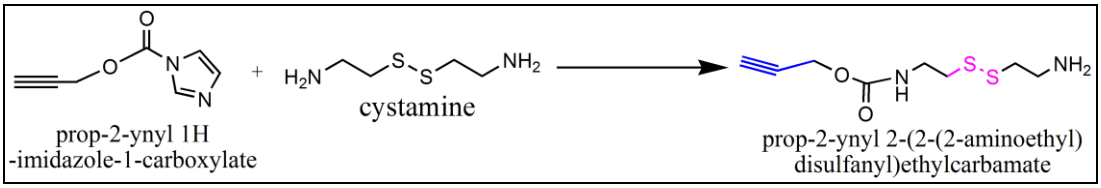

Scheme 6.11: *Synthesis of prop-2-ynyl 2-(2-(2-aminoethyl)disulfanyl)ethylcarbamate*

The structure of prop-2-ynyl 2-(2-(2-aminoethyl)disulfanyl)ethylcarbamate was confirmed by ^{1}H-NMR spectrum and the details are given below, ^{1}H-NMR using $CDCl_3$ δ (ppm): 2.49 (t, 1H, *H*C≡C-), 2.77 (m, 2H, -S-S-C*H*$_2$-CH$_2$-NH$_2$), 2.79 (m, 2H, -HN-CH$_2$-C*H*$_2$-S-S-), 3.01 (m, 2H, -S-S-CH$_2$-C*H*$_2$-NH$_2$), 3.54 (m, 2H, -HN-C*H*$_2$-CH$_2$-S-S-), 4.69 (s, 2H, HC≡C-C*H*$_2$-O-).

6.2.4.1.8. Synthesis of alkyne modified HA-Na

The alkyne modified HA-Na was then prepared by a coupling reaction between carboxyl groups of HA-Na and amine of prop-2-ynyl 2-(2-(2-

aminoethyl)disulfanyl)ethyl carbamate using EDC/NHS as coupling agent in MES buffer at room temperature. The reaction pathway is shown in **Scheme 6.12**

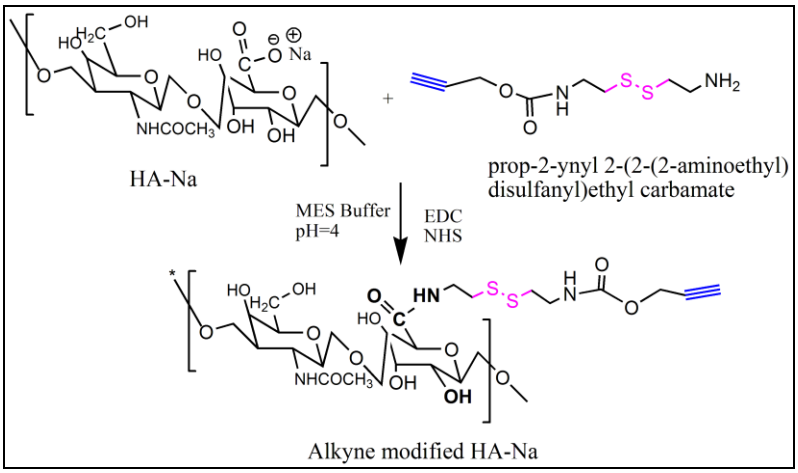

Scheme 6.12: *Synthesis of alkyne modified HA-Na*

The structure of an alkyne modified HA-Na was confirmed by ^{1}H-NMR spectrum and the details are given below,^{1}H-NMR using D_2O δ (ppm): 2.47 (2H, *H*C≡C-CH_2), 4.55 (2H, HC≡C-C*H*$_2$), 4.83 (1H, HA, -O-C*H*(CH-OH)-O), 5.07 (1H, HA, -O-C*H*(CH-O-CH_2-C=OO-)-O).

6.2.4.1.9. Synthesis of azide modified HA-Na

Similarly, the azide modified HA-Na was prepared by a coupling reaction between HA-Na and 2-azidoethaneamine using EDC/NHS as coupling agent in MES buffer at room temperature. The reaction pathway is shown in **Scheme 6.13**

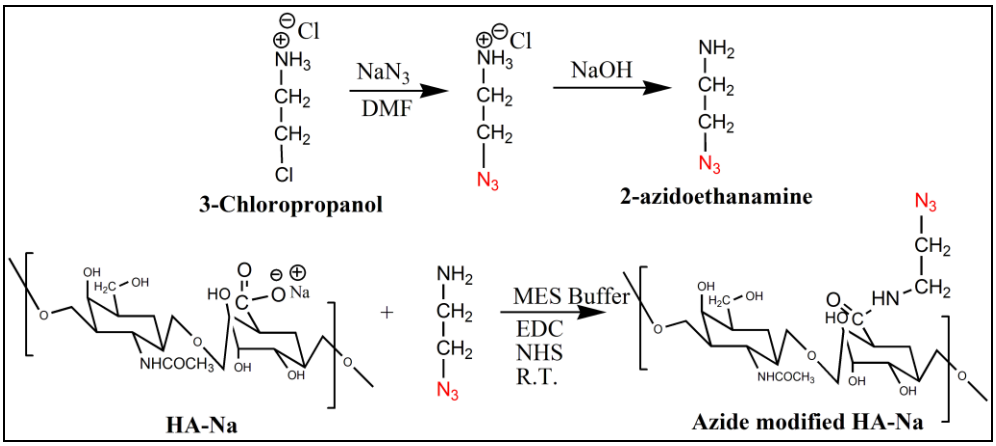

Scheme 6.13: *Synthesis of azide modified HA-Na*

The structure of an azide modified HA-Na was confirmed by ^{1}H-NMR spectrum and the details are given below, ^{1}H-NMR using D_2O δ (ppm): 1.93 (2H, -CH_2-C*H*$_2$-CH_2-), 4.92 (1H, HA, -O-C*H*(CH-OH)-O), 4.26 (t, 2H, -CH_2-C*H*$_2$-O-).

6.2.4.1.10. Click reaction between alkyne and azide modified HA-Na

HA-Na hydrogels was synthesized by rapid vortexing of an aqueous mixture of alkyne modified HA-Na and azide modified HA-Na containing PEG. Due to the immiscibility of the two phases, a water-in-water emulsion was obtained. Subsequently, a click reaction between the HA-Na pendent alkyne and azide moieties was initiated (**Scheme 6.14**).

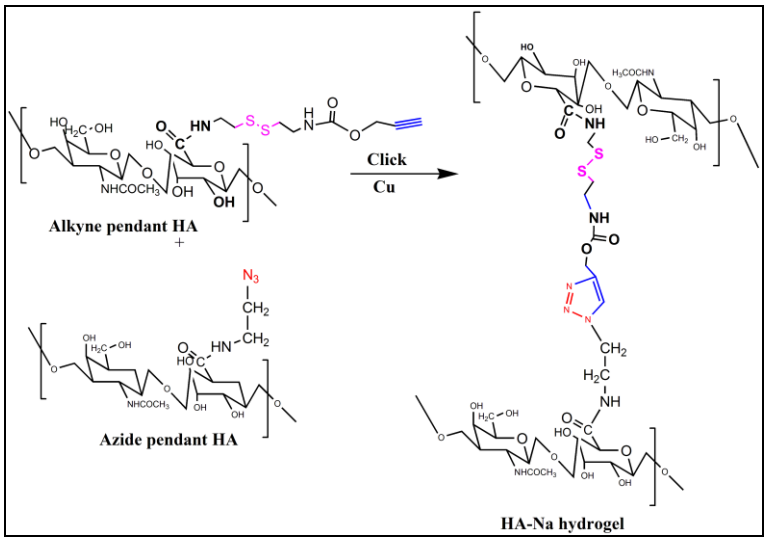

Scheme 6.14: *Click reaction between alkyne modified and azide modified HA-Na*

The product obtained after the click reaction was insoluble opaque, gummy mass. However, the product was evaluated for the click reaction by FT-IR spectroscopy. It was observed that there was still a small azide/alkyne stretching peak at about 2100 cm^{-1}, which can come from some of the unreacted alkyne/azide functionalities. The presence of triazole ring formation was also confirmed by the peak at 845 cm^{-1} for o-

substituted aromatic ring. The C=N and C=C stretching at 1600 cm^{-1} in the FT-IR spectra of the gel confirms the click reaction.

6.3. Conclusions

In this work, new alkyne and azide modified HA-TBA with hydrolysable carbonate esters and alkyne and azide modified HA-Na with cleavable disulphide linkages were successfully synthesized and characterized by IR and ^{1}H-NMR spectroscopy. Further HA hydrogels were obtained by the Cu(I)-catalyzed Huisgen 1,3-dipolar cycloaddition between an azide and an alkyne modified HA-TBA and similarly with azide and alkyne modified HA-Na. Although after the click reaction, the product was an insoluble mass, qualitative determination of functional groups was performed by FT-IR spectroscopy which indicated the presence of triazole ring. These studies need detailed investigations further which can be taken-up in future.

6.4. References:

1. Lutz, J.-F., 1,3-Dipolar Cycloadditions of Azides and Alkynes: A Universal Ligation Tool in Polymer and Materials Science. *Angewandte Chemie International Edition* **2007,** 46, (7), 1018-1025.

2. Burdick, J. A.; Prestwich, G. D., Hyaluronic acid hydrogels for biomedical applications. *Advanced Materials* **2011,** 23, (12), H41-H56.

3. Xu, X.; Jha, A. K.; Harrington, D. A.; Farach-Carson, M. C.; Jia, X., Hyaluronic acid-based hydrogels: from a natural polysaccharide to complex networks. *Soft matter* **2012,** 8, (12), 3280-3294.

4. Malkoch, M.; Vestberg, R.; Gupta, N.; Mespouille, L.; Dubois, P.; Mason, A. F.; Hedrick, J. L.; Liao, Q.; Frank, C. W.; Kingsbury, K., Synthesis of well-defined hydrogel networks using Click chemistry. *Chemical communications* **2006**, (26), 2774-2776.

5. Ossipov, D. A.; Piskounova, S.; Hilborn, J. n., Poly(vinyl alcohol) Cross-Linkers for in Vivo Injectable Hydrogels. *Macromolecules* **2008,** 41, (11), 3971-3982.

6. Hu, X.; Li, D.; Zhou, F.; Gao, C., Biological hydrogel synthesized from hyaluronic acid, gelatin and chondroitin sulfate by click chemistry. *Acta Biomaterialia* **2011,** 7, (4), 1618-1626.

7. Huerta-Angeles, G.; Šmejkalová, D.; Chládková, D.; Ehlová, T.; Buffa, R.; Velebný, V., Synthesis of highly substituted amide hyaluronan derivatives with tailored degree of substitution and their crosslinking via click chemistry. *Carbohydrate Polymers* **2011,** 84, (4), 1293-1300.

8. Tizzotti, M.; Creuzet, C.; Labeau, M.-P.; Hamaide, T.; Boisson, F.; Drockenmuller, E.; Charlot, A. l.; Fleury, E., Synthesis of Temperature Responsive

Biohybrid Guar-Based Grafted Copolymers by Click Chemistry. *Macromolecules* **2010,** 43, (16), 6843-6852.

9. Chelsea M. Nimmo, S. C. O., and Molly S. Shoichet, Diels-Alder click cross-linked hyaluronic acid hydrogels for tissue engineering. *Biomacromolecules* **2011,** 12, 824-830.

10. Crescenzi, V.; Cornelio, L.; Di Meo, C.; Nardecchia, S.; Lamanna, R., Novel hydrogels via click chemistry: synthesis and potential biomedical applications. *Biomacromolecules* **2007,** 8, (6), 1844-1850.

11. Testa, G.; Di Meo, C.; Nardecchia, S.; Capitani, D.; Mannina, L.; Lamanna, R.; Barbetta, A.; Dentini, M., Influence of dialkyne structure on the properties of new click-gels based on hyaluronic acid. *International journal of pharmaceutics* **2009,** 378, (1), 86-92.

12. De Geest, B. G.; Van CampThis, W.; Du Prez, F. E.; De Smedt, S. C.; Demeester, J.; Hennink, W. E., Biodegradable microcapsules designed via click chemistry. *Chemical communications* **2008**, (2), 190-192.

13. Zhang, J.; Li, C.; Wang, Y.; Zhuo, R.-X.; Zhang, X.-Z., Controllable exploding microcapsules as drug carriers. *Chemical communications* **2011,** 47, (15), 4457-4459.

14. Bulpitt, P.; Aeschlimann, D., New strategy for chemical modification of hyaluronic acid: preparation of functionalized derivatives and their use in the formation of novel biocompatible hydrogels. *Journal of biomedical materials research* **1999,** 47, (2), 152-169.

15. Pelletier, S.; Hubert, P.; Lapicque, F.; Payan, E.; Dellacherie, E., Amphiphilic derivatives of sodium alginate and hyaluronate: synthesis and physico-chemical

properties of aqueous dilute solutions. *Carbohydrate Polymers* **2000,** 43, (4), 343-349.

16. Tomihata, K.; Ikada, Y., Preparation of cross-linked hyaluronic acid films of low water content. *Biomaterials* **1997,** 18, (3), 189-195.

17. Oh, E. J.; Park, K.; Choi, J. S.; Joo, C.-K.; Hahn, S. K., Synthesis, characterization, and preliminary assessment of anti-Flt1 peptide hyaluronate conjugate for the treatment of corneal neovascularization. *Biomaterials* **2009,** 30, (30), 6026-6034.

Summary and Conclusions

Chapter - VII

The aim of this thesis work was to design and synthesize new APs and hydrogels based on renewable resource materials, such as Carboxymethyl Guar Gum (CMG), Carboxymethyl Tamarind (CMT), Hydroxypropyl Guar Gum (HPG) and Hyaluronic acid (HA) which have not been fully explored in APs and hydrogels areas.

Extensive literature search on APs in terms of their synthesis, chemical structure, rheology etc. along with general techniques for characterization of APs is given in the first chapter.

Thermo-associating APs based on CMG and CMT graft copolymers were designed and synthesized using LCST grafted chains such as, poly(*N*-isopropylacrylamide) (PNIPAm) and poly(ethylene oxide-co-propylene oxide) (PEPO). The graft copolymers, CMG-g-PNIPAm, CMG-g-PEPO and CMT-g-PEPO exhibited interesting thermo-associating behaviour, where the sol-gel transitions could be observed with increasing temperature. The phenomenon of thermo-associations was attributed to the self assembely of LCST grafts due to temperature driven hydrophobic associations without undergoing macrophase separation of the solution. The MW and percentage of grafting of LCST chains play an important role in determining the thermo-associating behaviour of these polymers. At moderate concentrations (C_p~10-30 g/L), the graft copolymer solutions showed gel-like behaviour and the viscoelastic behaviour (G' and G") was studied using oscillatory rheological experiments. The temperature of association (T_{ass}) was determined by measuring the ^1H line width of a peak of LCST grafted chain w.r.t. temperature. This temperature of association (T_{ass}) matched very well with the observed associating behaviour investigated by rheology. The influence of external parameters, such as salts and surfactants on the thermo-associating behaviour was studied. The salts decreased the T_{ass} due to salting out effect whereas, the presence of surfactant increased the T_{ass}. The thermo-associating

behaviour of these graft copolymers was further confirmed by pyrene emission fluorescence measurements. These thermo-associating polymers with biodegradable nature of CMG and CMT can have potential applications as smart injectables in controlled release technology.

We also demonstrated the use of thermo-associating polymers in the synthesis of metal nanoparticles. Silver nanoparticles (AgNPs) were synthesized using thermo-associating polymers namely, CMG-g-PEPO. The polymer acts as reducing agent as well as stabilising / capping agent during the synthesis of AgNPs. The conformation of formation of AgNPs was done by UV/Vis spectroscopy, which gave a surface plasmon resonance in the range of 400-420 nm. The TEM images indicated the size of nanoparticles in the range of 10-20 nm. The crystalline nature of AgNPs was studied by XRD. XPS and Raman spectroscopy study confirmed the binding of Dox onto AgNPs encapped with thermo-associating polymer. Further, the release profile of the drug could be controlled by varying the properties of thermo-associating polymer.

SAPs are a class of hydrophilic, highly crosslinked polymers which can absorb and hold large amount of water and body fluids (~100-1000 g of fluid per gram of polymer). Most of the commercially available SAPs are synthetic and do not have biodegradability, which can cause environmental problems. In this thesis work, we have reported on the synthesis and characterization of new SAPs based on crosslinked polysaccharides namely, CMG and HPG. These polymers are supposed to be biodegradable and biocompatible. The crosslinking of CMG and HPG in combination was effected using two crosslinking agents namely, Citric acid (CA) and Divinyl sulphone (DVS). The SAPs exhibited good swelling characteristics and particularly, SAPs with DVS crosslinking showed better mechanical strength in the swollen state as determined by Dynamic Mechanical Analysis (DMA). These SAPs were found to

be biodegradable (~ 90% in 30 days), non-toxic with good cell-proliferation which was confirmed by biodegradability and Cytotoxicity/Cell viability studies.

Finally we made an attempt to synthesize APs based Hyaluronic acid (HA) using "Click Chemistry" approach. The alkyne and azide modified HA was synthesized by incorporating hydrolysable carbonate esters and cleavable disulphide linkages. The structures were well characterized by FT-IR and ^{1}H-NMR spectroscopy. Both the clickable moieties of azide and alkyne modified HA showed highly viscous and jelly-behaviour even before the click reaction between them. This could be due to high intermolecular associations within the polymer and needs further detailed investigation.

Future Work

The development of new products and materials, especially those which are non-petrochemical reserves and based on renewable organic resources, using innovative sustainable processes is of increasing interest and deserves the major attention of both academic and industrial research.

Thermo-associating polymers based on polysaccharides are becoming increasingly important. Therefore, it is essential to understand the properties of the polymers in terms of molecular structure, polydisperse nature of natural polymers and the grafting techniques & mechanisms. A more detailed study of the aggregation behaviour/number via fluorescence studies associations in water and their direct application as bioinjectables have to be performed.

Although we have demonstrated the use of thermo-associating polymers for synthesis of AgNPs, a more detailed study on the mechanism of reduction, influence of concentrations of polymer, on the synthesis of AgNPs is to be performed. The incorporation of various drugs and their interaction with polymer encapped drug, drug release properties needs to be studied carefully.

The SAPs can be further evaluated as eco-friendly water manageable materials for agricultural and horticultural applications or for controlled release formulation in pharmaceutical formulations. Finally, a detailed investigation on the gelling behaviour of carbonate ester modified HA and the click reaction of the carbonate esters and disulphide modified HA respectively, to form hydrogels is warranted.